

# Carrier-Based Ion-Selective Electrodes and Bulk Optodes. 1. General Characteristics

Eric Bakker,<sup>\*,†</sup> Philippe Bühlmann,<sup>\*,‡</sup> and Ernö Pretsch<sup>\*,§</sup>

Department of Chemistry, Auburn University, Auburn, Alabama 36849, Department of Chemistry, School of Science, The University of Tokyo, Hongo, Bunkyo-ku, Tokyo 113, Japan, and Department of Organic Chemistry, Swiss Federal Institute of Technology (ETH), Universitätstrasse 16, CH-8092 Zürich, Switzerland

Received February 26, 1997 (Revised Manuscript Received July 10, 1997)

## Contents

I. Introduction	3083
II. Characteristics of Potentiometric and Optical Sensors	3087
1. Ion-Selective Electrodes	3087
A. Response Mechanism	3087
B. Selectivity	3090
C. Detection Limit	3098
D. Measuring Range	3101
E. Response Time	3102
2. Ion-Selective Optodes	3103
A. Response Mechanism	3103
B. Selectivity	3107
C. Detection Limits	3109
D. Measuring Range	3111
E. Response Time	3111
3. Comparison of Optical and Potentiometric Transduction Schemes	3112
A. Response Mechanism	3112
B. Selectivity	3113
C. Detection Limit	3114
D. Measuring Range	3114
E. Response Time	3114
F. Lifetime	3115
III. Specific Requirements for Ionophores and Membrane Matrices	3115
1. Ionophores	3115
A. General Considerations	3115
B. Modeling of Ionophores	3118
C. Exchange Kinetics, Reversibility	3120
D. Lipophilicity	3122
2. Other Membrane Components	3123
A. Membrane Solvent (Plasticizer)	3123
B. Ionic Additives	3125
C. The Polymer Matrix	3126
IV. Conclusions	3128
V. Acknowledgments	3128
VI. References	3128

## I. Introduction

Over the past 30 years, the application of carrier-based ion-selective electrodes (ISEs) has evolved to a well-established routine analytical technique. The

College of American Pathologists Comprehensive Chemistry Survey in 1980, for example, showed only 22% of the participating laboratories as making potentiometric Na<sup>+</sup> or K<sup>+</sup> measurements. By 1991, on the other hand, the Chemistry Survey listed 96% of 6041 participating laboratories as using Na<sup>+</sup> ISE analyzers and only 4% as using flame atomic emission spectrometry.<sup>1,2</sup> It was estimated that in the United States about 200 million clinical assays of K<sup>+</sup> are made every year with valinomycin-based ISEs.<sup>3</sup> Since several other biologically relevant ions are also monitored with solvent polymeric membrane electrodes, it can be safely stated that yearly well over a billion ISE measurements are performed world-wide in clinical laboratories alone. Moreover, ISEs are also utilized in many other fields, including physiology, process control, and environmental analysis. They thus form one of the most important groups of chemical sensors. The analytes for which carrier-based ISEs and their counterparts with optical detection have been developed so far are shown in Table 1 and will be discussed in part 2 of this pair of reviews. The key components of both types of sensors are lipophilic complexing agents capable of reversibly binding ions. They are usually called ionophores or ion carriers. The latter name reflects the fact that these compounds also catalyze ion transport across hydrophobic membranes. As will be shown here, their implementation in ion-selective electrodes or optodes is now straightforward.

The essential part of a carrier-based ISE is the ion-sensitive solvent polymeric membrane, physically a water-immiscible liquid of high viscosity that is commonly placed between two aqueous phases, i.e., the sample and the internal electrolyte solution (cf. Figure 1). It contains various constituents, commonly an ionophore (ion carrier) and a lipophilic salt as ion exchanger. The sensor responds to the activity of the target ion and usually covers an extraordinarily large sensitivity range, from about 1 to 10<sup>-6</sup> M. Its selectivity is related to the equilibrium constant of the exchange reaction of target and interfering ions between the organic and aqueous phases. It strongly depends on the ratio of complex formation constants of these ions with the ionophore in the membrane phase (cf. Figure 2 and section II.1.B).

Ionophores are in their uncomplexed (or unassociated) form either charged or electrically neutral (cf. Figure 2). The first neutral ionophores used in ISE membranes were antibiotics.<sup>4,5</sup> They were followed by a large number of natural and synthetic, mainly uncharged carriers for cations and a series of charged

<sup>†</sup> Auburn University.

<sup>‡</sup> The University of Tokyo.

<sup>§</sup> Swiss Federal Institute of Technology (ETH).

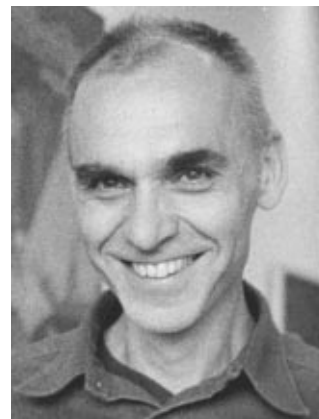


Eric Bakker is Assistant Professor of Chemistry since 1995 at the Department of Chemistry, Auburn University, Auburn, AL. He earned his doctoral degree at the Swiss Federal Institute of Technology (ETH) in Zurich, Switzerland, in 1993. In the same year he moved to the University of Michigan in Ann Arbor for a two-year postdoctoral stay. Since 1991 he has published over 40 scientific papers on various aspects of carrier-based optical and potentiometric sensors. His main research interests are the theory of selectivity; charged-carrier-based chemical sensors; potentiometric and optical sensors for polyions, anions, small cations, and heavy metals; pH electrodes; and new reference electrode concepts. His research group at Auburn maintains a web page at <http://www.duc.auburn.edu/~bakkeer> where current information is posted. His e-mail address is bakkeer@mail.auburn.edu.



Philippe Bühlmann received a Ph.D. from the Swiss Federal Institute of Technology (ETH) in Zürich, Switzerland, in 1993. After a one-year postdoctoral stay at The University of Tokyo, Japan, as a fellow of the Japan Society of the Promotion of Science, he joined in 1994 the faculty of the Department of Chemistry, School of Science, The University of Tokyo as a Research Associate. His main research interests are in the development and theory of electrochemical and optical sensors, with a special focus on the implementation of molecular recognition of inorganic anions and organic analytes. His e-mail address is buhlmann@utsc.s.u-tokyo.ac.jp.

and uncharged ones for anions (part 2<sup>6</sup>). Another motivation for developing carriers is the design of systems for separating ions or molecules by selective transport through membranes.<sup>7,8</sup> Potentiometric and ion-transport selectivities are correlated since both are governed by the selective extraction of ions.<sup>9</sup> In spite of this correlation, it must be kept in mind that the best ion carriers and membrane compositions for potentiometric and optical sensors do not necessarily give optimal ion transport systems in terms of high turnover.<sup>8,10</sup> Once an ISE membrane is conditioned with a solution of the target ion it responds to, no significant transport occurs within the membrane when the activity of this ion in the sample solution



Ernö Pretsch received his Ph.D., *venia legendi*, and the title of Professor from the Swiss Federal Institute of Technology (ETH) in Zürich, Switzerland, in 1968, 1980, and 1991, respectively. He has been working in the field of chemical sensors since 1970. Further topics of his interest are spectroscopic databases, automatic spectra interpretation, and modeling of structure–property relationships. He has published over 170 papers and 7 books. Current activities are documented on the web page <http://www.ceac.ethz.ch/pretsch/>. His e-mail address is pretsch@org.chem.ethz.ch.

is altered.<sup>11</sup> Optode membranes, on the other hand, are always reconditioned after every sample change.

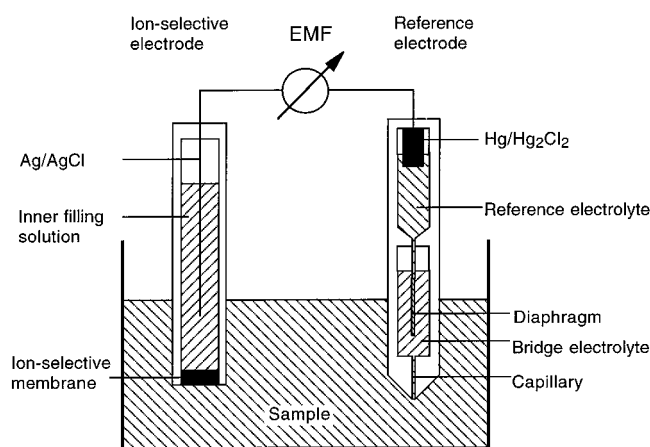
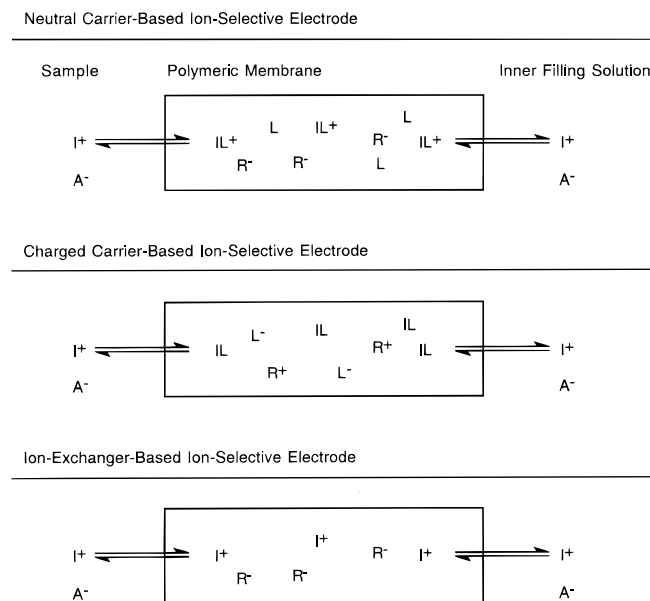
Historically, a fortuitous coincidence of several independent developments in the 1960s contributed to the rapid success in the systematic search for carrier-based ISEs. After the discovery, in 1964, by Moore and Pressman<sup>12</sup> that some antibiotics (cf. Figure 3) induce ion transport in mitochondria, Simon and Stefanac<sup>4,13,14</sup> showed in 1966 that the phenomenon is mainly due to the selective formation of complexes between these compounds and certain cations. They introduced the first neutral-carrier-based ISE and demonstrated that these antibiotics induce *in vitro* selectivities similar to those observed *in vivo*. At about the same time, Pedersen<sup>15</sup> and Lehn<sup>16,17</sup> synthesized macrocyclic polyethers and macroheterobicyclic compounds (cf. Figure 3) and showed them to act as complexing agents for alkali and alkaline-earth metal ions. The following years saw the structure determination of a large number of synthetic and natural ionophores and their complexes.<sup>18</sup> The third important contribution to the development of modern liquid membrane ISEs came from Shatkay and co-workers<sup>19,20</sup> and Ross,<sup>21</sup> who introduced solvent polymeric membranes. A Ca<sup>2+</sup>-selective electrode with a lipophilic organophosphoric acid<sup>21</sup> (cf. Figure 3) as the most prominent finding in this line of research is still in use. Poly(vinyl chloride) (PVC) was quickly widely accepted and, even though the use of various other polymer matrices has been demonstrated (cf. section III.2.C), it still remains the standard matrix for carrier-based ISEs.<sup>22,23</sup>

On the basis of previous results and with a view to their application in ISEs, an intensive systematic search for cation-selective ionophores started, whereas progress in the development of anion carriers was much slower. Within a few years after preparing the first electrically neutral Ca<sup>2+</sup>-selective ionophore (cf. Figure 3),<sup>24</sup> ISE membranes containing uncharged carriers<sup>25</sup> were developed for a series of alkali and alkaline-earth metal and some other cations (for a

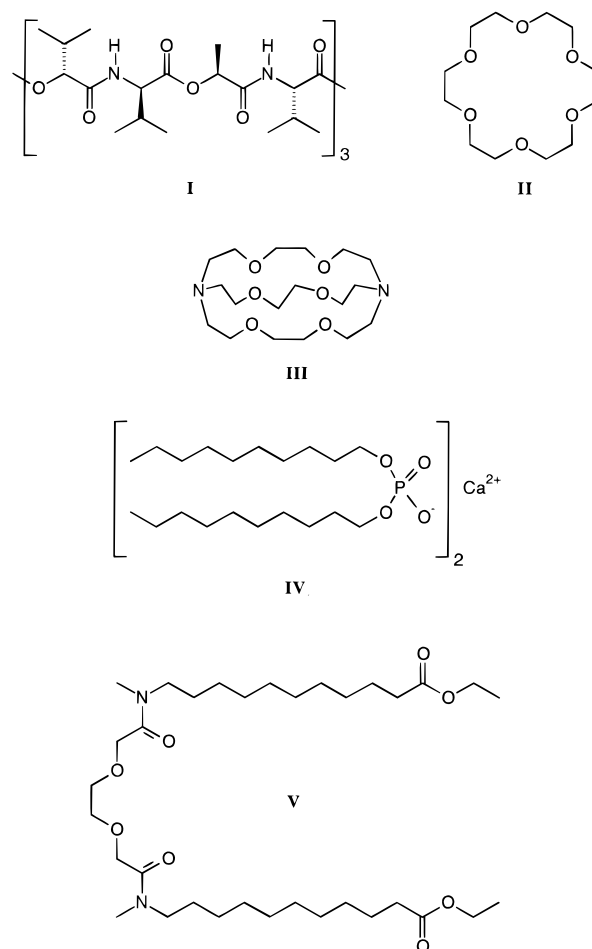
**Table 1. Analytes for Which Carrier-Based Ion-Selective Electrodes and Bulk Optodes Have Been Described So Far<sup>6,43</sup>**

analyte group	ion-selective electrodes	bulk optodes
inorganic cations	H <sup>+</sup> , Li <sup>+</sup> , Na <sup>+</sup> , K <sup>+</sup> , Rb <sup>+</sup> , Cs <sup>+</sup> , (Be <sup>2+</sup> ), Mg <sup>2+</sup> , Ca <sup>2+</sup> , Sr <sup>2+</sup> , Ba <sup>2+</sup> , Mo(IV), Fe(III), Cu <sup>2+</sup> , Ag <sup>+</sup> , Zn <sup>2+</sup> , Cd <sup>2+</sup> , Hg <sup>2+</sup> , Tl <sup>+</sup> , Bi <sup>3+</sup> , Pb <sup>2+</sup> , U(IV), Sm(III), NH <sub>4</sub> <sup>+</sup>	H <sup>+</sup> , Li <sup>+</sup> , Na <sup>+</sup> , K <sup>+</sup> , Mg <sup>2+</sup> , Ca <sup>2+</sup> , Ag <sup>+</sup> , Zn <sup>2+</sup> , Hg <sup>2+</sup> , Pb <sup>2+</sup> , U(IV), NH <sub>4</sub> <sup>+</sup>
inorganic anions	CO <sub>3</sub> <sup>2-</sup> , HCO <sub>3</sub> <sup>-</sup> , SCN <sup>-</sup> , NO <sub>2</sub> <sup>-</sup> , OH <sup>-</sup> , phosphate, sulfite, SO <sub>4</sub> <sup>2-</sup> , Cl <sup>-</sup> , SeO <sub>3</sub> <sup>2-</sup> , I <sup>-</sup>	CO <sub>3</sub> <sup>2-</sup> , SCN <sup>-</sup> , NO <sub>2</sub> <sup>-</sup> , sulfite, Cl <sup>-</sup> , I <sup>-</sup>
organic cations <sup>a</sup>	1-phenylethylamine, 1-(1-naphthyl)-ethylamine, ephedrine, norephedrine, pseudoephedrine, amphetamine, propranolol, amino acid methyl esters, α-amino-ε-caprolactam, amino acid amides, benzyl amine, alkyl amines, dopamine, mexiletine, local anaesthetics (procaine, prilocaine, lidocaine, bupivacaine, lignocaine), diquat and paraquat (herbicides), tetramethyl- and tetraethylammonium, guanidine, metformin, phenformin, creatinine, protamine	1-phenylethylamine, propranolol, norephedrine, octylamine
organic anions	salicylate, phthalate, maleate, 2-hydroxybenzhydroxamate, nucleotides, heparin	salicylate, guanosine triphosphate, heparin
neutral analytes	CO <sub>2</sub> , NH <sub>3</sub> (indirectly)	H <sub>2</sub> O, NH <sub>3</sub> , SO <sub>2</sub> , ethanol, O <sub>2</sub>

<sup>a</sup> For cations that can be deprotonated, the name of the corresponding neutral compound is indicated.

**Figure 1.** Schematic diagram of a membrane electrode measuring circuit and cell assembly.**Figure 2.** Schematic view of the equilibria between sample, ion-selective membrane, and inner filling solution for the special case of equal sample and inner electrolytes: top, electrically neutral carrier (L) and anionic sites (R<sup>-</sup>); center, charged carrier (L<sup>-</sup>) and cationic sites (R<sup>+</sup>); and bottom: cation exchanger (R<sup>+</sup>).

review, see ref 26). The ionophores were all non-macrocyclic, thus disproving the initial notion that complexing agents should be macrocyclic. Owing to

**Figure 3.** Structural formulas of the first relevant ion carriers and related compounds: **I**, valinomycin; **II**, 18-crown-6; **III**, cryptand [2,2,2]; **IV**, calcium didecyl phosphate; and **V**, the first lipophilic uncharged Ca<sup>2+</sup>-selective ligand.<sup>24</sup>

their low lipophilicity and limited selectivity,<sup>15</sup> the crown ethers known at that time were not suitable for use in ISE membranes. Cryptands, although highly selective, also lacked lipophilicity, and in addition, their slow complexation<sup>16,17</sup> may also hamper an application in sensor membranes. From the chemistry of macrocyclic ligands a great many studies of host-guest and supramolecular chemistry have evolved<sup>27</sup> but, unfortunately, seldom focused on chemical sensors.

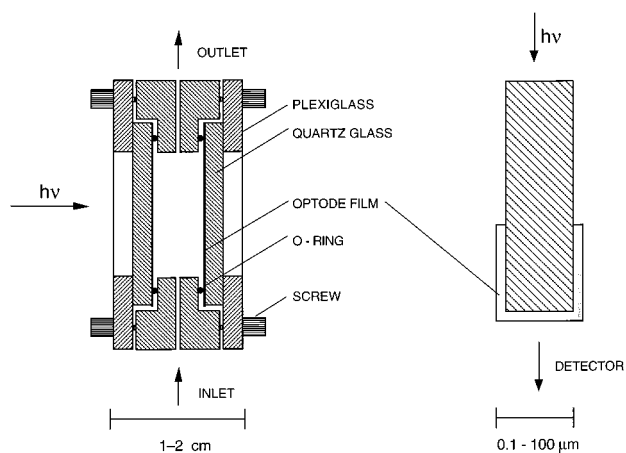
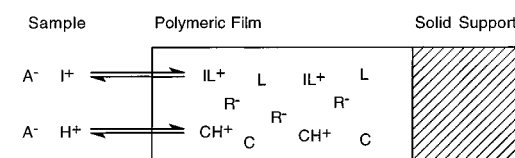


**Figure 4.** Schematic diagram of two kinds of bulk optode measuring setups: left, two membrane films are placed at the inner surface of a flow-through cell; right, membrane film on a waveguide.

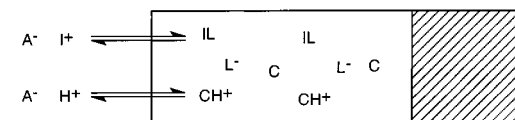
The theory of ISE response is well-established, especially owing to the pioneering work of Eisenman's group<sup>28</sup> and others.<sup>29,30</sup> Formally, the membrane potential can be described as the sum of the two phase boundary potentials and the diffusion potential within the membrane,<sup>31,32</sup> the latter being negligible in electrodes of practical relevance.<sup>33–35</sup> The selectivity dependence on ion exchange and complex formation properties is also well-understood,<sup>29</sup> but only recently a proper description of the ISE response to solutions containing ions of different valences was given.<sup>36</sup> The extended semiempirical Nicolskii–Eisenman equation, which had been generally used, is not appropriate in such cases.

The working mechanisms of a certain group of optical sensors are based on chemical equilibria analogous to those of ISEs and, furthermore, solvent polymeric films of similar compositions are employed (cf. Figures 4 and 5). In addition to a selective ionophore, they often contain a lipophilic counterion and a second ionophore that specifically interacts with a reference ion and, on complexation, undergoes a change in its optical characteristics. Such ionophores are known as chromoionophores<sup>37</sup> or fluoroionophores.<sup>38</sup> Usually, a lipophilic pH indicator is used as chromoionophore. Its degree of protonation and hence its color depend on the activity of both competing ions, i.e.,  $H^+$  and the target ion, in the measuring solution. If the pH of the sample is known (e.g., by buffering or from independent measurement), the activity of the target ion can be calculated from the absorbance changes of the sensing film. This type of optical sensors has been developed since the late 1980s only and is referred to as *bulk optodes*. The name alludes to the fact that the analyte is extracted into the bulk and not only a surface layer of the membrane (cf. Figure 5). Another type of bulk optodes contains only one lipophilic, chromo- or fluorophoric complexing agent that responds to the extraction of neutral species or to the coextraction of cations and anions. Such optodes do not have potentiometric equivalents. In contrast to ISEs, the response of bulk optodes to single salt solutions has always been fitted to equations derived on the basis of all equilibria involved, whereas their response to mixed salt solutions was originally described by an

#### Neutral Carrier-Based Ion-Selective Optode



#### Charged Carrier-Based Ion-Selective Optode



#### Ion-Exchanger-Based Ion-Selective Optode

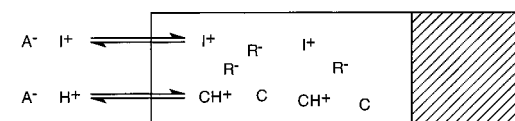


**Figure 5.** Schematic view of the equilibria between sample and bulk optode membrane containing a neutral  $H^+$ -selective chromoionophore C and (top) an electrically neutral carrier L with anionic sites  $R^-$ , (center) a charged carrier  $L^-$ , and (bottom) a cation exchanger  $R^-$ .

equation similar to that of Nicolskii–Eisenman.<sup>39</sup> A thermodynamically correct definition was introduced later.<sup>40</sup> A unique feature of the ISEs and bulk optodes discussed in this review is that the signal obtained depends on the *activity* of the target ion. For ISEs, local thermodynamic equilibrium at the sample–membrane interface is assumed, which results in a direct dependence of the interfacial potential on the sample activity. The bulk of optode films, on the other hand, is assumed to be in equilibrium with the sample. This equilibrium process depends, again for thermodynamic reasons, on ion activities and not concentrations. Both of the above statements seemingly contradict the thermodynamic principle that single-ion activities cannot be measured. However, in both cases, an extrathermodynamic assumption is involved: For ISEs, the potential of the reference half-cell is supposed to be sample-independent, while for optodes, the pH or in rarer cases the activity of another reference ion in the sample solution is assumed to be known.<sup>41,42</sup>

Section II of this review gives a summary of the relevant theoretical background. Emphasis is laid on simple and readily comprehensible formulations. For the first time, ISE and bulk optode theories are discussed in parallel with regard to all relevant analytical parameters, i.e., response function, selectivity, detection limits, and interferences. It is shown that an intimate relationship exists between the potentiometric and optical techniques in spite of basic differences between them. Indeed, the measured electromotive force of a cell containing an ion-selective electrode primarily depends on the potential change across the interface of the sample and membrane phase. While extraction processes are primarily used to describe deviations from ideal behavior, a Nernstian response is only observed if the organic phase boundary concentrations are not significantly altered as a function of the sample concentration.

Owing to this phase boundary behavior, the ISE response is mainly dictated by localized surface phenomena. On the other hand, optodes rely on concentration changes within the bulk of the sensing film, and the optical response itself can be rigorously described by bulk extraction processes. The underlying response mechanisms of both sensing schemes are therefore in many ways complementary. Section III deals with the demands on the various components used in both types of sensing films. Finally, part 2<sup>6</sup> will present a selection of important sensors, both from a historical and analytical perspective. The list is bound to be incomplete since a comprehensive documentation of published sensors<sup>43</sup> would be beyond the scope of this review.

The sensing elements described can be implemented in many different ways, i.e., in macro-, mini-, and microelectrodes, flow-through systems, and field effect transistors on one side and by using absorbance, fluorescence, evanescent wave, and refractive index measurements with various possible configurations of wave-guides on the other. Microelectrodes have been used for many years to assess ion activities in single living cells. More recently they have been applied as detectors for HPLC and capillary zone electrophoresis with detection volumes on the order of femtoliters. Disposable arrays, paper strips, and all solid-state devices are examples for various practical realizations. Although these technical aspects are not discussed here, it must be kept in mind that the principles presented are also unique with respect of the versatility of the sensors which can be constructed.

## II. Characteristics of Potentiometric and Optical Sensors

### 1. Ion-Selective Electrodes

#### A. Response Mechanism

The basic theory of the response of solvent polymeric membrane electrodes was developed many decades ago.<sup>29,31,32,44,45</sup> However, the relevance of the various contributions to the membrane potential has been the subject of long-lasting debates.<sup>33,46</sup> Only since it had been fully recognized that such membranes have intrinsic cation-exchange properties could very intuitive models be developed. Indeed, neutral-carrier-based membranes with poly(vinyl chloride) as membrane matrix without the addition of lipophilic ionic sites have been shown to give cationic response only because of anionic impurities present in the membrane.<sup>44,47,48</sup> In fact, membranes based on rigorously purified membrane components yielded ISEs that, even with the extremely selective valinomycin as neutral ionophore, had completely lost their cation permselectivity,<sup>49,50</sup> showing that the presence of ion-exchanger sites is crucial for the functioning of these sensors.

Ion-selective electrode membranes are typically investigated under zero-current conditions in a galvanic cell such as the following (see Figure 1):

Hg | Hg<sub>2</sub>Cl<sub>2</sub> | KCl(sat.) : 3 M KCl :: sample solution || liquid membrane || internal filling solution | AgCl | Ag.

**Table 2. Liquid Junction Potentials (in mV) for Various Sample and Bridge Electrolytes As Calculated According to the Henderson Equation<sup>51</sup>**

sample	liquid junction potentials <sup>a</sup>				
	1 M KNO <sub>3</sub>	1 M LiOAc	1 M NaCl	3 M KCl	10 <sup>-3</sup> M KCl
10 <sup>-1</sup> M HCl	-7.2	-12.4	-17.4	-4.5	-93.9
10 <sup>-3</sup> M HCl	3.7	-2.6	-28.4	-1.3	-25.2
10 <sup>-1</sup> M NaCl	3.0	0.8	-11.5	-0.1	22.4
10 <sup>-3</sup> M NaCl	4.7	-2.5	-33.0	-1.4	3.8
10 <sup>-1</sup> M CaCl <sub>2</sub>	4.8	4.1	-6.2	-1.0	45.1
10 <sup>-3</sup> M CaCl <sub>2</sub>	4.4	-2.2	-29.9	-1.2	10.4
10 <sup>-1</sup> M NaOH	6.8	7.0	-4.4	1.9	76.2
10 <sup>-3</sup> M NaOH	4.5	-2.1	-30.3	-1.2	17.0

<sup>a</sup> Small values are observed if the bridge electrolyte is concentrated and the mobilities of the cation and anion are similar (e.g., 1 M LiOAc or 3 M KCl).

The electromotive force (emf) across this cell is the sum of all individual potential contributions. Many of these are sample-independent, and the measured emf can usually be described as

$$\text{emf} = E_{\text{const}} + E_J + E_M \quad (1)$$

where  $E_M$  is the membrane potential, and  $E_J$  is the liquid junction potential at the sample/bridge electrolyte interface, which can either be kept reasonably small and constant under well-defined conditions or be estimated according to the Henderson formalism (for typical values, see Table 2).<sup>51</sup> It is important to note that it is this liquid junction potential that prohibits the true assessment of single ion activities with ion-selective electrodes; the role of the reference electrode on the overall emf measurement should, therefore, not be overlooked.<sup>52</sup> On the other hand, galvanic cells without liquid junctions (i.e., containing two ion-selective electrodes) respond to ratios or products of ion activities, again prohibiting single ion activity measurements. In this work, however, we will only focus on the membrane potential  $E_M$  of one electrode which is ideally a function of the sample ion activity.

**Phase Boundary Potential.** Since the membrane is usually interposed between the sample and an inner reference electrolyte, it is common to divide the membrane potential  $E_M$  into three separate potential contributions, namely the phase boundary potentials at both interfaces and the diffusion potential within the ion-selective membrane.<sup>31,32,53</sup> While the potential at the membrane/inner filling solution interface can usually be assumed to be independent of the sample, the diffusion potential within the membrane may become significant if considerable concentration gradients of ions with different mobilities arise in the membrane. Historically, there have been some debates about the relevance of the membrane diffusion potential.<sup>46</sup> While one reason was that no obvious explanation could be found for the observed permselectivity, another was the excellent correlation between the potentiometric and transport selectivities of such membranes. As a consequence, rather complex models have been used<sup>29</sup> that often make an intuitive understanding difficult.

Recently, various pieces of experimental evidence have, however, been collected which show that the

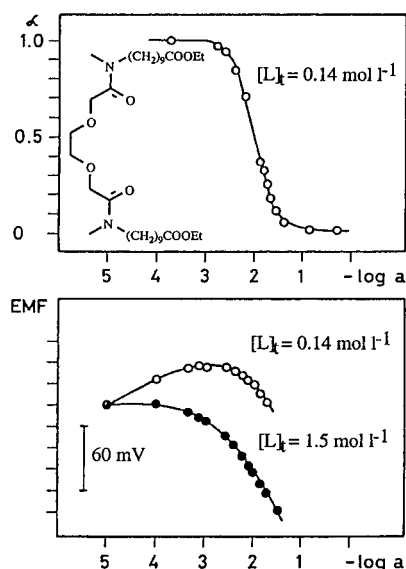


**Figure 6.** Correlation between salt extraction and potential response of a PVC-*o*-NPOE membrane based on a  $\text{Ca}^{2+}$ -selective ionophore:<sup>55,56</sup> top, degree of complexation ( $\alpha = [L]/[L]_t$ ) as a function of the aqueous  $\text{Ca}(\text{SCN})_2$  concentration, obtained from  $^{13}\text{C}$ -NMR spectra of the membrane; bottom, EMF-response of two membranes with different ligand concentrations. The cationic response of the electrode turns to an anionic one (bottom) in the concentration range above ca.  $10^{-2}$  M, where the coextraction of  $\text{Ca}(\text{SCN})_2$  from the aqueous to the membrane phase is strong (top).

diffusion potential is negligible in most cases of practical relevance<sup>33,35,54</sup> and that the cation permselectivity of PVC-based membranes without ionic additives can be explained by the presence of anionic impurities from the polymer matrix.<sup>47–50</sup> As it turns out, the phase boundary potential model can be used to describe the response of carrier-based ion-selective electrodes very accurately. This model provides straightforward results if ion activities in the membrane phase are approximated by concentrations so that simple relationships for mass balances and electroneutrality can be used. This formalism was applied earlier by Morf and others to predict the optimum amount of lipophilic ionic sites to be added to the membrane.<sup>55,56</sup> It also correlates well with findings from NMR (cf. Figure 6),<sup>57,58</sup> IR,<sup>34</sup> and UV/vis<sup>35</sup> experiments as well as impedance measurements<sup>59</sup> which show a massive coextraction of  $\text{I}^+\text{X}^-$  into the PVC membrane at concentrations where the interference from lipophilic counterions  $\text{X}^-$  in  $\text{I}^+$ -selective electrodes occurs.

For ion-selective electrodes, the membrane internal diffusion potential is zero if no ion concentration gradients occur. This is often the case for membranes that show a Nernstian response. For the sake of simplicity, diffusion potentials are treated here as secondary effects in other cases as well and are neglected in the following discussion. We therefore postulate:

$$E_M = E_{\text{const}} + E_{\text{PB}} \quad (2)$$

where  $E_{\text{PB}}$  is the phase boundary potential at the membrane-sample interface, which can be derived from basic thermodynamical considerations. First,

the electrochemical potential,  $\tilde{\mu}$ , is formulated for the aqueous phase:<sup>60</sup>

$$\tilde{\mu}(\text{aq}) = \mu(\text{aq}) + zF\phi(\text{aq}) = \mu^0(\text{aq}) + RT \ln a_1(\text{aq}) + zF\phi(\text{aq}) \quad (3)$$

and for the contacting organic phase:

$$\tilde{\mu}(\text{org}) = \mu(\text{org}) + zF\phi(\text{org}) = \mu^0(\text{org}) + RT \ln a_1(\text{org}) + zF\phi(\text{org}) \quad (4)$$

where  $\mu$  is the chemical potential ( $\mu^0$  under standard conditions),  $z$  is the valency and  $a_1$  the activity of the uncomplexed ion I,  $\phi$  is the electrical potential, and  $R$ ,  $T$  and  $F$  are the universal gas constant, the absolute temperature and the Faraday constant. It is now assumed that the interfacial ion transfer and complexation processes are relatively fast and that, therefore, equilibrium holds at the interface so that the electrochemical potentials for both phases are equal. This leads to a simple expression for the phase boundary potential:<sup>60</sup>

$$E_{\text{PB}} = \Delta\phi = -\frac{\mu^0(\text{org}) - \mu^0(\text{aq})}{zF} + \frac{RT}{zF} \ln \frac{a_1(\text{aq})}{a_1(\text{org})} \quad (5)$$

Often, the term comprising of the standard chemical potentials is combined to the symbol  $k_1$ ; i.e.,  $k_1 = \exp\{(\mu^0(\text{aq}) - \mu^0(\text{org}))/RT\}$ . Apparently, a simple function of the phase boundary potential on sample ion activities is expected if  $a_1(\text{org})$  is not significantly altered by the sample. Complexation reactions with a lipophilic neutral carrier within the organic membrane phase influence  $a_1(\text{org})$  and, therefore, also the phase boundary potential. This is demonstrated in Figure 7 where the emf responses of different solid contact PVC membranes are shown as a function of the concentration of the ion carrier.<sup>49</sup> Due to strong complexation with the carrier, the concentration of the free ion in the membrane is small relative to that of the complex. Consequently, the concentration of the complex is approximately equal to that of the anionic sites and remains unaltered if an excess of carrier is added. The excess carrier concentration is, therefore, inversely proportional to the activity of the free cations in the membrane. In accordance to eq 5, this increases the potential by  $RT/zF$ , i.e. by 59.2 mV for  $z = 1$  at 298 K, for every 10-fold concentration increase of carrier. Such an effect is not detectable with classical ion-selective electrodes (cf. Figure 1) since the change of activity influences the membrane potential at the inner filling solution simultaneously. Therefore, a polymeric solid contact electrode was used in which the membrane adheres on the internal reference electrode.<sup>49</sup>

The fundamental equation 5 will be used throughout this work to describe the behavior of ion-selective electrode membranes. By combining eqs 5 and 2 one obtains

$$E_M = E_{\text{const}} + E_{\text{PB}} = E_{\text{const}} - \frac{\mu^0(\text{org}) - \mu^0(\text{aq})}{zF} - \frac{RT}{zF} \ln a_1(\text{org}) + \frac{RT}{zF} \ln a_1(\text{aq}) \quad (6)$$

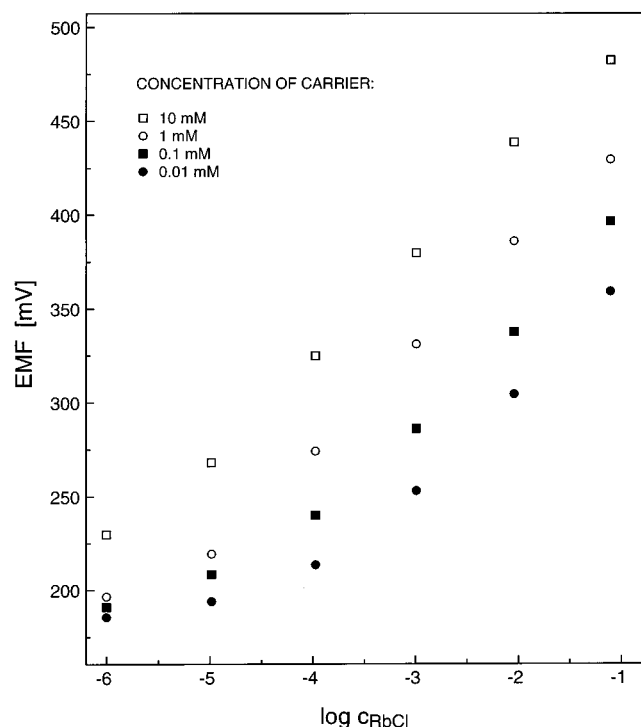


**Figure 7.** Potentiometric responses of analogous PVC–dibutylphthalate membranes with different concentrations of the ionophore 5-[[2,3-bis(octadecyloxy)-1-propyl]oxy]-4,4'-azobis(benzo-15-crown-5).<sup>47</sup> A 10-fold increase of the carrier concentration increases the potential by about 59 mV.

Under the condition that  $a_1(\text{org})$  remains unaltered, it can, together with all other sample-independent potential contributions, be included in one term ( $E^0$ ) and eq 6 reduces to the well-known Nernst equation:

$$E_M = E^0 + \frac{RT}{zF} \ln a_1(\text{aq}) \quad (7)$$

According to eq 6 it is evident that the composition of the surface layer of the membrane contacting the sample must be kept constant in order to obtain an exact Nernstian response of the electrode.<sup>61</sup> Only within the extremely thin charge separation layer at the very interface, where electroneutrality does not hold, are sample-dependent changes in the concentrations of complex and ionophore and ionic sites allowed to occur.<sup>61</sup> Nevertheless, if eq 5 is valid, the exact structure of this space charge region is not really relevant to the sensor response. To achieve a constant composition of the membrane bulk, several conditions must be met:

(1) The membrane must have ion-exchanger properties. The simultaneous coextraction equilibrium of sample counterions occurs according to the following reaction:  $\text{I}^+(\text{aq}) + \text{X}^-(\text{aq}) \rightleftharpoons \text{I}^+(\text{org}) + \text{X}^-(\text{org})$ . The major factor determining  $a_1(\text{org})$  is the presence of a lipophilic ion-exchanger within the membrane, and hence, the concentration of extracted anions  $\text{X}^-(\text{org})$  is insignificant. This characteristic is, somewhat misleadingly, called permselectivity. If, however, the concentration of the lipophilic ion exchanger is small relative to that of  $\text{X}^-(\text{org})$ , the concentration of primary ions in the organic phase,  $a_1(\text{org})$ , is roughly proportional to  $a_1(\text{aq})$  and the electrode does not respond to ion activity changes in a Nernstian way.<sup>45,49,50</sup>

(2) The membrane must be sufficiently hydrophobic in nature to prohibit substantial coextraction of sample counterions according to the reaction shown under condition 1. This allows one to measure samples with high electrolyte concentrations. Clearly, hydrophilic polymers such as hydrogels<sup>62</sup> are not suited as membrane bulk materials for ion-selective electrodes.

(3) If ion-exchange reactions with interfering ions of the same charge type occur, the activity  $a_1(\text{org})$  of the uncomplexed analyte ion in eq 7 is decreased and a sub-Nernstian mixed ion response is expected.<sup>36</sup> This can be prevented by incorporating a lipophilic complexing ligand (ionophore or carrier) in the membrane that selectively binds the target analyte ion.

(4) However, the ligand employed should not bind to the analyte ion too tightly, since then coextraction of  $\text{I}^+(\text{aq})\text{X}^-(\text{aq})$  increases  $a_1(\text{org})$  and leads to a breakdown of the permselectivity of the membrane. This effect is increasingly likely at high activity and lipophilicity of the sample electrolyte and is known as Donnan failure (cf. Figure 6).

(5) Other (electrically neutral) interfering species that can be extracted into the membrane and alter  $a_1(\text{org})$  must not be present in the sample. Examples for this effect include the complexation of analyte ions by neutral surfactants in tetraphenylborate based membranes<sup>63</sup> or in certain pH-selective electrodes,<sup>64</sup> where the binding of the surfactant with the electroactive species alters  $a_1(\text{org})$  and, therefore, the cell potential significantly. Similarly, the extraction of higher alcohols into valinomycin-based membranes has been shown to induce considerable emf shifts,<sup>65</sup> probably due to changes in the complex formation constant of valinomycin in the now altered matrix. The observed uptake of homogenous water into ion-selective membranes,<sup>66</sup> although not yet studied extensively, is expected to have similar effects (see also section III.2.C), especially in an asymmetric setup such as with solid contact electrodes, where this influence cannot be counterbalanced at the second membrane/aqueous solution interface.

While the permselectivity of the membrane is guaranteed by its ion-exchange properties and hydrophobicity, which prohibits substantial coextraction of counterions, it is the selective complexation of the analyte ion by a ligand, the so-called ion carrier or ionophore, in the organic phase that ensures that the membrane responds selectively to the target ion within a complicated sample matrix. In Figure 8, a classification of such selective ligands based on their charge type is presented. Since the widely used uncharged carriers are neutral when uncomplexed and the complexes have the same charge as the analyte ion, the respective membranes require the additional incorporation of lipophilic ions of opposite charge to ensure permselectivity. In practice, alkali salts of tetraphenylborate derivatives are used for cation-selective membranes and tetralkylammonium salts for anion-selective membranes. Since poly(vinyl chloride) as membrane matrix already contains ionic impurities with cation-exchanger properties, neutral-carrier-based cation-selective membranes are usually functional without the incorporation of anionic sites. However, their selectivity and lifetime behavior is

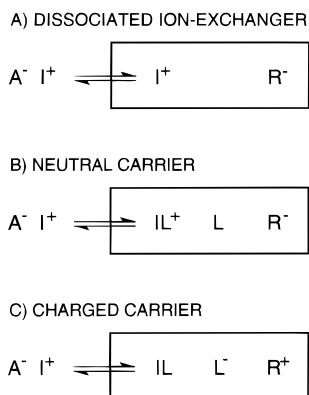


**Figure 8.** Classification of ion-selective membranes (shown for cationic analytes).

often not optimal. To a second important group of ionophores belong compounds that are electrically charged when uncomplexed and neutral when ligated to the analyte ion (see Figure 8). Important representatives of such carriers are metalloporphyrins and cobyrinates that bind selectively to anions by axial ligation of the metal center. With charged carriers, permselectivity can be achieved without the incorporation of additional ionic sites, e.g., with pure organic solvents as membranes.<sup>67,68</sup> However, as recently shown, the selectivity is only optimal for membranes containing ionic sites of the same charge type as the analyte ion, so that ionic sites of opposite charges are required for neutral and charged carriers.<sup>69–71</sup> More recently, carriers have been identified that cannot be easily fitted into one of these two general categories. Some of these are apparently insensitive to small amounts of added anionic or cationic sites in the membrane. While the exact carrier mechanism varies from case to case, these ionophores are now often called mixed-mode carriers. Examples for such carriers include the classical  $Ca^{2+}$  ionophore bis[4-(1,1,3,3-tetramethylbutyl)phenyl] phosphate<sup>72</sup> as well as a range of anion carriers.<sup>73</sup>

### B. Selectivity

The selectivity is clearly one of the most important characteristics of a sensor, as it often determines whether a reliable measurement in the target sample is possible. It is especially critical in clinical applications where for whole blood or serum measurements the allowed emf deviation (error) may sometimes not be larger than 0.1 mV.<sup>74</sup> A theoretically thorough selectivity description allows researchers to identify the key parameters for optimizing the performance of potentiometric sensors, e.g., by adjusting weighing parameters (i.e., absolute membrane concentrations) or choosing different plasticizers or matrices.<sup>55,69</sup>

Virtually all selectivity considerations were based in the past on the semiempirical Nicolskii–Eisenman equation.<sup>43</sup> In this section, we will demonstrate, on one hand, both the limitations and inaccuracies of that equation and, on the other, the usefulness of the Nicolskii coefficient itself. On the basis of the phase boundary potential model (eq 5), a new and more rigorous description of the mixed ion response of solvent polymeric membrane ISEs has been derived recently.<sup>36</sup> This new formalism allows a clear interpretation of the matched potential method introduced

by Christian<sup>75</sup> and also includes an earlier selectivity treatment of one specific case by Morf that had never found its way into general practice.<sup>76,77</sup>

**The Nicolskii–Eisenman Formalism.** Under ideal conditions, the electrode response function follows the Nernst equation

$$E = E_1^0 + \frac{RT}{z_1 F} \ln(a_1(I)) \quad (8)$$

where  $a_1(I)$  is the primary ion activity in the sample without interference from other sample ions. The constant potential contributions (see eq 6) are unique for every ion measured and included in  $E_1^0$ . According to the Nicolskii–Eisenman formalism,<sup>21,78</sup> the activity term in the Nernst equation is replaced by a sum of selectivity-weighted activities

$$E = E_1^0 + \frac{RT}{z_1 F} \ln(a_1(IJ) + K_{IJ}^{\text{pot}} a_j(IJ)^{z_1/z_j}) \quad (9)$$

where  $a_1(IJ)$  and  $a_j(IJ)$  are the activities of I and J in the mixed sample. The activity  $a_1(I)$  can be related to  $a_1(IJ)$  of the mixed sample that gives the same potential E by combining eqs 8 and 9:

$$a_1(I) = a_1(IJ) + K_{IJ}^{\text{pot}} a_j(IJ)^{z_1/z_j} \quad (10)$$

For extremely selective electrodes, the Nicolskii coefficient  $K_{IJ}^{\text{pot}}$  is very small and  $a_1(IJ)$  approaches  $a_1(I)$ . If interference is observed, a lower activity  $a_1(IJ)$  of the mixed sample will give the same response as the activity  $a_1(I)$  of a solution containing no interfering ions.

The Nicolskii coefficient is often determined by the so-called separate solution method by comparing two solutions, each containing a salt of the primary and interfering ion only. If both samples induce the same emf, eq 10 may be further simplified ( $a_1(IJ) = 0$ , and therefore  $a_j(IJ) = a_j(J)$ ) to give the following after rearranging:

$$K_{IJ}^{\text{pot}} = \frac{a_1(I)}{a_j(J)^{z_1/z_j}} \quad (11)$$

A different method is the fixed interference method (see below), where calibration curves for the primary ion are determined in a constant background of interfering ions. However, even in this case, two separate Nernst sections of the calibration curve, each relating to ranges where only one ion is potential-determining, are used to calculate the Nicolskii coefficient. Equation 11 can be brought to the following concentration-independent form by inserting the Nernstian equation 8 for both primary and interfering ion (where  $E_J^0$  is defined for the interfering ion in complete analogy to  $E_1^0$  for the primary ion according to eq 8):

$$K_{IJ}^{\text{pot}} = \exp\{(E_J^0 - E_1^0)z_1 F/RT\} \quad (12)$$

This shows that the Nicolskii coefficient,  $K_{IJ}^{\text{pot}}$ , as determined with separate solutions, is expected to be a constant parameter for a particular ISE. As long as the emf follows the Nernstian function for every



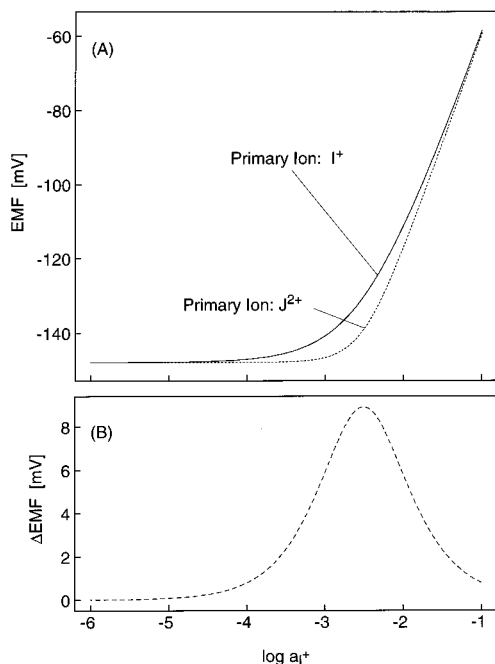


**Figure 9.** Top, calculated emf response function according to the Nicolskii–Eisenman equation (eq 9) as a function of  $\log a_I^+$  for a sample containing a constant background of  $J^{2+}$  if  $I^+$  (solid line) or  $J^{2+}$  if  $I^+$  (dotted line) is assumed to be the primary ion (parameters used:  $E_1^0 = 0$ ,  $\log K_{IJ}^{\text{pot}} = -1$ ,  $a_J(\text{IJ}) = 0.001 \text{ M} = \text{const}$ ); bottom, vertical distance between the two curves shown in the top part. The deviation shows the inconsistency of eq 9.

ion under consideration,  $K_{IJ}^{\text{pot}}$  should be independent of the sample activities. With these respects, the Nicolskii coefficient is indeed a useful characteristic of any particular ISE.

The Nicolskii–Eisenman formalism can be brought into the following compact form by combining eqs 10 and 11:

$$\frac{a_I(\text{IJ})}{a_I(\text{I})} + \left( \frac{a_J(\text{IJ})}{a_J(\text{J})} \right)^{z_I/z_J} = 1 \quad (13)$$

Again, this relationship shows that for ideally selective ISEs  $a_I(\text{I})$  equals  $a_I(\text{IJ})$ , i.e., identical primary ion activities in the absence and presence of interfering ions are expected to give the same membrane potential. If interference is observed, the Nicolskii–Eisenman equation predicts that  $a_I(\text{IJ}) < a_I(\text{I})$ ; i.e., too high potential readings are observed for the mixed sample. For extremely large interference by ions J, the electrode eventually becomes ideally responsive to  $a_J$ , and  $a_J(\text{J}) = a_J(\text{IJ})$ . Since  $a_I(\text{I})$  and  $a_J(\text{J})$  are separate sample activities giving the same potential  $E$ , interference will be increased for increasing interfering ion activities  $a_J(\text{IJ})$  and for decreasing  $a_J(\text{J})$ , i.e., when the electrode does not sufficiently discriminate against J. One serious drawback of eq 13 is, however, that for  $z_I \neq z_J$ , the Nicolskii–Eisenman equation is inconsistent, i.e., exchanging the indices for I and for J does not give identical analytical expressions (see Figure 9). Therefore, the predicted mixed ion response of an ion-selective electrode depends on which ion is treated as the primary and which as the interfering ion. This is a serious limitation of the Nicolskii–Eisenman equation that can lead to substantial errors in practice.

**New Selectivity Formalism: Mixed Electrode Response to Ions of Different Charge.** To remedy this situation, a formalism was recently developed that relies on the phase boundary potential model and phase transfer equilibria at the sample/membrane interface.<sup>36</sup> The general result can be expressed as follows:<sup>36</sup>

$$a_I(\text{I}) = a_I(\text{IJ}) + (K_{IJ}^{\text{pot}})^{z_I/z_J} a_I(\text{I})^{1-(z_I/z_J)} a_J(\text{IJ}) \quad (14)$$

This equation is a direct replacement of eq 10, which was obtained from the Nicolskii–Eisenman formalism. It is quite generally valid but cannot be applied to membranes where the concentration of free carrier significantly changes upon contact with interfering ion solutions. This situation is for example observed with highly optimized  $\text{Mg}^{2+}$ -selective electrodes, where the relative concentration of anionic sites is high. For these cases, extended equations have been suggested that are not discussed in this review.<sup>79</sup> The formalism presented here assumes that mass and charge balances are not altered as a function of time due to membrane inhomogeneities or gradients of total membrane concentrations. Again, such adverse effects are also more likely with membranes containing only a small excess of free carrier.<sup>79</sup> Recently, an alternative mathematical route was presented to describe the mixed-ion response of solvent polymeric membrane electrodes, and the result was effectively identical to the one discussed here.<sup>80</sup>

For ions of the same charge, the new formalism gives the same result as the Nicolskii–Eisenman equation:

$$a_I(\text{I}) = a_I(\text{IJ}) + K_{IJ}^{\text{pot}} a_J(\text{IJ}) \quad (15)$$

The new formalism still makes use of the Nicolskii coefficient, which is, theoretically, independent of sample solution conditions (see above). Therefore, it is still most useful in characterizing ISE selectivities in tabular form. Equation 14 can be brought into an analytically intuitive form in several ways. One possibility is to introduce a new selectivity factor,  $k_{IJ}^{\text{psel}}$ :

$$k_{IJ}^{\text{psel}} = \frac{a_I(\text{I})}{a_J(\text{J})} \quad (16)$$

to yield the following after inserting into eqs 8, 11, and 14:

$$E_1 = E_1^0 + \frac{RT}{z_1 F} \ln(a_I(\text{IJ}) + k_{IJ}^{\text{psel}} a_J(\text{IJ})) \quad (17)$$

If ions of different charge are compared, the selectivity factor  $k_{IJ}^{\text{psel}}$  is, in contrast to the Nicolskii coefficient  $K_{IJ}^{\text{pot}}$ , not a constant parameter of a particular electrode since the separate calibration curves are not parallel (see eq 8 and Figure 10). For this reason, it would be very difficult to compare reported  $k_{IJ}^{\text{psel}}$  values from different sources if the experimental conditions are not exactly known. Tabulation of such values is, therefore, not encouraged and reporting of Nicolskii coefficients should be generally preferred.

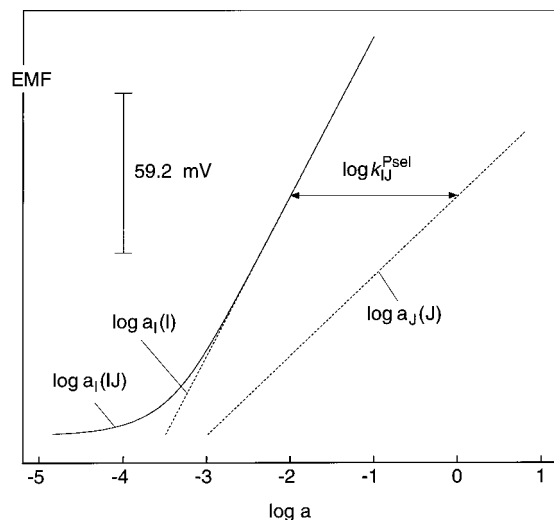


**Figure 10.** Calculated electrode responses as a function of primary ( $\log a_I(I)$ ) and interfering ( $\log a_J(J)$ ) ion alone and toward the primary ion with a constant interfering ion background of 0.001 M according to eqs 15 and 16.

The most compact form of the new selectivity formalism can be obtained as follows by directly substituting  $K_{IJ}^{\text{pot}}$  in eq 14 via eq 11:

$$\frac{a_I(IJ)}{a_I(I)} + \frac{a_J(IJ)}{a_J(J)} = 1 \quad (18)$$

This equation can now be directly compared to eq 13, which was obtained from the Nicolskii–Eisenman formalism. Qualitatively, most considerations discussed for eq 13 apply here as well. However, in contrast to eq 13, a permutation of the indices for I and J in the new formalism does not change the analytical expression in any way so that eq 18 yields consistent results also for ions of different charge.

Unfortunately, eq 14 is an implicit equation so that different explicit solutions have to be derived for every particular combination of  $z_I$  and  $z_J$ . This is accomplished by solving eq 14 for  $a_I(I)$  and inserting the result in eq 8. Explicit response functions are given here for some important cases:

for  $z_I = 1$  and  $z_J = 2$  (see Figure 11)

$$E = E_1^0 + \frac{RT}{F} \ln \left( \frac{a_I(IJ)}{2} + \frac{1}{2} \sqrt{a_I(IJ)^2 + 4a_J(IJ)(K_{IJ}^{\text{pot}})^2} \right) \quad (19)$$

for  $z_I = 2$  and  $z_J = 1$  (see Figure 12)

$$E = E_1^0 + \frac{RT}{F} \ln \left( \sqrt{a_I(IJ) + \frac{1}{4}K_{IJ}^{\text{pot}} a_J(IJ)^2} + \sqrt{\frac{1}{4}K_{IJ}^{\text{pot}} a_J(IJ)^2} \right) \quad (20)$$

For trivalent ions, explicit solutions can be obtained as well. For simplicity, the symbol  $u$  stands here for

$$u = a_J(K_{IJ}^{\text{pot}})^{z_I/z_J} \quad (21)$$

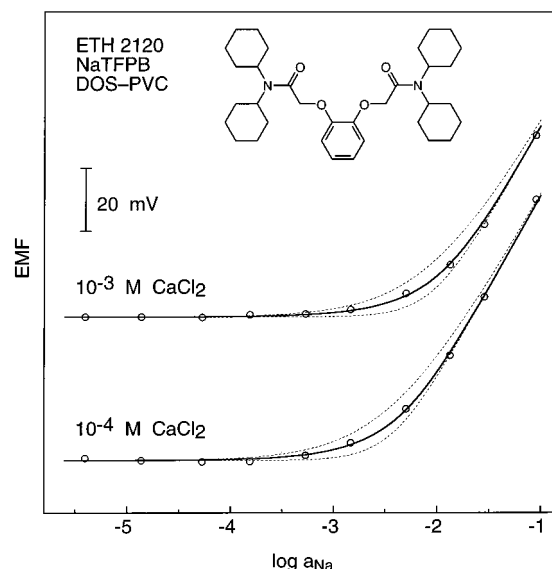


**Figure 11.** Electrode response to NaCl in a background of 0.001 or 0.0001 M  $\text{CaCl}_2$ , for a sodium ion-selective electrode.<sup>36</sup> The solid line is plotted according to eq 19; the dotted lines are plotted according to eq 9 if  $\text{Na}^+$  (upper curve) or  $\text{Ca}^{2+}$  (lower curve) is assumed to be the primary ion.

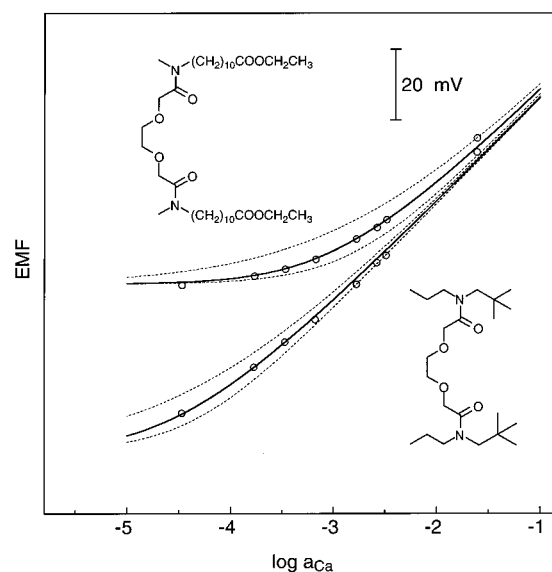


**Figure 12.** Electrode response to  $\text{CaCl}_2$  in a background of 0.150 M NaCl, 0.003 M KCl and 0.001 M  $\text{MgCl}_2$  for two calcium-selective electrodes.<sup>77</sup> The solid line is plotted according to eq 20; the dotted lines according to eq 9 if  $\text{Na}^+$  (upper curve) or  $\text{Ca}^{2+}$  (lower curve) is assumed to be the primary ion.

Accordingly, the following relationships are obtained

for  $z_I = 1$  and  $z_J = 3$

$$E = E_1^0 + \frac{RT}{F} \ln \left( \frac{a_I}{3} + \frac{a_I^2}{9b^{1/3}} + b^{1/3} \right) \quad (22)$$

with

$$b = \frac{u}{2} + \frac{a_I^3}{27} + \sqrt{\frac{u^2}{4} + \frac{ua_I^3}{27}} \quad (23)$$

for  $z_I = 2; z_J = 3$

$$E = E_1^0 + \frac{RT}{2F} \ln \left( \frac{2a_1}{3} + \frac{a_1^2}{9b^{1/3}} + b^{1/3} \right) \quad (24)$$

with

$$b = \frac{u^2}{2} - \frac{a_1^3}{27} + \sqrt{\frac{u^4}{4} + \frac{u^2 a_1^3}{27}} \quad (25)$$

for  $z_I = 3; z_J = 2$

$$E = E_1^0 + \frac{RT}{3F} \ln \left( a_1 + \frac{u^3}{3b^{1/3}} + b^{1/3} \right) \quad (26)$$

with

$$b = \frac{u^3 a_1}{2} + \sqrt{\frac{u^6 a_1^2}{4} - \frac{u^9}{27}} \quad (27)$$

for  $z_I = 3; z_J = 1$

$$E = E_1^0 + \frac{RT}{3F} \ln \left( \frac{u^3 + 3a_1}{3} + \frac{u^6 - 6u^3 a_1}{9b^{1/3}} + b^{1/3} \right) \quad (28)$$

with

$$b = \frac{u^9}{27} + \frac{u^6 a_1}{3} + \frac{u^3 a_1^2}{2} + \sqrt{\frac{u^9 a_1^3}{27} + \frac{u^6 a_1^4}{4}} \quad (29)$$

Equations 19–29 quantitatively describe the mixed ion response in the range of cation interference, but are relatively cumbersome to use since a different relationship applies for every charge pair considered. In practice it would be desirable to use a general explicit equation that describes the response function in the presence of interfering ions independent of the charges  $z_I$  and  $z_J$ . This can be accomplished for relatively small interference (ca. 10%), where  $a_I(I)$  on the left hand side of eq 14 is nearly equal to  $a_I(IJ)$ ; i.e.,  $a_I(I) \approx a_I(IJ)$ . In this case, eq 14 can be approximated by<sup>36</sup>

$$a_I(I) = a_I(IJ) + (K_{IJ}^{\text{pot}})^{z_I/z_J} a_I(IJ)^{1-(z_I/z_J)} a_J(IJ) \quad (30)$$

which, after inserting into eq 8, gives the explicit response function of the ISE when interference is small:

$$E = E_1^0 + \frac{RT}{z_I F} \ln(a_I(IJ) + (K_{IJ}^{\text{pot}})^{z_I/z_J} a_I(IJ)^{1-(z_I/z_J)} a_J(IJ)) \quad (31)$$

In Figure 13, the theoretical response functions according to Nicolskii–Eisenman (eq 9), the exact equation (eq 19), and the approximation for small interference (eq 31) are shown for one particular charge set ( $z_I = 1$  and  $z_J = 2$ ). While the simplified function describes the initial range of interference much more accurately than the Nicolskii–Eisenman equation, it cannot be used to describe the full measuring range. According to the approximate eq

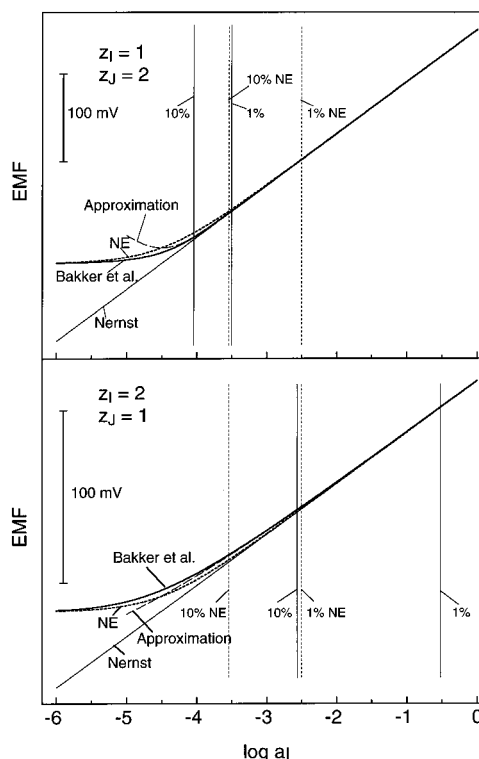


**Figure 13.** Response functions of a monovalent (top) and divalent (bottom) ion-selective electrode calculated by the Nicolskii–Eisenman equation (NE; eq 9), by the more exact model of Bakker et al. (eq 19 and 20, respectively), and with the approximation for small interference (eq 31). The values of the selectivity factors are  $\log K_{IJ}^{\text{pot}} = -4.00$  and  $-2.51$ , respectively. Vertical lines show the activities for 1 and 10% errors if the Nicolskii–Eisenman or the approximate model is used instead of the exact formalism.

31, no Nernstian electrode response toward  $a_J$  would be observed if no primary ions  $I^{z_I+}$  were present in the sample. Therefore, the approximation (eq 31) should only be used to describe the activity range of small interference. Overall, the formalism based on the phase boundary potential model predicts smaller deviations from the Nernstian response for monovalent primary and divalent interfering ions as compared to the Nicolskii–Eisenman equation and larger ones for divalent primary and monovalent interfering ions. This discrepancy has also been observed experimentally (see Figures 11 and 12) and is quantified below.

**Required Nicolskii Coefficients for Measurement in Mixed Ion Solutions According to the New Selectivity Formalism.** On the basis of eq 31 a simple general expression can be derived that calculates the required Nicolskii coefficient for a given target sample containing  $a_I(IJ)$  and  $a_J(IJ)$  and a specified maximum tolerable error  $p_{IJ}$  in percent, which is valid as long as  $p_{IJ}$  is smaller than about 10%.<sup>36</sup>

$$K_{IJ}^{\text{pot}}(\text{required}) = \frac{a_I(IJ)}{a_J(IJ)^{z_I/z_J}} \left( \frac{p_{IJ}}{100} \right)^{z_I/z_J} \quad (32)$$

Equation 32 can be conveniently used in practice to assess the feasibility of a specified measurement with a given ion-selective electrode. It is significantly different from the one used traditionally, which was

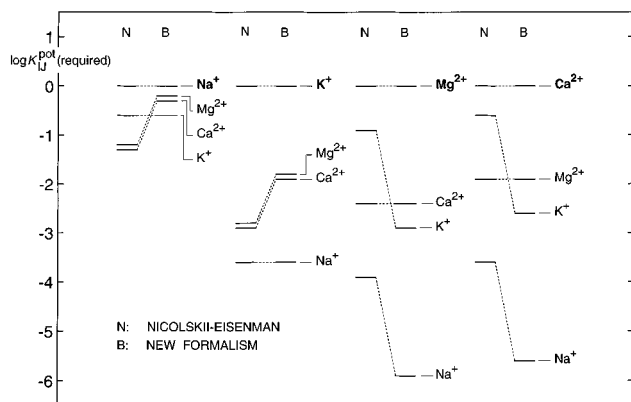


**Figure 14.** Required Nicolskii coefficients according to the Nicolskii–Eisenman equation (eq 9, indicated with N) and the new formalism (eq 19 or 20, B) for measurements of  $\text{Na}^+$ ,  $\text{K}^+$ ,  $\text{Mg}^{2+}$ , and  $\text{Ca}^{2+}$  in undiluted whole blood or serum, if a maximum tolerable error of 1% in the determination of the analyte ion activity is assumed.

derived on the basis of the Nicolskii–Eisenman equation<sup>74</sup> and yields required values that differ sometimes by many orders of magnitude depending on the charges of the ions compared (see Figure 14).<sup>36</sup> This significant discrepancy of required selectivity coefficients originates in the differing formulations of the mixed ion response of ion-selective electrodes and depends on the level of allowed interference.

**Influence of Membrane Compositions on the Nicolskii Coefficient: Optimization of Membrane Selectivity.** In the following, the influence of various membrane parameters on the selectivity coefficient is investigated. Such an analysis is helpful for optimizing the selectivity of ion-selective electrodes in view of a particular application. By combining the separate phase boundary potentials for the primary and the interfering ion with eq 11, the Nicolskii coefficient can be written as a function of the uncomplexed primary and interfering ion concentration in its most general form as follows

$$K_{IJ}^{\text{pot}} = K_{IJ} \frac{[\text{I}^{z_1^+}(\text{I})]}{[\text{J}^{z_2^+}(\text{J})]^{z_1/z_2}} \quad (33)$$

where  $K_{IJ}$  is the equilibrium constant for the ion-exchange between uncomplexed primary and interfering ions between the sample and organic phase:

$$K_{IJ} = \left( \frac{a_{\text{I}}(\text{aq})}{[\text{I}^{z_1^+}]} \right) \left( \frac{[\text{J}^{z_2^+}]}{a_{\text{J}}(\text{aq})} \right)^{z_1/z_2} \quad (34)$$

It is important to note that  $[\text{I}^{z_1^+}(\text{I})]$  and  $[\text{J}^{z_2^+}(\text{J})]$  in eq 33 are the concentrations of the ions in the phase boundary layer of the organic film when measured separately, i.e., when the respective organic layer contains either  $[\text{I}^{z_1^+}]$  or  $[\text{J}^{z_2^+}]$  and its complex. They are therefore not identical to the symbols shown in eq 34. In principle, these equations are valid on the basis of ion activities and not concentrations, because of the assumed phase boundary equilibrium. However, the use of concentrations for the organic phase allows one to obtain explicit results on the basis of complex formation constants, mass balances, and electroneutrality conditions for the two separate experimental situations. Accordingly, the selectivity

coefficient can be related to the total membrane concentrations, stability constants, and stoichiometric factors of the formed complexes. Successful examples of optimizing ISE selectivity by using this approach have been presented in the past.<sup>36,69,81,82</sup> One important example is shown here for membranes containing an electrically neutral carrier forming stable complexes with the respective ions. In this case, eq 33 can be extended by considering the overall complex formation constants  $\beta_{\text{IL},n_1}$  for the primary cation-carrier complex with the stoichiometric factor  $n_1$ ,

$$\beta_{\text{IL},n_1} = \frac{[\text{IL}_{n_1}^{z_1^+}]}{[\text{I}^{z_1^+}][\text{L}]^{n_1}} \quad (35)$$

and the respective complex formation constant  $\beta_{\text{JL},n_2}$  for the interfering ion, which is defined in complete analogy to eq 35, to give:

$$K_{IJ}^{\text{pot}} = K_{IJ} \frac{(\beta_{\text{JL},n_2})^{z_1/z_2}}{\beta_{\text{IL},n_1}} \frac{[\text{IL}_{n_1}^{z_1^+}(\text{I})]}{[\text{I}(\text{I})]^{n_1}} \left( \frac{[\text{L}(\text{J})]^{n_2}}{[\text{JL}_{n_2}^{z_2^+}(\text{J})]} \right)^{z_1/z_2} \quad (36)$$

Again, the concentrations of the complexed and the free carrier in the membrane relate to the two different experimental situations where only  $\text{I}^{z_1^+}$  or  $\text{J}^{z_2^+}$  partitions into the membrane, as indicated by (I) and (J) in eq 36. This equation can further be related to the membrane weighing parameters (i.e., absolute membrane concentrations of carrier and ionic sites) by inserting the respective charge and mass balances to obtain

$$K_{IJ}^{\text{pot}} = K_{IJ} \frac{(\beta_{\text{JL},n_2})^{z_1/z_2}}{\beta_{\text{IL},n_1}} \frac{R_{\text{T}}^-}{z_1[L_{\text{T}} - n_1(R_{\text{T}}^-/z_1)]^{n_1}} \times \left( \frac{z_2[L_{\text{T}} - n_2(R_{\text{T}}^-/z_2)]^{n_2}}{R_{\text{T}}^-} \right)^{z_1/z_2} \quad (37)$$

where  $L_{\text{T}}$  and  $R_{\text{T}}^-$  are the total membrane concentrations of carrier and anionic sites, respectively. For eq 37 to strictly hold, a number of simplifications are assumed: each ion is strongly complexed by the ionophore and forms a complex of only one stoichiometry. Furthermore, effects of ion pairing are neglected. Since these assumptions cannot be generally valid, eq 37 represents a rather qualitative relationship. Nonetheless, the influence of weighing parameters on the selectivity factor was successfully described with eq 37 in a recent investigation aimed at the quantification of ionic impurities of the membrane phase.<sup>83</sup> It is quite obvious from eq 37 that, in general, the selectivity coefficient, i.e. the Nicolskii coefficient, is not an equilibrium constant and not only depends on the stability constants of the involved ion–carrier complexes and relative lipophilicities of the uncomplexed sample ions but also on the total concentrations of ionic sites and ion carrier. Therefore, the selectivity-modifying influence of added ionic sites to carrier-based membranes can be well understood with eq 37 (see also section III.2.B. below).<sup>56</sup> Assuming that each ion forms a complex with one given stoichiometric factor only, an optimum concentration of anionic sites can be calculated for

**Table 3. Concentration of Anionic Sites ( $R_T^-$ ) in Neutral-Carrier-Based Cation-Selective Membranes Relative to Total Concentration of Ligand ( $L_T$ ) Inducing an Optimum Selectivity for the Ion I (charge  $z_i$ , ion/ligand stoichiometry of the complex  $n_i$ ) with Respect to the Interfering Ion  $J$ <sup>56</sup>**

I (analyte), $z_i$	J (interfering ion), $z_j$	stoichiometry of complex: ligand/ion (I or J)		ratio $R_T^-/L_T$ <sup>a</sup>
		$n_i$	$n_j$	
2	2	1	2	1.41
2	2	2	3	0.77
2	2	3	4	0.54
2	1	1	1	1.62
2	1	2	2	0.73
2	1	3	3	0.46
1	1	1	2	0.71

<sup>a</sup> Inducing optimal selectivity for analyte cation (I) with respect to interfering cation (J).

many cases (see Table 3). It is assumed that the stoichiometry of the complexes cannot change and, therefore, excess interfering ions remain uncomplexed. After extending eq 37 accordingly, the derivative of  $K_{IJ}^{\text{pot}}$  with respect to  $R_T^-$  is set equal to zero for the various stoichiometric factors  $n_i$  and  $n_j$  to obtain the optimal ionic site concentrations (see Table 3). These values have for example been extremely useful in the design of  $\text{Mg}^{2+}$ -selective sensors. Optimum  $\text{Mg}^{2+}$  selectivity over  $\text{Ca}^{2+}$  has been achieved when a hexadentate ionophore is forced to form 1:1 complexes with the divalent metal ion, since  $\text{Ca}^{2+}$  prefers higher coordination numbers. This is accomplished by incorporating a high amount of anionic sites into the membrane relative to total ionophore leaving only a small portion of the ionophore uncomplexed (see Table 3). However, the mixed ion response of such an electrode cannot be described by the simplified results discussed here. While an extended model has been proposed,<sup>79</sup> there is more recent evidence that this system is far more complicated and a variety of complexes with different stoichiometry are simultaneously present.<sup>84</sup> This makes it extremely difficult to model the expected response behavior without prior knowledge of all involved equilibria. Moreover, long-term potential drifts are often observed because the simultaneous extraction of the two ions induces a concentration gradient of uncomplexed ionophore that leads to a depletion of ionophore at the phase boundary of the membrane and the inner filling solution.<sup>79</sup> The concept of severely destabilizing the interfering ion with a high concentration of ionic sites has therefore its drawbacks, both from an empirical and descriptive view.

For the simple case of equal charge of the primary and interfering ion and equal stoichiometry of their complexes ( $z_i = z_j$  and  $n_i = n_j$ ), the selectivity coefficient is indeed an equilibrium constant and, therefore, independent of total ionophore and site concentrations, as eq 37 can then be simplified to:

$$K_{IJ}^{\text{pot}} = K_{IJ} \frac{\beta_{JL, n_j}}{\beta_{IL, n_i}} \quad (38)$$

In this case, the observed selectivity is directly proportional to the ratio of the stability constants of

the involved complexes. A thermodynamic cycle can be applied to relate the ion selectivity to the complex formation constants measured in polar solvents. In some cases, an excellent correlation between selectivity coefficients and the ratio of experimental complex formation constants has been observed.<sup>85,86</sup> A major drawback of this method, however, is that most ion carriers form extremely weak complexes in common polar solvents.<sup>87,88</sup> Therefore, a direct measurement of complex formation constants within the solvent polymeric membrane phase as introduced recently has been shown to yield more meaningful results.<sup>84</sup>

**Selectivity of Charged-Carrier-Based Ion-Selective Electrodes.** Recently, the above treatment of the Nicolskii coefficient has been extended for cation-selective membranes containing electrically charged carriers (see also section III.2.B below). For primary and interfering ions of equal charge and complexes of equal stoichiometry, the following relationship between the Nicolskii coefficient on one hand and equilibrium constants and weighing parameters on the other hand has been developed<sup>69</sup>

$$\log K_{IJ}^{\text{pot}} = \log \left( \frac{k_J \beta_{JL}}{k_I \beta_{IL}} \times \frac{R_T^+ \beta_{IL} + 1 - \sqrt{(R_T^+ \beta_{IL} + 1)^2 + 4\beta_{IL}(L_T - R_T^+)}}{R_T^+ \beta_{JL} + 1 - \sqrt{(R_T^+ \beta_{JL} + 1)^2 + 4\beta_{JL}(L_T - R_T^+)}} \right) \quad (39)$$

where  $R_T^+$  is the concentration of lipophilic cationic sites (see Figure 53). For anionic sites  $R_T^-$  instead of  $R_T^+$ , the appropriate equation is obtained by substituting  $R_T^+$  with  $-R_T^-$  in eq 39 (i.e.,  $R_T^+ \rightarrow -R_T^-$ ). For anion-selective sensors, the same relationships are valid after reversing the charge sign of all ionic species. Interestingly, eq 39 reduces only to eq 38, which allows one to determine conditions for optimum selectivity, if ionic sites of the same charge as the analyte ion are present in the membrane. If no ionic sites are present at all, the concentration of uncomplexed carrier will be determined by the dissociation constant of the complex. For discriminated ions, i.e. weaker complexes, this concentration will be larger than for the primary ion, and a less-than-optimal selectivity is observed. On the other hand, the presence of ionic sites of opposite charge as the analyte ion, as required for neutral carriers, forces uncomplexed ions to be extracted for electroneutrality reasons, which gives a selectivity sequence that reflects the relative lipophilicity of the sample ions and is not influenced by the complexation with the charged ligand. These theoretical expectations have been confirmed for anion-selective electrodes based on a vitamin B12 derivative (cf. Figure 15)<sup>69</sup> as well as with selected metalloporphyrins,<sup>71</sup> thereby introducing a new approach for the optimization of ISEs based on electrically charged carriers. Accordingly, nitrite-selective microelectrodes could be successfully fabricated for the first time.<sup>70</sup> More recently, it has been shown that there are carriers that apparently behave in a so-called mixed mode, for which neither a pure classical neutral carrier nor a charged carrier mechanism apply.<sup>72,73</sup> (See Note Added in Proof.)

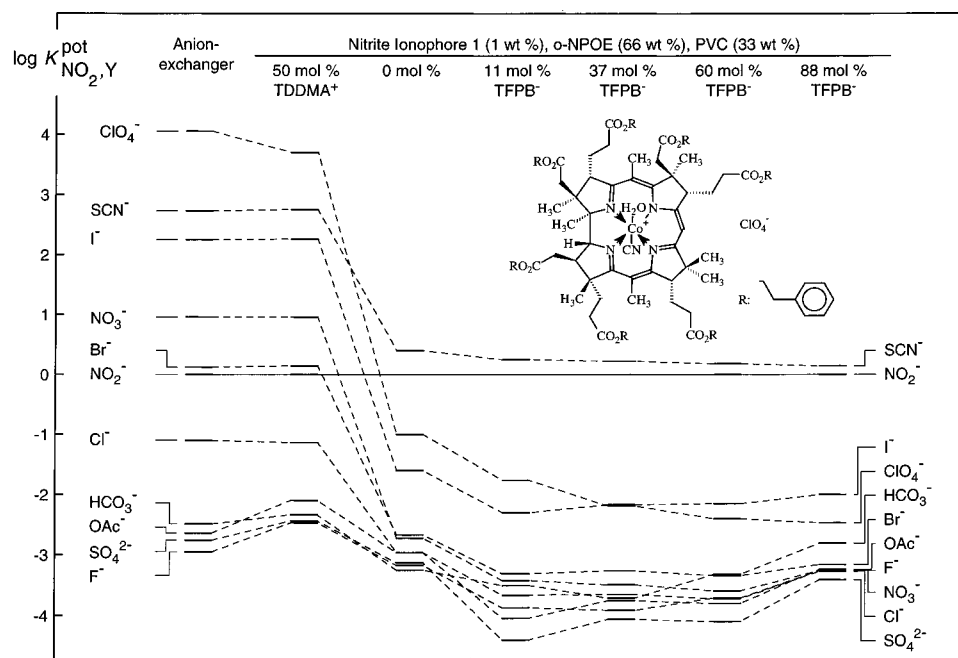


**Figure 15.** Potentiometric selectivity coefficients of nitrite-selective electrodes based on a charged carrier as a function of charge and concentration of lipophilic ionic sites.<sup>69</sup> For comparison, the selectivity of a membrane based on the anion exchanger tridodecylmethylammonium (TDDMA<sup>+</sup>) chloride alone is shown in the first column. The addition of negatively charged ionic sites (potassium tetrakis[3,5-bis(trifluoromethyl)phenyl]borate, K<sup>+</sup> TFPB<sup>-</sup>) is beneficial while positive sites suppress the selectivity of the ionophore.

#### Determination of Selectivity Coefficients.

**Classical Procedures.** The IUPAC commission of 1976 recommended the use of two different procedures to determine the Nicolskii coefficients of ISEs, namely the so-called separate solution method (SSM) and the fixed interference method (FIM).<sup>89</sup> The SSM involves the measurement of two separate solutions, each containing a salt of the determined ion only. The Nicolskii coefficient is then calculated from the two observed emf values (cf. Figure 16). In the FIM, an entire calibration curve is measured for the primary ion in a constant interfering ion background ( $a_J(BG)$  in Figure 16). The linear (i.e., Nernstian) response curve of the electrode as a function of the primary ion activity is extrapolated until, at the lower detection limit  $a_I(DL)$ , it intersects with the observed potential for the background alone. The Nicolskii coefficient is calculated from these two extrapolated linear segments of the calibration curve, each relating the analytical response of the ISE to one respective ion only. In addition, other methods have been used by various authors.<sup>43</sup> Only recently, the actual mixed ion response has been fitted to the Nicolskii–Eisenman equation.<sup>90,91</sup> As it stands, it seems unfortunate that in many cases the chosen theoretical model is not appropriate to describe the analytically relevant mixed response range. Nonetheless, with the use of more accurate models such a procedure will ultimately be very convincing from a practical standpoint. With other, traditional methods to determine selectivity coefficients, the part of the calibration curve that is not correctly described by the Nicolskii–Eisenman equation (see above) is not considered for calculating selectivity coefficients. Therefore, any of these latter experimental procedures should ideally give identical selectivity values. However, they all

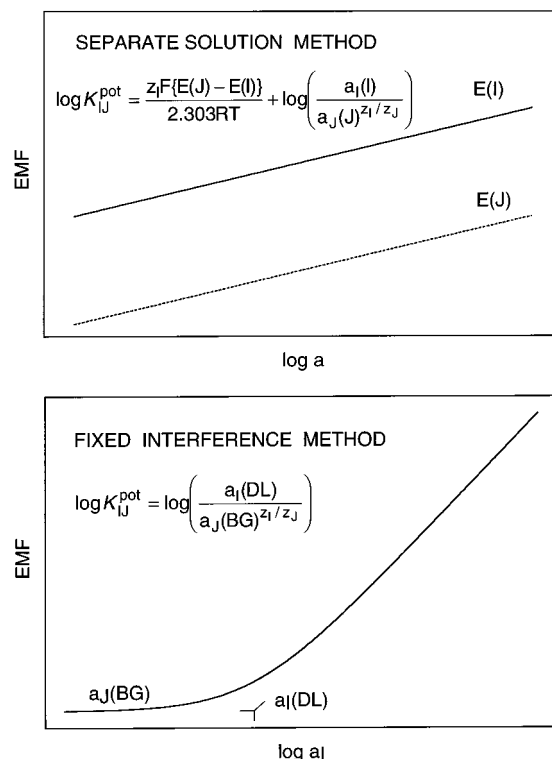


**Figure 16.** Determination of the Nicolskii coefficients according to the separate solution method (SSM, top) and the fixed interference method (FIM, bottom) as proposed by the IUPAC commission.<sup>89</sup>

rely on the assumption that the interfering ion completely displaces the primary ion from the interfacial layer of the membrane, i.e., no mixed ion response is observed.<sup>92</sup> Indeed, it has repeatedly been stated that the reporting of Nicolskii coefficients

is only meaningful if Nernstian slopes are observed for every ion involved.<sup>93,94</sup> However, in many practical situations, this is observed for primary ions only and heavily discriminated ions often show non-Nernstian behavior. Umezawa and co-workers have pointed out that it is actually desirable to discriminate other ions to an extent that no response to them is observed and the requirement of Nernstian slopes toward all ions in the Nicolskii equation is in fact a paradox. Indeed, a recent study on the issue found that only very few electrodes showed Nernstian slopes toward all ions of interest.<sup>93</sup> The reason for non-Nernstian slopes can vary. If the interfering ion is highly discriminated, the response is partially dictated by the detection limit of the sensor, which is a characteristic that is still under current investigation. To date, it is most likely that low levels of primary ions constantly released from the membrane often dictate this detection limit. In this case, nonzero levels of primary ions are continuously present at the sample-membrane interface and successfully compete with the measured discriminated ion in the exchange process. This leads to only partial ion exchange at the interface and, therefore, to non-Nernstian slopes for the discriminated ion. As a consequence, Nicolskii coefficients calculated from such experiments are too large compared to values that reflect the true ion-exchange selectivity. An additional effect is sometimes seen for analyte ions that can be protonated, complexed, or form ion pairs in solution. In these cases, the activity of the potential determining species (usually the free ion) is often not proportional to the total sample concentration and an apparent non-Nernstian electrode slope can be observed. Examples for such analytes are mercury, uranyl, or salicylate ions. Such effects can, however, be corrected by calculating the equilibrium concentration of the extracted species or be prevented by employing a pH or ion buffer.<sup>29</sup> In principle, analogous equilibria within the membrane phase could also lead to non-Nernstian behavior. Another disturbing effect is the electrolyte coextraction into the membrane and therefore loss of membrane permselectivity (i.e., Donnan failure).<sup>95,96</sup> Therefore, Nicolskii coefficients should only be calculated from the Nernstian portion of the calibration curves. In contrast, a nonclassical response is sometimes even preferred, as this is for example required for successful analytical use of polyion sensors.<sup>97</sup> Here, the selectivity can be either described for experimental conditions that closely resemble those of intended samples<sup>97,98</sup> or determined in an equilibrium mode where the thermodynamic preference of different polyions can be evaluated.<sup>99</sup>

The reporting of Nicolskii coefficients of real-world liquid membrane electrodes that show non-Nernstian slopes is in most cases not meaningful. In fact, this dilemma is one of the important reasons why published Nicolskii coefficients for similar membrane compositions vary so much from author to author. Non-Nernstian slopes are often not very reproducible, and the Nicolskii coefficients obtained depend heavily on the experimental conditions, such as sample concentrations, characteristics of previously measured solutions (memory effect), and sample stirring

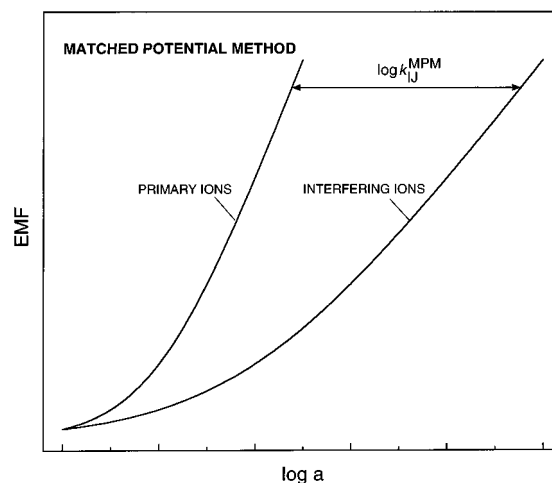


**Figure 17.** Determination of empirical selectivities by the matched potential method (MPM).<sup>75</sup> The activity increase of the primary ion I and interfering ion J leading to the same potential is determined in two different experiments.

rate, to mention a few. Two main solutions to this dilemma have been proposed. One is to introduce a different selectivity formalism that describes the empirical situation as closely as possible,<sup>75,93</sup> while the other is to change the experimental conditions in order to observe Nernstian slopes as required by the formalisms discussed above.<sup>92,100</sup> Which approach is preferred depends on the question that is addressed with the experiment.

**Empirical Selectivities: The Matched Potential Method.** The so-called matched potential method was introduced in the mid 1980s by Gadzekpo and Christian to offer a selectivity formalism that would give empirically more meaningful results.<sup>75,101</sup> In practice, a specified amount of primary ions is added to a reference solution and the membrane potential is measured. In a separate experiment, interfering ions are successively added to an identical reference solution until the membrane potential matches the one obtained before with the primary ion (see Figure 17). The matched potential method selectivity coefficient is then defined by the ratio of the primary ion and interfering ion activity increases in the two experiments.

$$k_{IJ}^{\text{MPM}} = \frac{\Delta a_I}{\Delta a_J} \quad (40)$$

The symbol  $k_{IJ}^{\text{MPM}}$  has been introduced (MPM = matched potential method) for the selectivity coefficient thus determined to clearly distinguish it from the Nicolskii coefficient.<sup>102</sup> A lowercase  $k$  is chosen since this selectivity coefficient is generally not constant for a particular electrode (as opposed to the Nicolskii coefficient) but depends on the exact experimental conditions.<sup>103</sup> The meaning of selectivity coefficients determined with this method is, of course, intuitively convincing because they clearly reflect what is observed with real-world sensors in relevant samples. In the special experimental case that Nernstian response slopes are observed for the involved ions, and for the case that  $a_i = \Delta a_i$  and  $a_j = \Delta a_j$  (i.e., the reference solution contains neither of the two ions), the value obtained by the matched

potential method is equal to the  $k_{IJ}^{\text{Psel}}$  coefficient established above ( $k_{IJ}^{\text{MPM}} = k_{IJ}^{\text{Psel}}$ ; see eq 16). Generally, the matched potential method can be used without regard to the electrode slopes being Nernstian or even linear. For these reasons, it has gained in popularity in the last few years and has even been advocated by IUPAC in a recent technical report.<sup>93</sup> Nonetheless, it is important to realize that the selectivity values obtained will widely vary under changing experimental conditions and large discrepancies among different authors have to be expected. Since the matched potential method does not rely on theoretical assumptions, it intrinsically has no predicting power for varying analytical situations, and the electrode has to be characterized in solutions that carefully match the target sample. Similarly, a correlation of the selectivity to the extraction behavior of the membrane is not directly possible and it is very difficult to obtain information about optimum membrane compositions or binding characteristics of ion carriers from these data. Neither do they allow one to judge whether the interference is due to thermodynamic reasons or, actually, kinetic effects, or even if experimental artifacts are masking the signal. If such information is needed, it will also be important to determine the underlying ion-exchange selectivity of the membrane as outlined below.

**Unbiased Selectivity Coefficients.** Various experimental conditions have been described that allow the determination of Nicolskii coefficients which are not biased by the difference of sample ion activities at the membrane surface and in the bulk. Hulanicki and co-workers have proposed to measure the response of calcium ion-selective electrodes in ion-buffered solutions to obtain the thermodynamic or so-called true selectivity coefficient.<sup>100</sup> It is well-known that the detection limit of ion-selective electrodes can be significantly lowered by employing ion buffers.<sup>104,105</sup> If this buffering can be accomplished to an extent that solely the interfering ions contained in the background electrolyte govern the ISE response, the observed detection limit is a direct measure for the Nicolskii coefficient. This procedure is an experimental modification of the fixed interference method for determining selectivity coefficients (see above). The drawback of the method is that usually no information about the electrode slope for the background ion is obtained. Therefore, the validity of the approach was usually not confirmed in the past. Moreover, the proposed method is only successful if the primary ion is effectively buffered while the interfering ion is not. This is not always easily accomplished and even quite impossible to achieve for characterizing  $\text{Na}^+$  or  $\text{K}^+$  selective sensors, since no suitable water-soluble ligands are available.

For these reasons, a novel method has been recently proposed to measure unbiased selectivity coefficients.<sup>92,106</sup> In the traditional procedure, the membrane is conditioned in a solution that contains a relatively high concentration of the primary ion. This ensures stable and reproducible electrode behavior and is recommended for practical use of the sensor. However, the presence of these primary ions is often the reason for the non-Nernstian response toward

highly discriminated ions (see above). In fact, a Nernstian response is only expected if the primary ion in the interfacial layer of the membrane that contacts the sample is fully exchanged by the discriminated ion, a requirement that is often not met in practice. To overcome this limitation, membranes are now chosen for the measurement that never have been in contact with the preferred ion. For cation-selective electrodes based on neutral carriers, the membranes contain tetraphenylborate derivative salt of a discriminated ion and are conditioned in a chloride solution of this cation. Indeed, this method enables one for the first time to obtain Nernstian responses for a series of strongly discriminated cations with various membranes.<sup>92,106</sup> After measuring calibration curves for a range of discriminated ions, the primary ion response is measured. Since these ions are preferred by the membrane, they exchange readily with the ions the membrane has been conditioned with and, again, a Nernstian response is observed. The feasibility of this method has been established for a range of cation-selective membranes containing neutral ionophores and lipophilic anionic sites.<sup>106</sup> Figure 18 shows the response functions of a  $\text{K}^+$ -selective DOS-PVC (2:1) electrode containing valinomycin and NaTFPB (cf., Figure 54) that was conditioned classically in KCl (a) and, according to the new procedure, in NaCl (b).<sup>92</sup> Apparently, the classically conditioned membrane shows a sub-Nernstian response toward  $\text{Na}^+$ ,  $\text{Mg}^{2+}$ , and  $\text{Ca}^{2+}$ , with potentials around the detection limit of the sensor, therefore prohibiting the proper calculation of Nicolskii coefficients. On the other hand, membranes conditioned in NaCl show near-Nernstian responses toward all measured ions and, consequently, the obtained Nicolskii coefficients more closely reflect the underlying ion-exchange selectivity of the membrane. In this particular example, of course, the experiments have to be performed with great care and a series of important points have to be closely followed, such as the nature of the initial counterion of the incorporated ionic site and sequence and length of exposure to different electrolytes.<sup>92</sup>

### C. Detection Limit

Every ion-selective electrode has a lower and upper detection limit where the response starts to deviate significantly from a Nernstian electrode slope. Generally, they fall into activity ranges where the electrode starts to lose sensitivity toward the primary ion. According to the IUPAC recommendation of 1976,<sup>89</sup> the detection limit is defined by the cross-section of the two extrapolated linear calibration curves (see Figure 19). A definition of the detection limit of ISEs in analogy to other analytical techniques has also been proposed.<sup>107</sup> It is useful if the electrode is intended to be used in an activity range of severe interference, i.e., low sensitivity. However, for general use, the IUPAC recommendation is useful since it is simple and widely accepted and experimental results from different authors can be easily compared.

**Lower Detection Limit.** There are two main possible explanations for the apparent loss of Nernstian response slope at low primary ion activities,



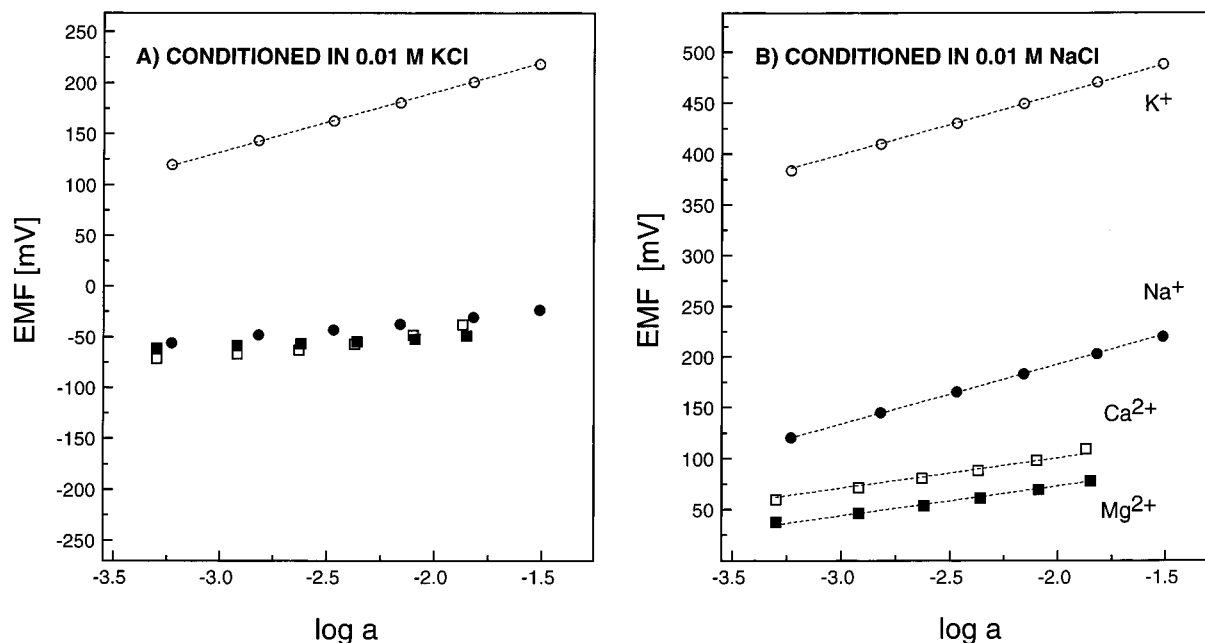


**Figure 18.** Determination of unbiased Nicolskii coefficients  $K_{IJ}^{\text{pot}}$  of potassium-selective plasticized poly(vinyl chloride) membranes containing valinomycin and a sodium tetraphenylborate derivative.<sup>92</sup> While the classical procedure involves conditioning the membrane in a 0.01 M KCl solution (A), only the electrode conditioned in a discriminated ion solution of 0.01 M NaCl (B) shows near-Nernstian response slopes toward all the ions (B) K<sup>+</sup>, (R) Na<sup>+</sup> (Q) Mg<sup>2+</sup>, and (A) Ca<sup>2+</sup>, thereby allowing the calculation of fundamentally meaningful selectivities. Dotted lines are Nernstian response slopes at 21.5 °C (58.4 and 29.2 mV dec<sup>-1</sup>, respectively).

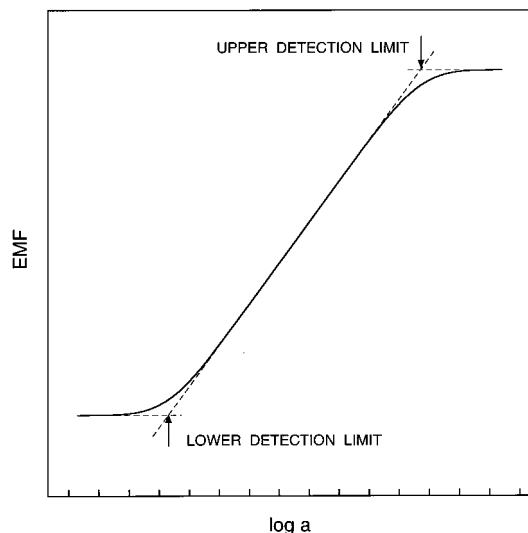


**Figure 19.** Definition of the upper and lower detection limits of an ion-selective electrode according to the IUPAC recommendations.<sup>89</sup>

namely (a) the perturbation of the interfacial sample activity by the membrane and (b) interference by competing sample ions. The most likely reason for the first effect is the constant release of a low amount of primary ions from the membrane into the sample, thereby inducing a local nonzero primary ion activity at the interface. Although the Nernst equation is still valid in this case, the ion activity at the interface is considerably higher than in the bulk, so the response of the electrode becomes insensitive to sample activity changes. The continuous release of small amounts of ions from ISE membranes has indeed been observed.<sup>49</sup> Similarly, silver ISE membranes showed anionic response toward sample halide ions,<sup>108</sup> suggesting that the free concentration of released silver ions is decreased with increasing chloride or iodide

sample concentration due to limited solubility, thereby decreasing the measured potential. Moreover, it is well-known that the detection limit of highly selective ISEs can be significantly lowered by adding a ligand to the sample that effectively buffers the primary ion. With neutral-carrier-based systems, detection limits as low as 10<sup>-12</sup> M (for pH electrodes) or 10<sup>-9</sup> M (for Ca<sup>2+</sup> and Pb<sup>2+</sup> selective systems) have been reported.<sup>109-111</sup> Again, this buffering effect can be explained with a concentration decrease of the free primary ions that are continuously released from the membrane. For an ISE with virtually unlimited selectivity, the maximum possible decrease can be expected to depend only on the degree of complex formation between added sample ligand and primary ion. However, deliberate sample buffering does not allow measurement of the total sample ion concentrations that are lower than the lower detection limit in unbuffered samples. Indeed, ion-selective electrodes seem, to date, still insufficient for total ion concentrations on the order of 10<sup>-6</sup> M or lower. There are, however, many applications where extremely low free sample concentrations/activities can be determined in an ion buffered matrix, such as in intracellular free calcium determinations, where ion-selective electrodes are indispensable tools.<sup>104</sup>

For ISEs of limited selectivity, interfering ions will eventually compete with the primary ion and the detection limit is then given by the selectivity of the sensor. In this case, the detection limit  $a_i(\text{DL})$  is related to the Nicolskii coefficient and the free interfering ion activity as follows:

$$a_i(\text{DL}) = K_{IJ}^{\text{pot}} a_j^{z_i/z_j} \quad (41)$$

With eq 41, the detection limit in a solution with given interfering ion activity can be predicted for

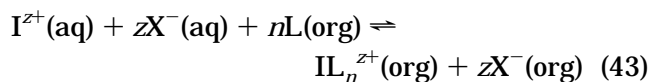
ISEs of known selectivity. In fact, eq 41 is also valid for ISEs that already show interference without added ion buffers. This is the basis for determining Nicolskii coefficients according to the so-called FIM as recommended by IUPAC.<sup>43,89</sup> Of course, the reverse approach can be used as well. This procedure has been recommended by Hulanicki and co-workers for the determination of so-called true selectivity coefficients of calcium ISEs (see above).<sup>100</sup> However, for the correct calculation of Nicolskii coefficients from such experiments, the free interfering ion activity has to be taken into account. This is especially important with added ligands that also buffer the interfering ion.

It can often be assumed that hydrogen ion carriers do not appreciably stabilize/complex any other ions than  $H^+$ .<sup>112</sup> As a recent study has shown, the same can be true for carrier-based silver ion-selective electrodes.<sup>113</sup> The description of the lower detection limit of neutral-carrier-based pH electrodes is, therefore, an important special case. If the lower detection limit (DL) is given by interference of a background ion  $J^+$ , eq 41 can here be modified to<sup>114</sup>

$$a_H(\text{DL}) = \frac{a_J}{L_T - R_T^-} \frac{k_J}{k_H} K_a \quad (42)$$

where, again,  $L_T$  and  $R_T^-$  are the membrane concentrations of ionophore and anionic site. Apparently, the lower detection limit is proportional to the acidity constant of the  $H^+$  carrier in the membrane and the activity and lipophilicity of the involved species. These expectations have been confirmed experimentally.<sup>115</sup>

**Upper Detection Limit.** For cation-selective membranes (anion-selective electrodes can be treated in complete analogy), the upper detection limit is a consequence of a coextraction process of primary cations and interfering anions from the sample into the ion-selective membrane, thereby leading to a loss of membrane permselectivity (so-called Donnan failure)<sup>96,116</sup>



with the corresponding co-extraction constant

$$K_{\text{coex}} = \frac{[IL_n^{z^+}][X^-]^z}{a_I[L]^n a_X} = k_I k_X^z \beta_{IL_n} \quad (44)$$

Equation 44 shows that this process is favored by greater stability of the complexes and higher lipophilicity of the sample anions. With increasing sample concentration, sample anions will be extracted along with primary cations that are complexed with the carrier. Eventually, all free carrier is used up and the membrane contains primarily cation-carrier complexes, lipophilic anionic sites, and extracted sample anions. Therefore, it now functions as a dissociated anion exchanger (permselective for anions), so an anion response of the electrode is expected (see range A in Figure 20). This response is usually observed for carrier-based ISEs and used

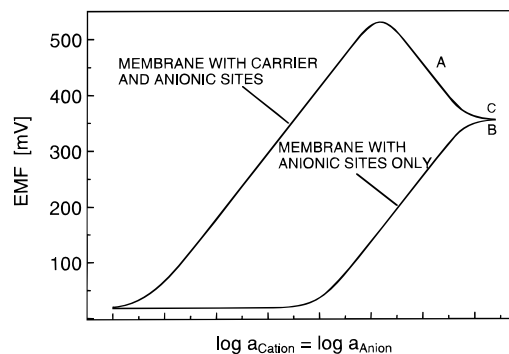


**Figure 20.** Predicted emf function in the anion interference range for ionophore-based and ion-exchanger membranes. In the former case the lipophilic complex acts as an anion exchanger and a negative potential response is expected with increasing sample activities.

for calculating the upper detection limit as the cross-section of the cationic and anionic response curves. A different behavior is expected for ISE membranes that contain only a lipophilic cation exchanger. Here, the concentration of extracted anion will increase continuously with increasing sample electrolyte concentration since no carrier whose complex can act as a lipophilic anion exchanger is present. This should lead to a nearly activity-independent phase boundary potential since the ion activity in the organic phase boundary is roughly proportional to the one in the aqueous phase (see eq 5 and range B in Figure 20). The same response is eventually also expected for neutral-carrier-based sensors for very high sample activities where the activity of the uncomplexed primary ion and counterion in the membrane become nearly equal (see range C in Figure 20).

An approximate equation for the description of the upper detection limit can be given in analogy to the formalism developed earlier for neutral-carrier-based pH electrodes.<sup>114</sup> The emf response as a function of the sample anion activity is obtained by combining eqs 44 and 6 and by inserting the complex formation constant of the carrier (see ref 114 for a detailed derivation):

$$E_X = E^0 + \frac{RT}{zF} \ln \left( \frac{1}{K_{\text{coex}}} \left( \frac{[X^-]}{a_X} \right)^z \right) \quad (45)$$

For the activity range where the electrode responds in a Nernstian way to the sample anion activity,  $[X^-]$  can be calculated from electroneutrality and mass balance considerations and inserted into eq 45 to give

$$E_X = E^0 + \frac{RT}{zF} \ln \left( \frac{1}{K_{\text{coex}}} \left( \frac{zL_T/n - R_T^-}{a_X} \right)^z \right) \quad (46)$$

where, as above,  $L_T$  and  $R_T^-$  are the total membrane concentrations of ionophore and anionic site. It is important to note that eq 46 is only valid if ion-pair formation within the organic phase can be neglected, an assumption that may only be valid for membrane materials of high polarity.<sup>114,117</sup> Finally, according to the IUPAC recommendation,<sup>89</sup> the upper detection limit (UDL) can be calculated by setting eq 46 equal to the respective Nernstian function for the primary

cation activity and solving for the latter:<sup>114</sup>

$$a_1(\text{UDL}) = \frac{1}{K_{\text{coex}}} \left( \frac{zL_T/n - R_T^-}{a_X} \right)^z \frac{R_T^-}{z(L_T - nR_T^-/z)^n} \quad (47)$$

Again, eq 47 must be considered to be semiquantitative since the ion-pair formation of extracted anions and cation complexes within the membrane will certainly have influence on the relevant equilibria. However, from eq 47 it can directly be seen that the upper detection limit is roughly proportional to the concentration of anionic sites,  $R_T^-$ , for membranes that contain a large excess of carrier over ionic sites.<sup>96,116</sup> In addition, eq 47 also shows that ion carriers are not allowed to bind the primary ion too strongly, since the coextraction constant  $K_{\text{coex}}$  is directly proportional to the complex formation constant of the cation-carrier complex,  $\beta_{\text{IL},r}$ . This poses serious limits to the improvement of selectivities by designing ligands that form much stronger complexes with the primary ion than the available ones, since the membranes could otherwise become nonspecific anion sensors. An excellent example for this behavior is the fact that lipophilic porphyrins cannot be used to develop cation-selective electrode membranes. Instead, the formed metalloporphyrins behave by themselves as selective anion exchangers and can be used for anion sensing purposes.

#### D. Measuring Range

The measuring range of ISEs is defined as the activity ratio of upper and lower detection limit and approximately corresponds to the range where the electrode responds according to the Nernst equation. The semiquantitative relationships for the quantification of the lower and upper detection limits of ion-selective electrodes have been established above and can be used to estimate the maximum possible measuring range of carrier-based ion-selective electrodes. The upper detection limit is given by mass extraction of primary cations together with sample anions into the membrane (see above). It can be assumed that the extracted anion is not specifically stabilized within the membrane phase and that, at most, nonspecific ion-pair formation can occur. Therefore, the upper detection limit is primarily dictated by the stability constant of the cation-carrier complex, the relative lipophilicity of the extracted salt, and the involved species concentrations (see eq 47). The lower detection limit of cation-selective sensors is ideally limited by cation interference. The more the interfering ion is stabilized, the smaller the measuring range will be. Therefore, a maximum range will be achieved if the interfering ion is not complexed at all by the carrier. This special limiting case is often approximately valid for  $\text{H}^+$ -selective sensors. Therefore, neutral-carrier-based pH electrodes are expected to have the maximal possible measuring ranges. While the lower detection limit of these systems has been developed above, the upper detection limit (UDL) can be described by simplifying eq 47 ( $z = n = 1$ , see eq 44) to give:

$$a_{\text{H}}(\text{UDL}) = \frac{R_T^- K_a}{a_Y k_{\text{H}} k_Y} \quad (48)$$

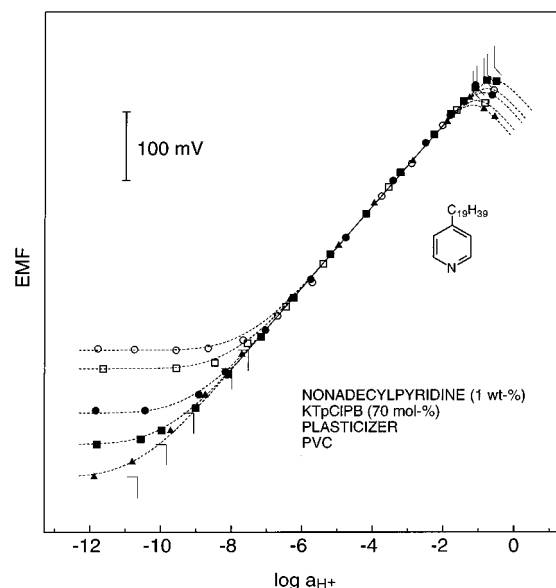


**Figure 21.** Potentiometric pH response of ion-selective electrodes based on 4-nonaecylpyridine (1 wt %) as neutral carrier and potassium tetrakis(*p*-chlorophenylborate) (70 mol % relative to the ionophore) as anionic additive in plasticized PVC membranes as a function of the plasticizer chosen:<sup>114</sup> (A) DOS (dielectric constant (DK) = 3.9<sup>118</sup>); (B) TOTM (DK = 4.7<sup>118</sup>); (R) Mesamoll (DK = 10.6<sup>118</sup>); (Q) *o*-NPOE (DK = 23.9<sup>119</sup>); (U) chloroparaffin (DK = 7.9<sup>119</sup>). Dotted curves are calculated according to the phase boundary potential model;<sup>114</sup> lower and upper detection limits according to eqs 42 and 47, respectively, are indicated by straight vertical lines.

Consequently, an expression for the measuring range is obtained by combining eqs 42 and 48:

$$\Delta\text{pH} = \log \frac{R_T^- (L_T - R_T^-)}{k_J k_Y a_Y} \quad (49)$$

According to eq 49, the maximum measuring range is not influenced by the complex formation constant of the ionophore since a change shifts the upper and lower detection limit simultaneously. Provided that any appreciable complexation of the carrier with interfering ions can be neglected, the measuring range can hardly be extended by searching ionophores with different complexing properties.

From eq 49 it is apparent that it is mainly the nature of the membrane and the kind and concentration of the interfering electrolyte that dictate the maximum measuring range. Different plasticizers<sup>118,119</sup> have been found to induce significantly different measuring ranges (cf. Figure 21).<sup>114</sup> Typically, a range of about 9 logarithmic activity units is achieved with DOS-PVC membranes and ca. 0.1 M KCl as background electrolyte.<sup>114,115</sup> From these data, the approximate value for the KCl coextraction constant (in analogy to eq 83; see below) can be estimated to be about  $10^{-12}$  for DOS-PVC, showing that these membranes indeed behave as hydrophobic matrices. This range has been found to be larger for *o*-NPOE as plasticizer, a fact that is surprising at first sight since a membrane with higher polarity should allow higher electrolyte extraction. Apparently, the stabilization/complexation of the extracted ions by the plasticizer and/or ionic sites within the

membrane matrix also plays a very important role in the overall electrolyte extraction.

The measuring range of common ISEs containing neutral carriers that also complex interfering ions can be described in complete analogy by replacing the Nicolskii coefficient in the eq 41 for the lower detection limit by eq 37. The combination of this result with eq 47 for the upper detection limit gives the following measuring range for monovalent interfering ions:

$$\Delta(\log a_i) = z_i \log \left( \frac{z_i L_T / n_i - R_T^-}{a_Y a_J k_Y k_J \beta_{JL_{ij}}} \frac{R_T^-}{(L_T - n_J R_T^-)^{n_J}} \right) \quad (50)$$

It is well-established that common carriers selective for other cations than  $H^+$  do complex interfering ions significantly, although there are exceptions, such as neutral carriers for silver ions.<sup>113</sup> Usually, stability constants on the order of  $10^4$ – $10^6$   $M^{-1}$  are common values for monovalent interfering ions forming 1:1 complexes in DOS–PVC membranes.<sup>84</sup> For monovalent ions, typical ISE measuring ranges of 5–7 orders of magnitude are therefore estimated ( $z_i = n_i = 1$ ,  $L_T = 10$   $mmol\ kg^{-1}$ ,  $R_T^- = 1$   $mmol\ kg^{-1}$ ,  $a_Y = a_J = 0.1$   $M$ , and  $k_Y k_J = 10^{-12}$ ), a range that is commonly observed experimentally. In contrast, divalent ion-selective electrodes are expected to have a larger measuring range, typically 10–14 orders of magnitude (with  $z_i = n_i = 2$  and otherwise the same parameters). This difference of measuring range between monovalent and divalent ions has often been observed experimentally<sup>110</sup> and is related to the lower electrode slopes for divalent ions.

While the considerations established here only provide a rough approximation for neutral-carrier-based ISE membranes in general, important optimization rules for pH sensors can be deduced from the above analysis. Apparently, the concentration of ionophore should be kept high, that of the anionic site must be 50 mol % relative to the ionophore,<sup>114</sup> and a membrane matrix that neither stabilizes interfering cations  $J^+$  nor anions  $Y^-$  is preferred to achieve a maximum measuring range of such pH sensors.<sup>114</sup> Recently, the present approach has been applied to explain the influence of nonionic surfactants, which are often used in clinical analyzers, on the response of carrier-based pH sensors, showing that the lower detection limit can be heavily shifted by such surfactants due to their cation binding properties.<sup>64</sup> As a further effect of nonionic surfactants on pH electrodes using carrier-free aminated PVC as the selective membrane matrix, additional large shifts in emf values over the entire Nernstian measuring range were observed. This effect was interpreted in terms of multidentate interactions between the surfactant molecules and the protonated polymeric amine in the membrane, leading to a change in the apparent  $pK_a$  values of the amine sites.<sup>64</sup>

### E. Response Time

Since the response time is a very important characteristic of ISEs, it has been thoroughly studied. A comprehensive review of the literature up to 1987 is

available.<sup>120</sup> In earlier IUPAC recommendations, it was defined as the length of time between the instant at which the ISE and a reference electrode are brought into contact with a sample solution (or the time at which the concentration of the ion of interest in a solution is changed on contact with an ISE and a reference electrode) and the first instant at which the potential of the cell becomes equal to its steady-state value within 1 mV<sup>89</sup> or has reached 90% of the final value.<sup>121</sup> More recently, it has been extended to be able to treat drifting systems as well. In this case, the second time instant is defined as the one at which the emf/time slope ( $\Delta E/\Delta t$ ) becomes equal to a limiting value.<sup>94,122</sup> Whichever definition is used, it must be kept in mind that a single time constant does not describe the form of the response function that might provide information on the prevailing time limiting mechanism. Responses of ISEs can be so fast that the electronic equipment may become limiting, especially when investigating electrodes with a high impedance such as microelectrodes.<sup>123</sup>

In the following, solely changes of the potential at the sample/membrane boundary are considered, since only few results are available with regard to long term drifts (over hours) caused by membrane internal diffusion or changes at the inner boundary surface.<sup>97,106,124</sup> The three possible time-limiting processes are (1) the interfacial ion-exchange, and the diffusion-controlled equilibration of (2) the sample with the aqueous side of the phase boundary and (3) the membrane side of the phase boundary with the membrane bulk. The latter was found to be only of importance in specific cases such as nonplasticised silicone rubber based membranes,<sup>125</sup> but for most ISEs of practical relevance, this process is fast (cf. section III.A.3). As a consequence, a virtually immediate shift of the phase boundary potential is expected after a change of the activity in either of the phases at the membrane surface. Therefore, potential drifts arise as a consequence of slow equilibration of the corresponding surface layers with the bulk of the solution and/or membrane upon a change of the sample. In the following sections the two cases are discussed independently. This is only justified if one of them dominates, but a more elaborate model is needed if both processes have comparable speeds.

For electrodes equilibrated with the salt of an ion to which they respond according to the Nernst equation, concentration changes in the membrane phase are negligible in most cases, and thus diffusion within the membrane is not relevant (cf. II.1.A. and see below). Therefore, diffusion through a stagnant aqueous layer is the slowest process which defines the response time in these situations. Although an exact solution of the corresponding diffusion equation is available,<sup>120</sup> for practical purposes the use of an approximate equation is more convenient<sup>29,126</sup>

$$E_t = E_\infty + \frac{RT}{z_i F} \ln \left( 1 - \left( 1 - \frac{a_i^0}{a_i} \right) \frac{4}{\pi} e^{-t/\tau} \right) \quad (51)$$

with  $a_i^0$  and  $a_i$  being the activities at the membrane surface at  $t = 0$  and at equilibrium, respectively, and  $\tau$  the time constant that depends on the thickness of the Nernst diffusion layer,  $\delta$ , and on the

diffusion coefficient,  $D_{\text{aq}}$ :

$$\tau' = \frac{\delta^2}{2D_{\text{aq}}} \quad (52)$$

Some frequent observations can be understood on the basis of these equations. As a consequence of the logarithmic response of ISEs, the response time is always significantly longer (by a factor of  $\approx 100$  in case of a 10-fold activity change) if a diluted solution is measured after a more concentrated one than in the opposite case. From eq 52 the massive influence of stirring is apparent. Because of the reduction of the thickness of the diffusion layer, fast stirring decreases the value of  $\tau'$  from  $\approx 1$  s (unstirred solution) to  $10^{-3}$  s.

In some instances, the change of sample may significantly influence the composition of the membrane surface layer and, therefore, internal diffusion so that membrane internal processes may be time limiting. This occurs when measurements close to the detection limit are made and is caused by an interfering ion that then partially exchanges with the primary ion. Another case is the selectivity measurement, which is only possible if the interfering ion replaces the primary one. A third possibility of drifts caused by membrane internal diffusion is coextraction of a primary ion salt from the sample into the membrane, a process that sets the upper detection limit (see above). However, the extent of coextraction in terms of potential drift is already significant if the membrane is in contact with more diluted solutions. While one or two logarithmic activity units below the upper detection limit the slope of the electrode function is still close to Nernstian, the effect of coextraction on the response time is already significant. It strongly depends on the polarity of the plasticizer: nonpolar phases reduce coextraction and accelerate the ISE response.<sup>126</sup> An increase of the concentration of anionic sites in the membrane reduces coextraction (cf. II.1.C) and, as expected from this interpretation, accelerates the response.<sup>127</sup> Finally, the use of components of limited lipophilicity might also give rise to response times determined by the diffusion in the membrane. Since the composition of the sample might influence their leaching out from the membrane, a new stationary state has to be established upon sample change. Hence, diffusion of membrane components to the interface might define the response time.

The mathematical analysis of the influence of diffusion processes within the membrane leads to a different response behavior: An inverse square root time dependence is expected instead of the exponential decay.<sup>126</sup> In some, but not all, cases a detailed analysis of the response curve may help to differentiate between these two mechanisms.<sup>128,129</sup>

## 2. Ion-Selective Optodes

The response of optical sensors may either rely on surface phenomena (surface optodes) or on concentration changes inside the bulk of a separate phase (so-called bulk optodes).<sup>41,42,130-132</sup> Both hydrophilic membranes/surfaces and water immiscible hydrophobic films are used as matrices. While the former

group often is based on poly(acrylamide) or other hydrogels and makes use of derivatives of classical water-soluble indicators, the latter, which is discussed here in greater detail, is typically based on PVC or similar polymers and exploits the extremely high selectivity of the same lipophilic ionophores that are employed in ion-selective electrode membranes. Some PVC films containing neutral ionophores have been shown to yield a useful optical response based on interfacial phenomena, e.g., with optical second harmonic generation<sup>133</sup> or by making use of potential-sensitive dyes.<sup>134</sup> They are, however, not yet very well explored or accepted, partly because the theoretical framework of their response is difficult to establish. In this review, we will focus on optical sensors based on bulk extraction equilibria into a hydrophobic water-immiscible film as studied by several research groups.<sup>130,135-147</sup>

### A. Response Mechanism

**Optical Sensors for Ionic Analytes.** While hydrophobic polymeric films containing neutral ionophores and lipophilic ionic sites are a well-suited matrix for ion-selective electrode membranes, the realization of optical sensors that exhibit similar selectivity and sensitivity as their ISE counterparts

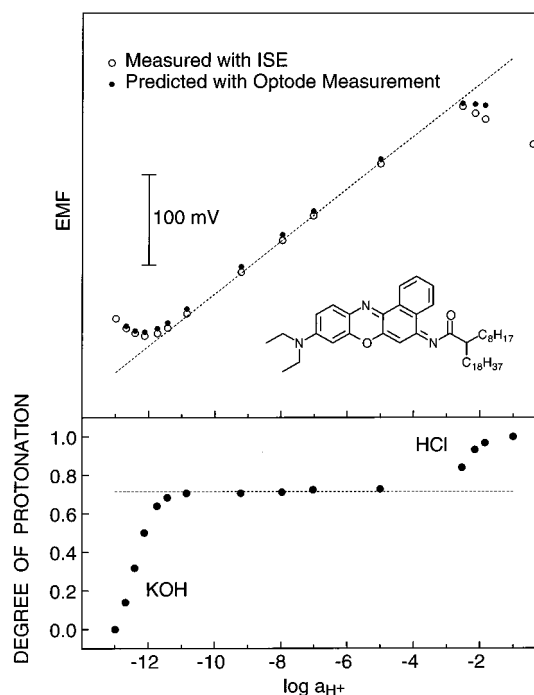
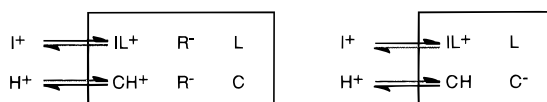


**Figure 22.** Bottom, degree of protonation ( $1 - \alpha$ ), evaluated from optical measurements, for the  $\text{H}^+$ -selective chromoionophore ETH 2458 (structure shown; 2.8 wt %) with 71 mol % (relative to ETH 2458) anionic additive (KTFPB) in a ca.  $2 \mu\text{m}$  thin DOS-PVC (2:1) film as a function of the sample pH (high pH values, dilute KOH; low pH values, dilute HCl; intermediate pH, standard pH buffers).<sup>35</sup> The changes at low and high pH are caused by ion-exchange with sample  $\text{K}^+$  and coextraction with  $\text{Cl}^-$  ions, respectively. Top, measured and predicted emf changes of a  $\text{H}^+$ -selective membrane having the same composition as the organic film used in the bottom figure as a function of the sample pH. Values are predicted according to concentration changes shown in the bottom panel and with the phase boundary potential  $\text{emf} = E^0 + 59 \log(a_{\text{H}^+} [\text{C}]/[\text{CH}^+])$ ,  $[\text{C}]$  and  $[\text{CH}^+]$  being the concentration of unprotonated and protonated ETH 2458 in the membrane.

## OPTODES WITH ELECTRICALLY NEUTRAL IONOPHORE L

FOR CATIONIC ANALYTES



FOR ANIONIC ANALYTES

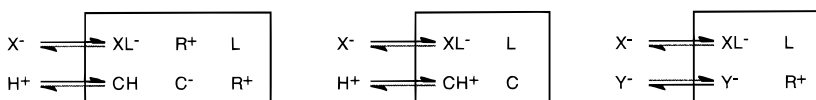
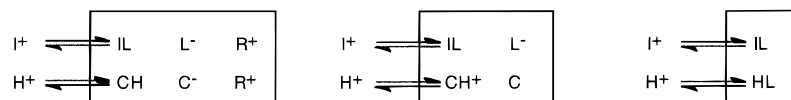


**Figure 23.** Types of neutral-carrier-based optodes with neutral or charged chromoionophores (L, neutral carrier; C and C<sup>-</sup>, neutral and charged H<sup>+</sup>-chromoionophores; R<sup>+</sup> and R<sup>-</sup>, positively and negatively charged ionic sites). Squares indicate species in the organic phase.

OPTODES WITH ELECTRICALLY CHARGED IONOPHORE L<sup>-</sup> OR L<sup>+</sup>

FOR CATIONIC ANALYTES



FOR ANIONIC ANALYTES

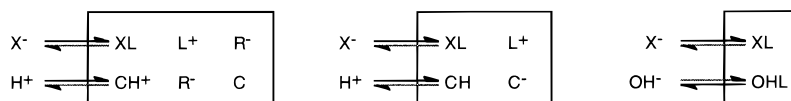


**Figure 24.** Types of charged-carrier-based optodes with neutral or charged chromoionophores (L<sup>+</sup> and L<sup>-</sup>, charged carriers; C and C<sup>-</sup>, neutral and charged H<sup>+</sup>-chromoionophores; R<sup>+</sup> and R<sup>-</sup>, positively and negatively charged ionic sites). Squares indicate species in the organic phase.

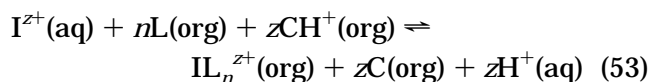
requires somewhat different considerations. An optical signal change must usually be induced by a concentration change of a component inside a thin polymeric film. Since ion-selective electrode membranes are ideally permselective ion exchangers, the concentrations of ionophore and its complex in the organic phase are practically constant as long as a Nernstian behavior of the electrode is observed. Considerable concentration changes of the analyte ion in the membrane are only obtained in the limiting activity ranges where significant coextraction and ion-exchange equilibria occur, but in this case the electrode potential is also dictated by the sample activity of the interfering ion that coparticipates in the equilibrium. On the other hand, a signal change of a corresponding bulk optode film (i.e., one that has the same composition as the ISE membrane) is expected outside the Nernstian response range of the electrode (see Figure 22). Since electroneutrality must hold for the bulk phase, bulk optodes based on hydrophobic films cannot be sensitive to one ion alone. Instead, a well-defined phase transfer equilibrium of two distinct ions has to be established. This process is shown schematically in Figure 23 for neutral ionophores and in Figure 24 for charged ones. Depending on the charge signs of the two involved ions, either a competitive ion exchange or a carrier-mediated coextraction equilibrium is responsible for the optode response. Preferably, a complexation reaction of at least one of the two ions should lead to an optical response, e.g. due to changes in absorbance, fluorescence, phosphorescence, or refractive index. Most reports on bulk optode films have made

use of the selective interaction of hydrogen ions with lipophilized or immobilized pH indicators as chromoionophores. This has obvious advantages, since the sample pH can be varied and buffered over a wide range and lipophilized pH indicators with a large variety of different basicities are now available. In addition, neutral H<sup>+</sup>-ionophores belong to the most selective ones and the complexation of these compounds with other cations can usually be neglected.<sup>112</sup> Of course, one obvious drawback of this type of sensor is its pH cross-sensitivity, which can be overcome by measuring pH simultaneously, e.g., with optical or potentiometric pH sensors, or by buffering the sample, such as with a continuous buffer stream in flow-injection analysis.<sup>148</sup> In a commercially available disposable product for single measurements,<sup>135</sup> a dried layer of pH buffer is applied to the optical film that dissolves upon contact with a drop of sample and adjusts its pH.

A wide range of neutral and electrically charged ionophores and pH-selective chromoionophores is available<sup>112,135,140</sup> that can be combined in sensing films to operate according to a variety of different sensing principles (see Figures 23 and 24). For cation-exchange optodes based on two electrically neutral ionophores, one being a chromoionophore, the simultaneous presence of lipophilic anionic sites that give the membrane cation exchange properties is required (Figure 23, first row, left side).<sup>130</sup> If the H<sup>+</sup>-selective chromoionophore is itself electrically charged (i.e., negatively charged when nonprotonated and neutral when protonated), no such trapped ionic sites are needed (see Figure 23, first row, right side).<sup>149</sup>

If, on the other hand, the ionophore is charged, ionic sites are needed with charged chromoionophores but not with neutral ones (Figure 24, first row, first two entries). Another type of optodes has been reported on the basis of compounds that act both as the ionophore and chromoionophore, i.e., the analyte ion and hydrogen ion can be selectively complexed by the same carrier, one of them inducing an absorbance change (Figure 24, first row, right side).<sup>143,144,150</sup> While such systems contain fewer components, they are less flexible since the chromoionophore and/or ion carrier content cannot be separately optimized (the second row, right side in Figure 24 shows an equivalent system that is anion responsive). For anion-sensing optodes based on coextraction equilibria, electrically neutral and/or charged carriers can be used, again with and without electrically charged trapped ionic sites, respectively. The second row in Figure 23 shows, in the first two entries from the left, neutral-carrier-based optodes containing an electrically charged chromoionophore  $C^-$  and cationic sites  $R^+$ , and an electrically charged chromoionophore  $C$  without added sites. On the other hand, the second row of Figure 24 shows, in the first two entries from the left, charged-carrier-based optodes containing an electrically neutral chromoionophore  $C$  and anionic sites  $R^-$ , and a charged chromoionophore  $C^-$  without added sites. On the other hand, films containing only a neutral  $H^+$ -chromoionophore also function as anion optodes. However, they show a Hofmeister-type selectivity pattern, i.e., a preference for lipophilic anions,<sup>151</sup> since the coextracted anions are not selectively complexed.

Here, we will focus on the theory of the ion-exchange mechanism that has been described most often for polymeric films containing a neutral ionophore  $L$  forming complexes  $IL_n^{z+}$  with the cationic analyte  $I^{z+}$ , a neutral chromoionophore  $C$  that binds  $H^+$  to form  $CH^+$ , and lipophilic anionic additives  $R^-$ . Other systems can often be described by complete analogy. The overall ion-exchange equilibrium between sample and organic film is written as<sup>136</sup>



with the corresponding exchange constant

$$K_{\text{exch}}^{IL_n} = \frac{(a_H[C])^z [IL_n^{z+}]}{[CH^+]^z a_I [L]^n} = \left(\frac{K_a}{k_H}\right)^z k_I \beta_{IL_n} \quad (54)$$

which is a function of the relative lipophilicities  $k_I$  and  $k_H$  of  $I^{z+}$  and  $H^+$  (see discussion of eq 5), respectively, the stability constant  $\beta_{IL_n}$  for the ion-ionophore complex, and the acidity constant  $K_a$  for the chromoionophore. The latter two are defined for the organic phase. It is assumed that concentrations within the organic phase are proportional to activities. This assumption considerably simplifies the mass and charge balances used for eq 54. Subsequently, eq 54 is combined with the electroneutrality condition ( $R_T^- = [CH^+] + z[IL_n^{z+}]$ ) and mass balances for the ionophore ( $L_T = [L] + n[IL_n^{z+}]$ ) and chromoionophore ( $C_T = [C] + [CH^+]$ ) in the polymeric

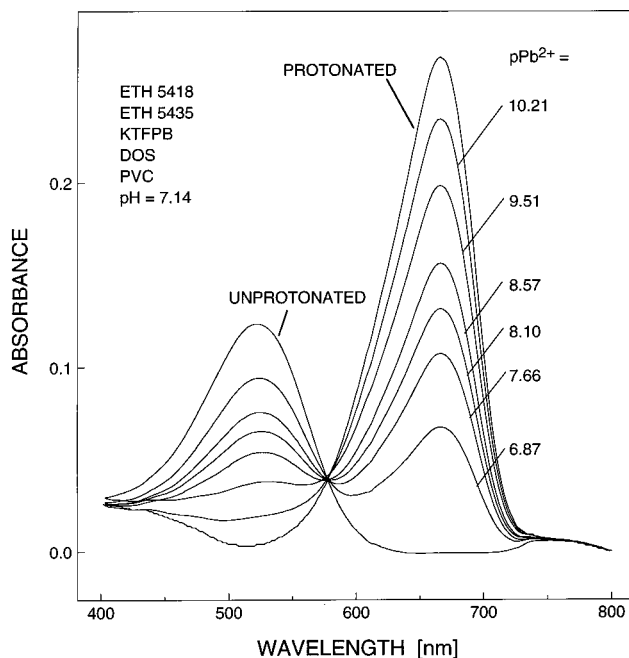


**Figure 25.** Spectra of a  $Pb^{2+}$ -selective optode film, containing ETH 5435 ( $Pb^{2+}$  ionophore), ETH 5418 (chromoionophore), and NaTFPB (see Figure 26), as a function of different lead ion activities in the sample, buffered with NTA as ligand at pH 7.14 ( $25 \pm 1$  °C).<sup>111</sup> The chromoionophore is subsequently deprotonated with increasing  $Pb^{2+}$  concentration in the sample. Absorbance maximum of the protonated form,  $\lambda_{\text{max}} = 666$  nm.

film, giving the optode response function as<sup>40</sup>

$$a_I = (zK_{\text{exch}}^{IL_n})^{-1} \left( \frac{\alpha}{1-\alpha} a_H \right)^z \times \frac{R_T^- - (1-\alpha)C_T}{\{L_T - (R_T^- - (1-\alpha)C_T)(n/z)\}^n} \quad (55)$$

where the normalized absorbance  $\alpha$  is the relative portion of the unprotonated form of the chromoionophore ( $\alpha = [C]/C_T$ ). Since the optode film is in chemical equilibrium with the sample solution, the ratio of free sample ion activities ( $a_I/a_H^z$ ), not of concentrations, is measured. Equation 55 describes an implicit sigmoidal response function that cannot generally be solved for  $\alpha$ . The measured absorbance  $A$  at a given equilibrium can be related to  $\alpha$  by measuring the absorbances of the fully protonated ( $A_P$ ) and nonprotonated form ( $A_D$ ) of the chromoionophore

$$\alpha = \frac{A_P - A}{A_P - A_D} \quad (56)$$

Analogous relationships have been developed for optodes that are operated in the fluorescence mode.<sup>145</sup> In Figure 25 the observed spectral changes as a function of different sample activities at pH 7.14 are shown for a  $Pb^{2+}$ -selective optode based on a DOS-PVC film doped with the  $Pb^{2+}$  ionophore ETH 5435, the  $H^+$ -chromoionophore ETH 5418, and the lipophilic anionic site TFPB $^-$  (see Figure 26). The individual normalized absorbances for the protonated form of the chromoionophore are shown in Figure 27 together with the theoretical response curve as

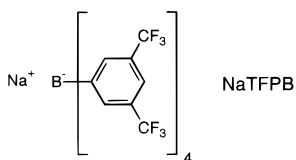
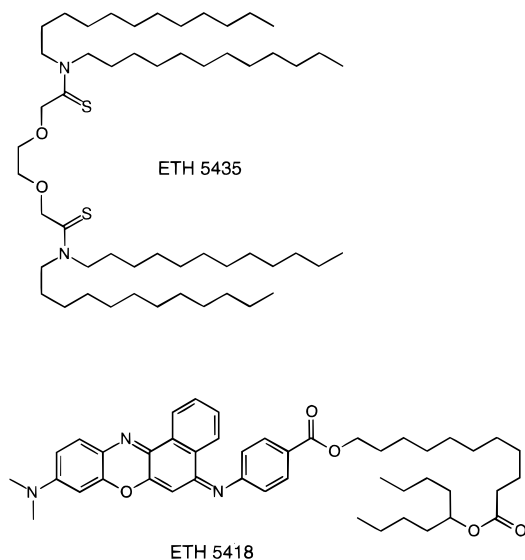


**Figure 26.** Structural formulas of the components used in the Pb<sup>2+</sup>-selective optode (cf. Figures 25, 27, and 28).

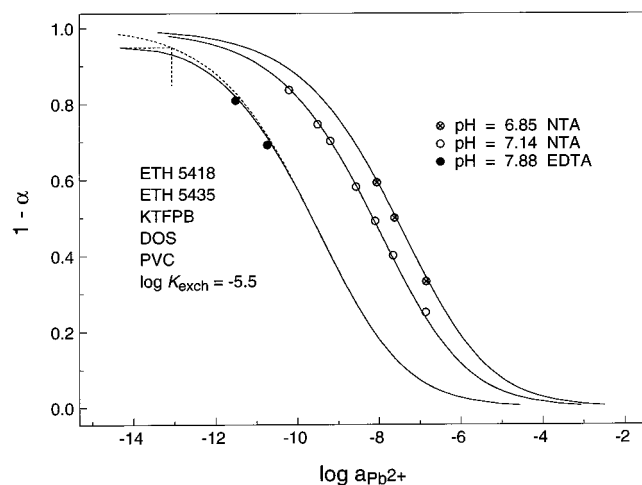


**Figure 27.** Response functions of the Pb<sup>2+</sup>-selective optode at various sample pH values (cf. Figures 25 and 26 and eq 55).<sup>111</sup> The complexing agents nitrilotriacetic acid (NTA) and ethylenediaminetetraacetic acid disodium salt (EDTA) were used to maintain low sample Pb<sup>2+</sup> activities.

calculated with eq 55. It is evident from eq 55 that the equilibrium not only depends on the Pb<sup>2+</sup> concentration but also on the pH value, i.e., the pH has to be kept constant or determined independently for accurate analyte ion activity measurements. As expected for a divalent ion, the response toward  $\log(a_{\text{Pb}^{2+}}/(a_{\text{H}^+})^2)$  is independent of pH (see Figure 28). On the other hand, this dependence can often be exploited to tune the sensitive range of the optode to the target sample activity. For example, the selectivity toward monovalent ions can be enhanced by a decrease of pH, as shown in Figure 29. Another consequence of eq 55 is the fact that the ion-exchange equilibrium can be shifted to lower or higher activity

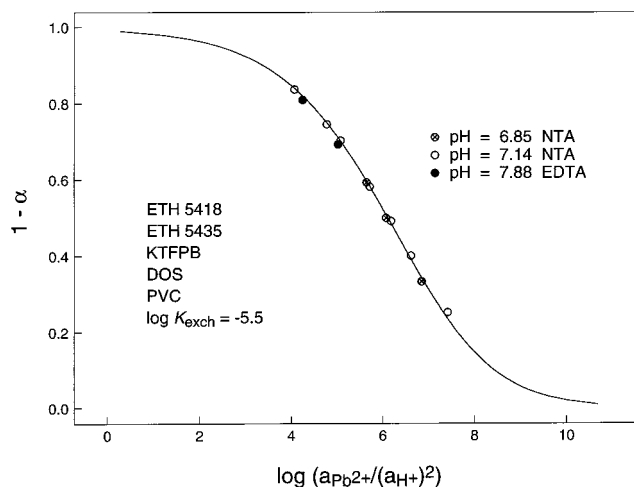


**Figure 28.** Response function of the Pb<sup>2+</sup>-selective optode plotted as a function of  $\log(a_{\text{Pb}^{2+}}/(a_{\text{H}^+})^2)$ .<sup>111</sup> As expected from eq 54, values measured at different sample pH values can be fitted to one single function.

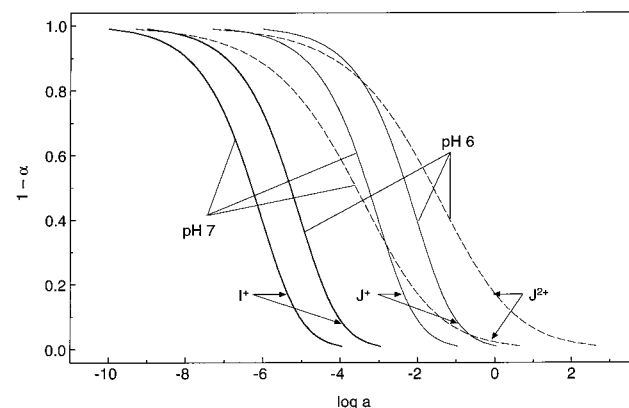


**Figure 29.** Calculated influence of the pH on the selectivity of an optode toward a monovalent ion I<sup>+</sup> relative to a monovalent (J<sup>+</sup>) or divalent (J<sup>2+</sup>) interfering ion. The selectivity toward an ion of lower valency can be improved by decreasing the pH of the sample and vice versa.

ranges by choosing a system with a different exchange constant, i.e., by changing either the ionophore or chromoionophore with one that forms a complex with a different stability. An additional important feature of such an optode response function is the dependence on the charge of the extracted cation and the stoichiometry of the complex. The latter information cannot be obtained from measurements within the Nernstian response range of corresponding ion-selective electrodes.

In some cases, the choice of a higher concentration of chromoionophore than of the anionic site may be of advantage. In this situation, the above equations are still valid. However, it is practically difficult to determine the absorbance for  $\alpha = 0$ , since the chromoionophore cannot be fully protonated. To remedy this situation, an effective  $\alpha$  value,  $\alpha_{\text{eff}}$ , can be introduced as

$$\alpha_{\text{eff}} = \frac{[\text{C}]}{R_{\text{T}}} = \frac{R_{\text{T}}^- - [\text{CH}^+]}{R_{\text{T}}} \quad (57)$$

This definition ensures that the practical limiting absorbances, as in eq 56, can be used without restric-



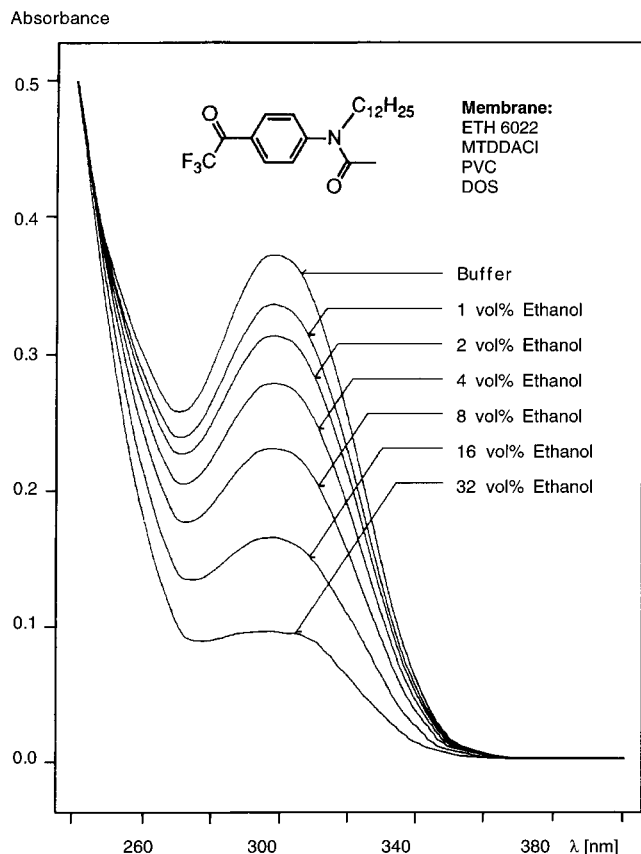


**Figure 30.** Absorption spectra of two 4  $\mu\text{m}$  thick optode films after equilibration with different ethanol concentrations in a phosphate buffer at pH 7.<sup>153</sup> The absorbance maximum of the ligand ETH 6022 is at 305 nm and that of its hydrate and its hemiketal below 210 nm.

tions. Of course, the optode response function has to be modified accordingly. Since the mass and charge balances remain unaffected, the optode response function based on  $\alpha_{\text{eff}}$  is given as

$$a_I = (zK_{\text{exch}}^{\text{IL}_n})^{-1} \times \left( \frac{C_T - (1 - \alpha_{\text{eff}})R_T^-}{(1 - \alpha_{\text{eff}})R_T^-} a_H \right)^z \frac{a_{\text{eff}}R_T^-}{\{L_T - (n/z)\alpha_{\text{eff}}R_T^-\}^n} \quad (58)$$

**Optical Sensors for Neutral Analytes.** In contrast to ion-selective electrodes, optical sensors for neutral species can be developed with relative ease. The description of such a sensor is in fact much more straightforward as compared to ion-selective optodes since no charge balances are involved. For a polymeric film that contains a lipophilic ligand C that changes its optical properties upon complexation with a neutral analyte N (with the stability constant  $\beta_{\text{NL}}$ ), the response function can be given as

$$[N]_{\text{aq}} = \frac{[N]_{\text{org}}}{P_N} = \frac{[NC]_{\text{org}}}{P_N \beta_{\text{NL}} [C]_{\text{org}}} = \frac{1 - \alpha}{P_N \beta_{\text{NL}} \alpha} \quad (59)$$

where  $P_N$  is the partition coefficient for N between the sample and the sensing film and  $\alpha$  is again the fraction of uncomplexed ligand that is accessible experimentally. Optical sensors have been presented for example for the measurement of humidity<sup>152</sup> and ethanol (cf. Figures 30 and 31),<sup>153</sup> both on the basis

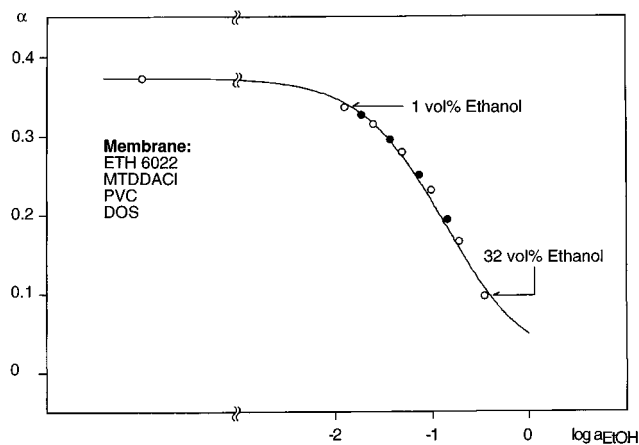


**Figure 31.** Relative absorbance values at 305 nm as a function of  $\log a_{\text{EtOH}}$  at 25 °C:<sup>153</sup> (○) 0.1 M phosphate buffer, (●) 0.1 M phosphate buffer with a constant background of 4 g L<sup>-1</sup> glucose, 4 g L<sup>-1</sup> fructose, 0.2 g L<sup>-1</sup> citric acid, 0.35 g L<sup>-1</sup> NaCl, 0.77 g L<sup>-1</sup> acetic acid, 2 g L<sup>-1</sup> lactic acid, and 1 g L<sup>-1</sup> tartaric acid.

of lipophilic trifluoroacetophenone derivatives that show strong absorbance changes upon reversible reactions with nucleophiles. Optical sensors for neutral species, however, can also make use of protonation and deprotonation equilibria of the analytes that lead to electrically charged species that can be complexed with appropriate ionophores. Sensors for aqueous and gaseous ammonia<sup>149,154</sup> as well as CO<sub>2</sub><sup>155</sup> and SO<sub>2</sub><sup>156,157</sup> have been developed according to this principle. The description of the response function in such cases is closely related to that of optodes for ionic analytes (see above).

### B. Selectivity

Since optodes are used to measure under equilibrium conditions, their response function can be directly derived from fundamental phase transfer and complexation equilibria. Therefore, fewer assumptions than for ISEs are involved in the description of the response to samples containing also interfering ions. While in the earliest papers, an equation equivalent to the extended Nicolskii–Eisenman equation was employed,<sup>39,158</sup> only shortly thereafter was a thermodynamically concise description presented<sup>40</sup> which enabled an improved characterization of ion optodes based on lipophilic ionophores.

The selectivity formalism is presented here only briefly. For this purpose, a second ion-exchange constant for the phase transfer equilibrium with interfering ions J is formulated in complete analogy to eq 55, using  $JL_{n_j}^{z_j+}$  and  $\beta_{JL}$  for the interfering ion–ionophore complex and the corresponding stability constant. These two ion exchange equilibria are simultaneously valid and are combined with the electroneutrality condition

$$R_T^- = [CH^+] + z_1[IL_{n_1}^{z_1+}] + z_J[JL_{n_J}^{z_J+}] \quad (60)$$

and mass balance for the ionophore

$$L_T = [L] + n_1[IL_{n_1}^{z_1+}] + n_J[JL_{n_J}^{z_J+}] \quad (61)$$

to give, for  $n_1 = n_J = 1$  and after rearrangements, an

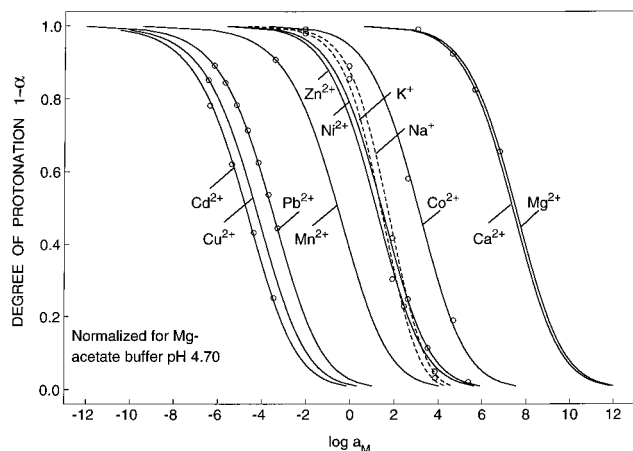


**Figure 32.** Response of the  $\text{Pb}^{2+}$ -selective optode (cf. Figure 25) to various sample ions.<sup>159</sup> The horizontal distance between the calibration curves for  $\text{Pb}^{2+}$  and any interfering ion  $\text{J}^{z+}$  gives the selectivity coefficient  $k_{\text{PbM}}^{\text{Osel}}$ .

extended response function for optode membranes in contact with a sample containing interfering ions  $\text{J}^{+}$ <sup>40</sup>

$$a_{\text{I}} + k_{\text{IJ}}^{\text{Osel}} a_{\text{J}} = (z_{\text{I}} K_{\text{exch}}^{\text{IL}})^{-1} \left( \frac{\alpha}{1 - \alpha} a_{\text{H}} \right)^{z_{\text{I}}} \times \frac{R_{\text{T}} - (1 - \alpha) C_{\text{T}}}{\{L_{\text{T}} - (R_{\text{T}} - (1 - \alpha) C_{\text{T}}) n_{\text{I}} / z_{\text{I}}\}^{n_{\text{I}}}} \quad (62)$$

with the selectivity factor  $k_{\text{IJ}}^{\text{Osel}}$

$$k_{\text{IJ}}^{\text{Osel}} = \frac{z_{\text{J}} K_{\text{exch}}^{\text{JL}}}{z_{\text{I}} K_{\text{exch}}^{\text{IL}}} \left( \frac{\alpha}{1 - \alpha} a_{\text{H}} \right)^{z_{\text{I}} - z_{\text{J}}} \times \frac{\{L_{\text{T}} - (R_{\text{T}} - (1 - \alpha) C_{\text{T}}) n_{\text{J}} / z_{\text{J}}\}^{n_{\text{J}}}}{\{L_{\text{T}} - (R_{\text{T}} - (1 - \alpha) C_{\text{T}}) n_{\text{I}} / z_{\text{I}}\}^{n_{\text{I}}}} \quad (63)$$

This relationship is exact for a large excess of ionophore and for  $n_{\text{I}} = n_{\text{J}} = 1$ , while it is a satisfactory approximation in other cases.<sup>40</sup> It is important to note that this description of the optode selectivity is analogous to the one developed above for ion-selective electrodes (cf. eqs 16 and 17). Similarly to  $k_{\text{IJ}}^{\text{Psel}}$ , the  $k_{\text{IJ}}^{\text{Osel}}$  values are only a constant characteristic for an optical sensor for ions of the same charge and complexes of the same stoichiometry. Therefore, it is advantageous to report measured exchange constants,  $K_{\text{exch}}$  (see eq 54), together with the assumed complex stoichiometries and weighing parameters of the active components. Ion optode selectivities can be reported graphically as individual response functions for every measured ion of interest at a particular pH.<sup>40,159</sup> Accordingly, the selectivity factor  $k_{\text{IJ}}^{\text{Osel}}$  is given by the ratio of primary to interfering ion activity at any given  $\alpha$ . It can be conveniently reported graphically as the horizontal distance between separate calibration curves on a logarithmic activity scale at one chosen pH value (see Figure 32).<sup>40,146,159</sup> For detailed selectivity studies of highly discriminated ions, the ion extraction can be enhanced by changing the sample pH value or employ-

ing an analogous optode with a less basic chromoionophore.<sup>159</sup> By normalizing the measured values, response curves of the optical sensor can be determined also for ions that are discriminated by many orders of magnitude. Examples for this approach are shown in recent works dealing with heavy-metal ion sensors,<sup>146,159</sup> where selectivities of more than 10 orders of magnitude have been determined. It is important to realize that, for ions of different charge, the value of  $k_{\text{IJ}}^{\text{Osel}}$  will heavily depend on the sample pH and the degree of protonation of the chromoionophore (see Figure 29). Of course, this is an important characteristic that can be exploited to optimize the measuring conditions.<sup>40</sup> However, it makes the tabulation of optode selectivity data difficult since they are sample-dependent. This problem exists in complete analogy for ion-selective electrodes if  $k_{\text{IJ}}^{\text{Psel}}$  values are reported (see eq 16). For improved comparison purposes and to relate optode selectivities with the ones obtained with ion-selective electrodes it is, therefore, convenient to formulate a selectivity coefficient for cation-exchange optodes in analogy to the Nicolskii coefficient for ISEs:

$$K_{\text{IJ}}^{\text{opt}} = (k_{\text{IJ}}^{\text{Osel}})^{z_{\text{I}}/z_{\text{J}}} a_{\text{I}}(\text{I})^{1-(z_{\text{I}}/z_{\text{J}})} \quad (64)$$

Inserting eqs 55 and 63 into 64 gives an explicit expression for this Nicolskii-like coefficient of neutral-carrier-based cation-exchange optodes that is independent of the sample pH value:

$$K_{\text{IJ}}^{\text{opt}} = \frac{\left\{ z_{\text{J}} K_{\text{exch}}^{\text{JL}} \left( L_{\text{T}} - \frac{n_{\text{J}}}{z_{\text{J}}} \{R_{\text{T}} - (1 - \alpha) C_{\text{T}}\} \right)^{n_{\text{J}}} \right\}^{z_{\text{I}}/z_{\text{J}}}}{z_{\text{I}} K_{\text{exch}}^{\text{IL}} \left( L_{\text{T}} - \frac{n_{\text{I}}}{z_{\text{I}}} \{R_{\text{T}} - (1 - \alpha) C_{\text{T}}\} \right)^{n_{\text{I}}}} \times \{R_{\text{T}} - (1 - \alpha) C_{\text{T}}\}^{1-(z_{\text{I}}/z_{\text{J}})} \quad (65)$$

This Nicolskii-like coefficient can be determined experimentally by separately measuring the activities of primary and interfering ion that induce a specified  $\alpha$  value. The two activities, together with the respective pH values (denoted with (I) and (J), if different), can then be inserted in the following equation<sup>160</sup>

$$K_{\text{IJ}}^{\text{opt}}(\text{SSM}) = \frac{a_{\text{I}}(\text{I})}{a_{\text{J}}(\text{J})^{z_{\text{I}}/z_{\text{J}}}} \left( \frac{a_{\text{H}}(\text{J})}{a_{\text{H}}(\text{I})} \right)^{z_{\text{I}}} \quad (66)$$

where SSM indicates that the values were measured according to the separate solution method. Apparently, if the pH in both experiments is equal, the equation simplifies to the one given for ion-selective electrodes in eq 11. In fact, the definition of the Nicolskii-like coefficient as shown in eq 66 is identical to the one used in earlier works on neutral-carrier-based optical ion sensors.<sup>160</sup> It is important to realize that, again, such Nicolskii type coefficients should be used with analogous modified equations as established above for the characterization of ISE selectivities. Accordingly, the optode response function for

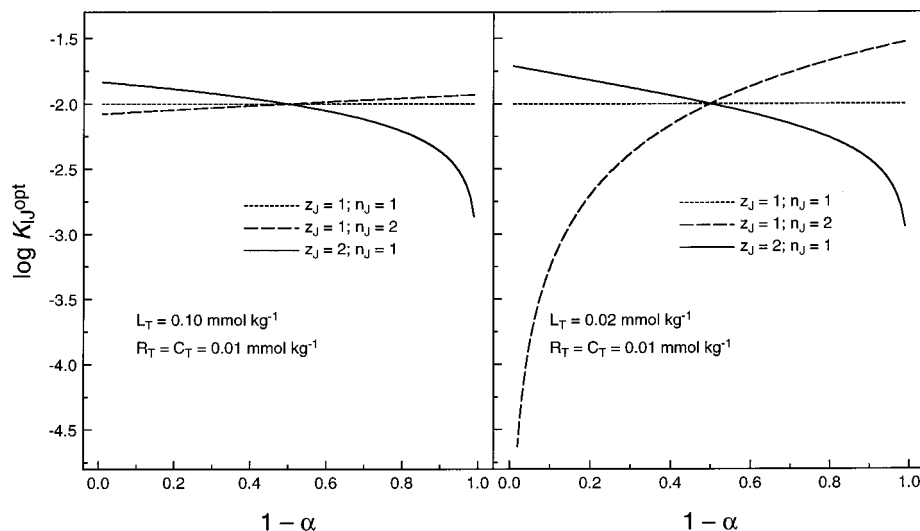


**Figure 33.** Variation of the Nicolskii-like coefficient  $K_{IJ}^{\text{opt}}$  for an optode selective for monovalent ions, forming 1:1 complexes with the carrier, as a function of the degree of protonation of the chromoionophore ( $1 - \alpha$ ) according to eq 65.<sup>161</sup> For divalent interfering ions, or for ions of the same charge but forming 1:2 complexes, significant changes of the selectivity coefficient are observed as the chromoionophore is protonated or deprotonated. This stands in contrast to ion-selective electrodes and is the main reason why the reporting of  $k_{IJ}^{\text{Osel}}$  values is generally preferred for optodes.

the mixed ion response can be described for  $z_I = 1$  and  $z_J = 2$  as

$$\frac{a_I}{2} + \frac{1}{2} \sqrt{a_I^2 + 4a_J(K_{IJ}^{\text{opt}})^2} = (K_{\text{exch}}^{IL_n})^{-1} \frac{\alpha}{1 - \alpha} a_H \frac{R_T - (1 - \alpha)C_T}{\{L_T - (R_T - (1 - \alpha)C_T)(n)\}^n} \quad (67)$$

and for  $z_I = 2$  and  $z_J = 1$  as

$$\left( \sqrt{a_I + \frac{1}{4}K_{IJ}^{\text{opt}} a_J^2} + \sqrt{\frac{1}{4}K_{IJ}^{\text{opt}} a_J^2} \right)^2 = (2K_{\text{exch}}^{IL_n})^{-1} \times \left( \frac{\alpha}{1 - \alpha} a_H \right)^2 \frac{R_T - (1 - \alpha)C_T}{\{L_T - (R_T - (1 - \alpha)C_T)(n/2)\}^n} \quad (68)$$

The required  $K_{IJ}^{\text{opt}}$  values for a particular target application can again be given by an equation analogous to eq 32 for ion-selective electrodes:

$$K_{IJ}^{\text{opt}}(\text{required}) = \frac{a_I(IJ)}{a_J(IJ)^{z_I/z_J}} \left( \frac{p_{IJ}}{100} \right)^{z_I/z_J} \quad (69)$$

However, the Nicolskii-like coefficient  $K_{IJ}^{\text{opt}}$  is, in contrast to ISE membranes, still somewhat dependent on the signal ( $\alpha$ ), as shown by Figure 33.<sup>161</sup> This originates from the fact that any absorbance or fluorescence change is coupled to concentration changes of the active species within the sensing film (see eq 55). One possible solution to this limitation is to report  $K_{IJ}^{\text{opt}}$  values that refer to one selected  $\alpha$  value;  $\alpha = 0.5$  has often been chosen in practice.<sup>39</sup> However, this dependence is one important reason why optode selectivities are usually reported as  $k_{IJ}^{\text{Osel}}$  values according to eq 63. Indeed, the reporting of  $k_{IJ}^{\text{Osel}}$  values, together with the determined  $K_{\text{exch}}$  values, is sufficient for a full characterization of optode selectivity since the response under other experimental conditions can be readily predicted from the given ion-exchange constants. It is therefore less

critical than with ISEs to report Nicolskii-like coefficients  $K_{IJ}^{\text{opt}}$  instead of  $k_{IJ}^{\text{Osel}}$  values. Therefore, Nicolskii coefficients are only preferred when optode and ISE selectivities are to be compared. It has been generally recommended to report both values from the same experiment, namely  $k_{IJ}^{\text{Osel}}$  in graphical form and numerical  $K_{IJ}^{\text{opt}}$  values for one chosen  $\alpha$  value, typically  $\alpha = 0.5$ .<sup>161</sup> In any case, it is extremely important to clearly indicate the definition used in the reporting of selectivity values, together with the determined ion-exchange constants and assumed complex stoichiometries.

### C. Detection Limits

**Lower Detection Limit.** The detection limit of ion-selective bulk optodes is given by various factors, including interference from other ions (with one recommended definition) and loss of sensitivity due to the sigmoidal shape of the response function (which has been defined in two different ways). Moreover, a practical lower limit of detection can be observed for limited sample volumes due to depletion of the sample caused by the extraction process. Accordingly, depending on the scope of the experiment, different possible definitions can be used.

*Detection Limit Because of Interference.* Here, the detection limit can be described in analogy to that of ion-selective electrodes (see above). If interfering ions are extracted into the membrane together with the primary ions, the response function starts to deviate from ideal behavior. In this respect, the detection limit is most conveniently defined by analogy to the recommendations of IUPAC for the characterization of ion-selective electrodes<sup>89</sup> and is given as follows:<sup>111</sup> The response curve of an ion-selective optode at a certain pH is evaluated by fitting the experimental data with eq 55 (curve labeled "ideal" in Figure 34) for the ideal response without interference. The intersection of this curve with the horizontal line corresponding to the degree of protonation

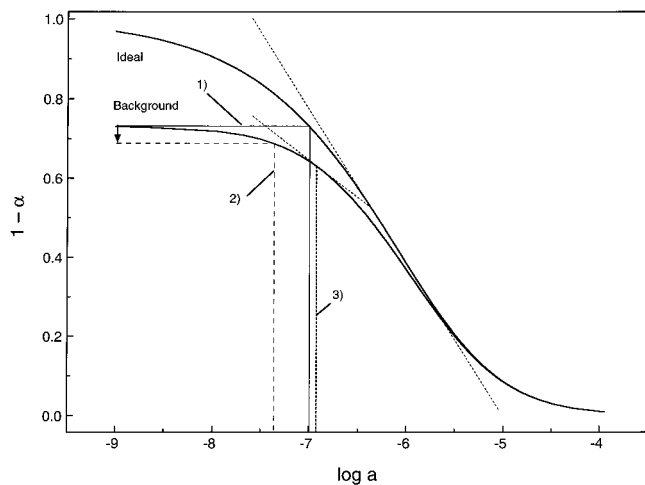


**Figure 34.** Various definitions of the lower detection limit of optodes: (1) the detection limit is given by the intersection of two extrapolated segments of the calibration curve in analogy to ion-selective electrodes,<sup>111</sup> (2) the detection limit is limited by the spectrophotometric uncertainty of the background signal by analogy to other analytical methods,<sup>159</sup> (3) the detection limit is given by a limiting sensitivity (slope) of the response function (shown here as half the maximum value).

determined in the background electrolyte (without primary ions) defines the detection limit  $a_1(\text{DL})$  (cf. 1 in Figure 34). If it is entirely given by the interference from the background, one can write with eqs 62 and 64:

$$a_1(\text{DL}) = K_{\text{IJ}}^{\text{opt}} a_{\text{J}}^{z_{\text{I}}/z_{\text{J}}} = k_{\text{IJ}}^{\text{Osel}} a_{\text{J}} \quad (70)$$

If the selectivity coefficient  $k_{\text{IJ}}^{\text{Osel}}$  is independent of sample concentration changes, the detection limit is proportional to the activity of the interfering ion in the sample.<sup>111</sup> However, no detection limit can be determined with this method if no interference is observed, i.e., the chromoionophore can be fully protonated for samples that contain no primary ions and the methods discussed below apply.

*Detection Limit Due to Loss of Sensitivity as a Consequence of the Sigmoidal Response Curve.* If no appreciable interference is observed, the apparent detection limit is given by the loss of response sensitivity owing to the sigmoidal response curve at low ion activities. For this case, two different approaches have been proposed to report the lower practical limit of detection. The first one defines the detection limit, in analogy to other analytical methods, as a function of the standard deviation of the background noise. For this purpose, the standard deviation of the spectrophotometric determination is calculated as a  $\Delta\alpha$  range and plotted as a vertical error bar at the maximum degree of protonation (signal without analyte ions), usually with a height of  $6 \Delta\alpha$ .<sup>159</sup> The intersection of the theoretical response function (see eq 62) and the lower value of this error bar defines the detection limit, again reported as limiting sample activity or concentration (cf. 2 in Figure 34). Another possibility is to define the limiting slope of the response function as a fraction, usually one-half or one-quarter, of the maximum slope (cf. 3 in Figure 34).<sup>130</sup> The corresponding activity is defined as detection limit.

The three definitions of the detection limit of optical sensors, including the one on the basis of ion interference, are illustrated in Figure 34. Apparently, widely varying lower detection limits will be reported from the very same experiment if different definitions are used. Since the definition based on ion interference conforms to practical usage with ion-selective electrodes, it is here recommended where applicable.

*Effective Detection Limit Due to Analyte Depletion in the Sample.* Extremely selective and sensitive optode films have been prepared for determining subnanomolar levels of heavy-metal ions.<sup>113,146,159</sup> The amount of sample ions that has to be extracted into the polymeric film for the sensor to give a sufficiently large signal change is on the order of  $10^{-9}$  mol for macroscale optodes.<sup>130</sup> This amount is contained in 1 mL of a  $10^{-6}$  M solution, or 1 L of a  $10^{-9}$  M sample. Hence, a significant perturbation of the sample is observed for low analyte concentrations and/or sample volumes, thereby defining a lower apparent detection limit. This effect has been quantitatively described for sensors being measured in the batch-mode<sup>130</sup> and often discussed for flow-through systems.<sup>146,159</sup> While with environmental applications, supply of sample or amount of time to reach the equilibrium signal is often not the limiting factor,<sup>159</sup> this will be a great challenge for designing heavy-metal sensors for application in clinical chemistry or in other areas where sample quantity is small. Some of these limitations might be overcome by decreasing the volume of the sensing film, e.g., by immobilizing the sensing film on the tip of an optical fiber, and/or choosing fluorescence as the detection mode.<sup>145</sup> Moreover, the overall uptake/release of sample ions may be kept small if the composition of the optode film is, between measurements, adjusted to be close to final equilibrium.

**Upper Detection Limit.** The upper detection limit of ion optodes has, until now, not been studied extensively. On one hand, there is a practical upper detection limit that is caused by the sigmoidal shape of the response function, i.e., the sensitivity decreases continuously with increasing sample activity. Such a detection limit can occur earlier if substantial coextraction of sample cations and anions into the solvent polymeric film occurs. This can be described in complete analogy to ion-selective electrodes (see above). While the cation-exchange constant according to eq 54 remains valid, the simultaneous coextraction of sample cations  $\text{I}^{z+}$  and anions  $\text{Y}^-$  into the polymeric film can be described as follows if the effect of ion-pair formation within the organic phase can be neglected:

$$K_{\text{coex}}^{\text{IL}_n} = \frac{[\text{Y}^-]}{a_{\text{Y}}} \left( \frac{[\text{IL}_n^{z+}]}{a_1[\text{L}]^n} \right)^{1/2} \quad (71)$$

This coextraction constant is given by the relative lipophilicity of the anion and cation and the complex formation constant of the ionophore. Simultaneous anion extraction shifts the ion-exchange equilibrium that is responsible for the optode response since the effective concentration of anionic sites continuously increases within the film. It is difficult to define the

**Table 4. Measuring Range [ $\Delta(\log a)$ ] of Neutral-Carrier-Based Optodes<sup>a</sup>**

$Z$	$n$	$\alpha_{\text{optimum}}$	$\alpha_{\text{upper limit}}$	$\alpha_{\text{lower limit}}$	$\Delta \log a$
Cation-Selective Optodes Based on Neutral Carriers					
for large excess of carrier $L_T$					
1	any value	0.586	0.894	0.192	2.22
2	any value	0.551	0.878	0.173	3.78
for $L_T = (n/z)R_T$					
1	0	0.586	0.894	0.192	2.22
1	1	0.500	0.854	0.146	3.06
1	2	0.449	0.827	0.122	3.78
1	3	0.414	0.808	0.106	4.44
2	1	0.500	0.854	0.146	4.59
2	2	0.464	0.835	0.129	5.33
2	3	0.436	0.820	0.116	6.01
Anion-Selective Optodes Based on Neutral Carriers					
for large excess of carrier $L_T$					
1	any value	0.414	0.106	0.808	2.22
2	any value	0.449	0.122	0.827	3.78
for $L_T = (n/z)R_T$					
1	0	0.414	0.106	0.808	2.22
1	1	0.500	0.146	0.854	3.06
1	2	0.551	0.173	0.878	3.78
1	3	0.586	0.192	0.894	4.44
2	1	0.500	0.146	0.854	4.59
2	2	0.536	0.165	0.871	5.33
2	3	0.564	0.180	0.884	6.01

<sup>a</sup>The two limiting slopes of the response function are allowed to be half the optimum value (see Figure 34, definition 3).  $Z$ , charge number of the analyte ion;  $n$ , stoichiometry of the ion–ligand complex;  $\alpha$ , mole fraction of nonprotonated chromoionophore;  $L_T$  and  $R_T$ , total concentrations of neutral carrier and ionic sites.

upper detection limit by analogy to ion-selective electrodes since the optode response function is not expected to flatten to a limiting value in a similar way. Since a detailed study of these processes has not been reported yet, this discussion has to remain rather qualitative. A possible measure for the upper detection limit is the limiting sample activity value that induces a specified optode signal in the presence of simultaneous anion interference. Because of the latter, responses in presence and absence of such salt extraction into the optode membrane differs significantly. Apparently, the coextraction is most pronounced for lipophilic sample anions and cations, for high complex formation constants, and for a low concentration of ionic sites relative to free carrier. Since similar effects are involved, such an upper detection limit should be observed under roughly similar experimental conditions as with the corresponding ion-selective electrodes.

#### D. Measuring Range

The two limiting activities at which the slope of the response function reduces to half its maximum value have been used to quantify the practical measuring range of the optodes described herein. In Table 4, calculated values for the detection limit of ion-selective optodes are shown. It is here assumed that the limiting upper and lower sample activities are given at the point where the sensitivity (slope) of the response function is decreased by a factor of 2 compared to its maximum value (see definition 3 in Figure 34). Measuring ranges typically cover 2–4

orders of magnitude and depend on the membrane composition, the charge of the analyte ion (they increase with increasing charge), and the stoichiometry of the formed complex in the polymeric film. For anionic compared to cationic analytes the limiting  $\alpha$  values differ since the sign of the response slope is opposite. The overall measuring range remains nonetheless the same (see the lower part of Table 4). This treatment is somewhat biased for ions of higher valency since the optode response slope toward monovalent ions is about double compared to the one for divalent ions. In practice, therefore, the values given here are for illustrative purposes only and the limiting optode response slopes should be evaluated on the basis of spectrophotometric accuracy. It is important to note that the response range of a particular sensor can be easily shifted within a wide range by changing the sample pH and by choosing a chromoionophore with a different  $pK_a$  value, until interference is the limiting factor. These parameters can be adjusted to obtain maximum sensitivity at the target concentration.<sup>145,159</sup> This is an advantage of bulk optodes relying on competitive ion-exchange or coextraction equilibria with organic films containing two different complexing agents. Consequently, the same selective ionophore can be used to fabricate sensors that are sensitive to widely varying ion concentration ranges.

#### E. Response Time

Since an equilibrium between optode film and sample must be reached for every measurement, the response time is most often determined by the time necessary to attain a uniform concentration of the optically relevant components, i.e., the unprotonated and protonated  $H^+$ -chromoionophore, in the membrane. Except for extremely thin membranes, diffusion within the organic phase is time-limiting. By assuming a mean diffusion coefficient  $D_m$  for all mobile species in an optode membrane of thickness  $d$ , the solution of the respective diffusion equation<sup>162</sup> leads to the following expression:<sup>136</sup>

$$A(t) = A(\infty) - \{A(\infty) - A(0)\} \times \frac{8}{\pi^2} \sum_{m=0}^{\infty} \frac{1}{(2m+1)^2} \exp\left(-\frac{(2m+1)^2 \pi^2 D_m t}{4d^2}\right) \quad (72)$$

The time needed to achieve 95% of the steady state response,  $t_{95\%}$ , is

$$t_{95\%} = 1.13 \frac{d^2}{D_m} \quad (73)$$

For a membrane of  $d \approx 1 \mu\text{m}$  with  $D_m \approx 10^{-8} \text{ cm}^2 \text{ s}^{-1}$ , eq 73 predicts 95% response times on the order of seconds, which were also observed experimentally.<sup>39,163</sup> A slightly faster response is observed with an acrylamide hydrogel membrane with a covalently immobilized calcium-selective fluorescent ligand, where the diffusion of ionic calcium is rate-limiting.<sup>164</sup> On the other hand, response times on the order of hours were measured with extremely diluted solutions ( $10^{-7}$ – $10^{-9} \text{ M}$ ), where the mass transfer from the bulk of the sample to the membrane interface

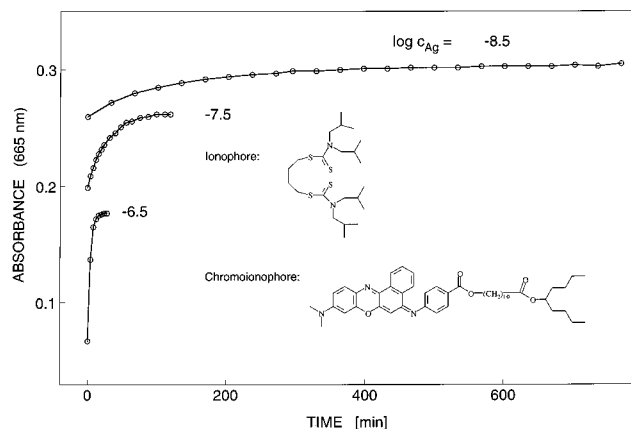


**Figure 35.** Response time curves for a silver ion-selective optode to various  $\text{AgNO}_3$  solutions at pH 4.70 ( $\text{Mg}(\text{OAc})_2$  buffer).<sup>113</sup>

becomes rate-limiting (see Figure 35).<sup>146,159</sup> Similar to ISEs, consistently much slower responses are observed for samples which are more diluted than the preceding ones.

### 3. Comparison of Optical and Potentiometric Transduction Schemes

#### A. Response Mechanism

Although both carrier based ion-selective electrodes and ion optodes rely on the same active components and polymeric materials as well as similar equilibria, they are in a certain way complementary in terms of response mechanism (see above). In ISEs, the measured potential is a direct function of the activities of the analyte ion in the sample and membrane phase. A Nernst response is therefore only expected if the free interfacial ion activity in the organic phase is not significantly altered by changing the sample composition. In the case of optical sensors, the reverse has to be achieved: changes in sample composition have to induce well-defined concentration changes in the sensing film that can be detected as an optical response. For these reasons, bulk optodes measure ratios or products of two sample ion activities. In order to obtain the activity of the target ion, one of the extracted species has to be measured by other means or must be kept constant.

In contrast to bulk optodes, the response of an ion-selective electrode can be expressed by the equilibrium activities of only one kind of analyte ion between two phases. For these reasons, ISEs could, in principle, be regarded as being responsive to single ion activities. However, two electrodes are needed to obtain emf values. If two ISEs are measured against each other in a galvanic cell, each selective for a different ion, it is again the ratio or product of activities that defines the potential. In practice, a reference electrode is used whose response is assumed to be nearly sample-independent. The invalidity of this assumption is the fundamental reason that prohibits the determination of true single ion activities with ion-selective electrodes.

The difference in response mechanism between ISEs and bulk optodes also shows in the variations of allowed concentration ratios of components within the polymeric material. For example, an ISE mem-

brane that contains an excess of ionic sites over ion carrier such that substantial quantities of uncomplexed sample ions are extracted into the membrane will hardly show any influence of the carrier on the selectivity. Since the response is dependent on the equilibrium activities of the free ion, such an ISE would respond as a nonspecific ion-exchange membrane with selectivities defined by the relative lipophilicity of the sample ions. To exploit the selectivity of the complex formation of the ion carrier it is, therefore, necessary to incorporate a sufficiently high concentration of carrier relative to ionic sites within the membrane. In contrast, it is customary to prepare bulk optodes with an excess of ionic sites over chromoionophore. This ensures that the indicator can be fully protonated. The excess of ionic sites is, at all times, partly counterbalanced by extracted sample ions that are complexed by the lipophilic carrier. This has only a marginal influence on the optode response that is observed when the incorporated pH indicator is deprotonated due to competing sample cations entering the polymeric film. Therefore, a typical bulk optode formulation for monovalent target ions forming 1:1 complexes contains the highest molar concentration of ion carrier, followed by ionic sites, and an equal or smaller concentration of  $\text{H}^+$ -chromoionophore ( $L_T > R_T > C_T$ ).

The response of bulk optodes is affected by changes in the optical properties of the polymeric film and, in the transmission mode, of the sample. The uptake of heterogeneous water as separate droplets within the film can lead to turbidity and, therefore, bias the optical response as well. It has been recently found for thick PVC membranes that the turbidity is sample-dependent.<sup>165</sup> However, such effects have typically not been observed with optode films which are only a few micrometers thick. Swelling of the film can be an additional problem because it alters the concentrations and the optical path length. While these two effects should cancel out in the transmission mode and give no net effect, they could pose more serious limitations with evanescent wave spectrometry<sup>166</sup> or similar detection principles. Additionally, the uptake of species that influence the ion activities within the polymeric film is expected to have considerable influence on the optode and ISE response. Indeed, some authors have argued that the sample-dependent extraction of dissolved water into these films could have a significant influence on the optode response.<sup>42</sup> While this is indeed a possible effect, theoretical models neglecting it have been used for real-world samples without apparent restrictions. An explanation might be the fast equilibration of these thin films with homogeneously dissolved water. Since analogous thermodynamic parameters apply for both systems, the same restrictions can also be expected for ion-selective electrodes. Indeed, changes in the activities of the extracted species have a direct influence on the measured potential. While some effects might be canceled owing to a similar change at the membrane–inner filling solution interface, a perfectly symmetric influence cannot be expected since the amount of extracted water is sample-dependent.<sup>165</sup> Similarly, the large response of valinomycin-based electrodes to higher alcohols<sup>65</sup> is most

likely caused by a change in the interfacial polymeric film composition due to alcohol uptake that, in turn, alters the complex formation constant of the  $K^+$ -valinomycin complex. Such an effect is also expected for bulk optodes if the change in the complex formation constant is not equal for both incorporated ionophores.

### B. Selectivity

A general selectivity description has been established above for optical and potentiometric sensors based on the same chemical recognition principles (see above). It is interesting to use them for evaluating whether one of the sensing schemes, in principle, is the more selective one. For this purpose, the relationship between the Nicolskii coefficient and measuring error can be compared for both measuring systems on the basis of eqs 32 and 69:

$$p_{IJ} = 100a_J(IJ) \left( \frac{K_{IJ}^{\text{pot}}}{a_I(IJ)} \right)^{z_I/z_J} = 100a_J(IJ) \left( \frac{K_{IJ}^{\text{opt}}}{a_I(IJ)} \right)^{z_I/z_J} \quad (74)$$

For ISEs based on neutral carriers forming complexes with a well-defined stoichiometry, the following relationship holds between selectivity coefficient and membrane composition (see above):

$$K_{IJ}^{\text{pot}} = K_{IJ} \frac{(\beta_{JL_{n_j}})^{z_I/z_J} [IL_{n_i}^{z_I^+}(I)]}{\beta_{IL_{n_i}} [L(I)]^{n_i}} \left( \frac{[L(J)]^{n_j}}{[JL_{n_j}^{z_I^+}(J)]} \right)^{z_I/z_J} \quad (36)$$

After inserting eq 74 into 36, a relationship between measuring error,  $p_{IJ}$ , the sample activities, membrane concentrations, and stability constants of the involved complexes is obtained:

$$p_{IJ} = 100a_J(IJ) \beta_{JL_{n_j}} \frac{[L(J)]^{n_j}}{[JL_{n_j}^{z_I^+}(J)]} \times \left( \frac{K_{IJ}}{a_I(IJ) \beta_{IL_{n_i}}} \frac{[IL_{n_i}^{z_I^+}(I)]}{[L(I)]^{n_i}} \right)^{z_I/z_J} \quad (75)$$

Interestingly, for bulk optodes based on the same carrier, an identical relationship can be derived. In this case, the Nicolskii-like coefficient,

$$K_{IJ}^{\text{opt}} = \frac{\left\{ z_J K_{\text{exch}}^{JL_{n_j}} \left( L_T - \frac{n_J}{z_J} \{ R_T - (1-\alpha) C_T \} \right)^{n_j} \right\}^{z_I/z_J}}{z_I K_{\text{exch}}^{IL_{n_i}} \left( L_T - \frac{n_I}{z_I} \{ R_T - (1-\alpha) C_T \} \right)^{n_i}} \times \{ R_T - (1-\alpha) C_T \}^{1-(z_I/z_J)} \quad (65)$$

is readily simplified by inserting the definitions for the respective overall ion-exchange constants,  $K_{\text{exch}}$  (see eq 54), and the charge and mass balances for the membrane phase and gives, after combining with eq 65, exactly the same eq 75. Therefore, no difference in selectivity is expected between potentiometric and optical sensing schemes as long as the respective equilibrium concentrations of free and complexed

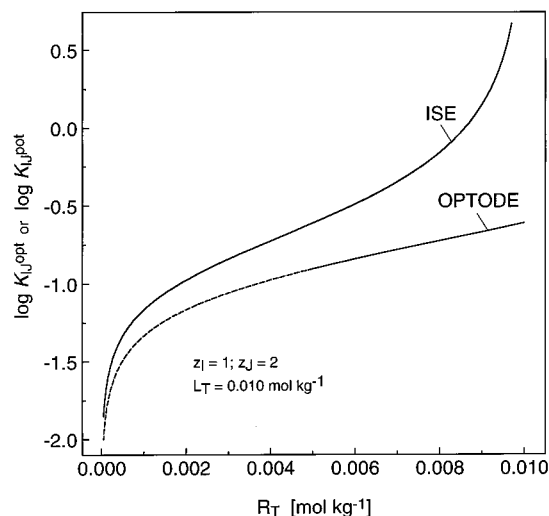


**Figure 36.** Nicolskii and Nicolskii-like selectivity coefficients for analogous potentiometric and optical sensing films containing  $10 \text{ mmol kg}^{-1}$  ionophore  $L_T$  and various concentrations of anionic sites  $R_T$ , calculated according to eqs 37 and 65. The primary ion is monovalent and the interfering ion divalent. The optode film contains in addition  $5.0 \text{ mmol kg}^{-1}$   $H^+$ -chromoionophore  $C_T$  and is assumed to be measured at  $\alpha = 0.5$  (half of chromoionophore is protonated). Other parameters are chosen arbitrarily. The dotted line shows the potentially impractical range for an absorbance-based optode since a decreased concentration of anionic sites is at the expense of sensitivity.

carrier within the membrane are identical. However, in practice, this is difficult to achieve, since, in contrast to ion-selective electrode membranes, the equilibrium concentrations for a bulk optode vary with changing sample activities. Only in the special case of equal charge of the competing ions and stoichiometry of the formed complexes, no such selectivity dependence is expected. For ions of different valencies, however, the dependence of the selectivity on the degree of protonation of the chromoionophore ( $1 - \alpha$ ) is especially pronounced. For a direct experimental comparison of selectivities, the concentrations of free and complexed carrier must, therefore, be equal for ISE and optode. In practice, one specific degree of protonation of the chromoionophore (usually  $\alpha = 0.5$ ) is chosen for the optode measurement. Figure 36 shows calculated selectivity coefficients for analogous ISEs and optodes that are selective for a monovalent ion, at varying concentrations of anionic sites, according to eqs 37 and 65. The selectivity coefficients for both systems are different, since at the assumed  $\alpha = 0.5$  ( $R_T = 0.005 \text{ mol kg}^{-1}$ ), the fraction of uncomplexed ionophore is higher for the optode than for ISE membrane. To accomplish the same equilibrium concentration of free to complexed ligand, the corresponding ISE has to be prepared with a higher carrier to ionic sites concentration ratio, i.e., with a lower concentration of  $R_T$  (ca.  $2.5 \text{ mmol kg}^{-1}$  in the case shown in Figure 36) than the optode. In general, such systems cannot be compared over the entire calibration curve, i.e., the increase in the free carrier concentration as  $\alpha$  is decreased will make a monovalent ion-selective optode more selective over divalent interfering ions than the ISE, and vice versa.

The selectivity of both optodes and ISEs can be effectively tuned by incorporating different concen-

trations of the active membrane components and adjusting the polarity of the membrane material. For example, the selectivity of a  $\text{Na}^+$ -selective sensor over  $\text{Ca}^{2+}$  can be optimized by using a large excess of  $\text{Na}^+$  carrier over anionic sites and a relatively nonpolar plasticizer such as dioctyl sebacate.<sup>167,168</sup> For ISEs, the lower concentration limit of ionic sites is usually given by the charged impurities already present in the polymer and plasticizer, which was for one system recently determined as about  $63 \mu\text{mol kg}^{-1}$  (see below section III.2.C),<sup>83</sup> and the solubility of the carrier on the other hand. However, for ion-selective optodes, the concentration of ionic sites controls the overall magnitude of the optical response via the electroneutrality condition within the polymeric film. Traditionally, therefore, the effective site concentration of such sensors has been chosen as  $5 \text{ mmol kg}^{-1}$  or higher, thus yielding optodes with worse selectivities for monovalent ions than the corresponding electrodes (see the left side of Figure 36).<sup>167</sup> The reverse problem is the case with sensors selective for divalent ions. Here, the concentration of free over complexed carrier has to be kept small to discriminate monovalent ions as much as possible. With electrodes, this is accomplished with membranes that contain as much as 70 or 160 mol % of anionic sites relative to carrier, depending on the stoichiometry of the formed complexes. Again, such exact concentration ratios cannot be achieved with ion optodes since the composition is a function of the sample solution. It should also be noted that ion-selective electrode membranes containing extremely high relative site concentrations are known to show nonrobust behavior such as long term drift that originate from concentration shifts within the polymeric membrane.<sup>79</sup>

One drawback of ion-selective electrodes is that only one kind of ion is allowed to partition between sample and membrane phase. Therefore, carriers that contain an additional binding site, for example for  $\text{H}^+$  ions, show considerable interference from that other ion. In contrast, such a behavior is not problematic with bulk optodes as long as this second ion is chosen as reference. Indeed, a number of lipophilic ligands that bind metal ions under the release of hydrogen ions are known from classical extraction chemistry. While these ligands are often not suited for ion-selective electrodes, they can sometimes be successfully used for optodes.<sup>150</sup> Consequently, the addition of a  $\text{H}^+$ -selective chromoionophore is successful here as well if it is more basic than the incorporated carrier. One possible application of the latter concept might be the design of an optical magnesium ion sensor on the basis of a basic magnesium ion carrier that shows high selectivity but considerable pH cross-interference if applied with ion-selective electrodes.<sup>169</sup>

### C. Detection Limit

It has repeatedly been observed that bulk optodes on the basis of highly selective carriers show much lower detection limits in unbuffered solutions than their ISE counterparts. (See Note Added in Proof.) This characteristic is, without doubt, one of the most striking advantages of bulk optodes over conventional ISEs. Generally, detection limits of ISEs are around

$10^{-6} \text{ M}$  and can only be significantly lowered if ion buffers are used. The reason for this difference is the constant release of low levels of analyte ions from the membrane into the sample, so the concentration at the interface is higher than in the bulk. This directly affects the signal of the ISE since the electrode response is dependent on the interfacial ion activities. Bulk optodes, unlike stationary ISE measurements, are at true equilibrium with the sample and no leaching of membrane ions from the polymer film can bias the sample concentration at the optode surface. Accordingly, subnanomolar analyte levels have been measured with some bulk optodes.<sup>111,146,159</sup> To minimize the perturbation of the sample due to extraction of ions into and from the optode film, the total amount of extracted ions has to be kept small relative to that in the sample. Moreover, the use of a flow-through system is advantageous since it ensures a continuous supply of unperturbed sample.

One possible drawback of this increased sensitivity of optodes relative to ISEs is that low levels of extremely preferred ionic impurities could more easily mask the response of optodes. With ISEs, it is known that small concentrations of such species are extracted into the polymeric membrane but continuously diffuse away from the interface into the membrane bulk.<sup>97,170</sup> Therefore, only impurity levels of about  $10^{-6} \text{ M}$  or higher have a significant influence on ISE responses. Due to this effect, experimental selectivity values for optodes can in certain cases differ quite significantly from those of ISEs.<sup>145,171</sup> This important effect can also be explained with the phase boundary potential after accounting for the depletion of analyte ions in the boundary region.<sup>97</sup>

### D. Measuring Range

The measuring range of ISEs is, with 5–9 orders of magnitude, much larger than that of optodes, with 2–4 orders of magnitude, depending on the valency of the measuring ion and stoichiometry of the formed complexes. The reason for this discrepancy lies in the difference in the two response mechanisms. However, for cation-selective optodes based on two different ionophores, the effective measuring range can be conveniently tuned by incorporating  $\text{H}^+$ -chromoionophores with varying basicities, thereby shifting the ion-exchange or coextraction equilibria to higher or lower activity values. In fact, since highly selective optical sensors show much lower detection limits than corresponding ion-selective electrodes, optical sensor arrays could be made with relative ease that cover a much larger activity range than one conventional ISE.

### E. Response Time

The response of potentiometric sensors is, in general, much faster than that of bulk optodes. In fact, the measured potential virtually immediately follows the activity changes in both phases at the membrane interface, and the rate-limiting step is the establishment of the equilibrium between the activities in the aqueous phases at the surface layer and in the bulk of the sample. Depending on the direction and magnitude of the sample activity change, response times are usually in the millisecond to second range. They are considerably longer if a diluted solution is



measured after a more concentrated one (cf. eq 51). In optodes, on the other hand, equilibrium between sample and the whole bulk of the film must be established. Here, diffusion within the polymeric phase is usually rate-determining (cf. eq 73). Reported response times are on the order of seconds to minutes. However, with very dilute sample solutions, where the net mass transfer of analyte ions into the optode film is rate-limiting, response times may be on the order of hours. Such systems may still be relevant for continuous monitoring, e.g., for environmental analysis but not for rapid measurements as needed for example in clinical analysis.

#### F. Lifetime

It is well-established that the loss of plasticizer, carrier, or ionic site from the polymeric film due to leaching into the sample is a primary reason for limited lifetimes of carrier-based sensors. In principle, this shifts the involved equilibria for both ISEs and optodes and, therefore, should lead to a slow deterioration of selectivity and response of both. For ISEs, the concentration decrease, if slow, would simultaneously occur at the membrane–inner filling solution interface, so that no net effect is expected in the measured potential, although the selectivity would still deteriorate. In contrast, solid contact ISEs indeed show potential shifts due to leaching (see section II.1.A). With classical electrodes, the critical concentration can be established on the basis of loss of selectivity and electrode slope. In most cases, this limit is reached when the concentration of incorporated ion carrier drops below that of the ionic site concentration. For membranes that contain no additional ionic sites and rely on charged impurities, a 100-fold concentration decrease is usually allowed before breakdown of selectivity and slope is observed.<sup>172</sup> For example, it has been demonstrated that valinomycin-based electrodes continued to function after 10 years of soaking.<sup>173</sup> For systems containing added ionic sites, the maximum allowed loss is much smaller and depends on the rate of simultaneous concentration decrease of these sites.<sup>174</sup>

In contrast to ISEs, the response of optical sensors directly depends on the concentration of active components. A loss of any compound (ionophore, chromoionophore, ionic site) leads to shifts in ion extraction equilibria and therefore in the signal (see eq 55). In such cases, recalibration is required to ensure accurate measurements. Fortunately, no sudden breakdown of response is expected for bulk optodes if the concentration of carrier falls below that of the ionic sites (see above).

One major drawback of optical sensors is that their thickness, owing to the necessity of equilibrating the bulk of the sensing film after each sample activity change, is about 100 times smaller than that of macroelectrodes (typically 1–2  $\mu\text{m}$  vs 200  $\mu\text{m}$ ). Since the leaching rate is directly proportional to the thickness of the sensing film, it is ca. 100 times faster for optodes than ISE membranes. However, modern screen printed ion-selective electrode arrays are much thinner (ca. 40  $\mu\text{m}$  or less) and higher leaching rates have to be expected in these cases as well. Moreover, bulk optodes usually rely on a higher

number of components than ISEs, complicating the lifetime issue even further. For optodes, it is unfortunate that the incorporated  $\text{H}^+$ -chromoionophores are critical components in terms of lifetime since their lipophilicity is drastically decreased in contact with acidic sample solutions due to the additional sample protonation equilibrium (see eq 82 below). The covalent immobilization of active components onto the polymeric backbone of the membrane<sup>82,158,175,176</sup> is certainly one way to ensure a high lifetime of both ISEs and optical sensors, especially for measurement of relatively lipophilic samples such as whole blood or organic solutions. For optodes, this goes at the expense of longer response times, however.<sup>158</sup> It should be noted that the loss of components due to chemical or photochemical processes is a limiting factor as well, especially for optical sensors. Indeed, tetraphenylborates are known to decompose under the influence of acid and light.<sup>82,177,178</sup> Similarly, photobleaching of chromoionophore can occur, especially with the strong excitation sources used in fluorescence detection.<sup>112,145</sup>

One important drawback of ISEs is that a physical hole in the membrane or an otherwise incomplete isolation of sample and inner filling solution will cause an electrical short and, therefore, complete breakdown in membrane response, an effect that does not occur with optical sensors since not a potential but a color change within the film is measured. This can lead to much longer lifetimes of optical sensors relative to ISEs in certain situations. This characteristic allows for a wider variety of designs of optical sensors, including extreme miniaturization.

### III. Specific Requirements for Ionophores and Membrane Matrices

#### 1. Ionophores

##### A. General Considerations

To act as ion carriers in biological membranes in which ions are transported by a potential gradient, ionophores require a fine-tuned balance between the free energies of ion–ligand interaction and ion hydration. Ion selectivities, as defined by the ion exchange constant,  $K_{IJ}$ , of the ions I and J in equilibrium between an aqueous and an organic phase (cf. eq 34), usually correspond to free energy differences on the order of a few tens of kilojoules/mol, while the free energies of hydration and complexation within the individual phases are between hundreds and thousands of kilojoules/mol. Thus, ion selectivity represents a small difference between two large effects. Since both natural<sup>4,13</sup> and synthetic ion carriers are capable of transporting cations through cell membranes,<sup>12,179,180</sup> it is still widely believed that their free energy of complexation must be on the same order of magnitude as that of hydration. This is incorrect because the total concentration of cations in sensing films is not determined by the strength of cation–ligand interactions but essentially by the amount of incorporated anions that remain in the organic phase owing to their lipophilicity or immobility. The range of adequate complex formation constants in the membrane covers several orders of

**Table 5. Reported Formation Constants of Valinomycin–Potassium Ion Complexes in Various Solvents**

solvent	$\log \beta_{\text{KL}}$	solvent	$\log \beta_{\text{KL}}$
H <sub>2</sub> O	0.37 <sup>184</sup>	EtOH	6.30 <sup>186</sup>
	0.09 <sup>85</sup>		6.08 <sup>187</sup>
MeOH	4.90 <sup>188</sup>	DOS–PVC (2:1)	9.30 <sup>84</sup>
	4.48 <sup>185</sup>		

**Table 6. Complex Formation Constants for Various Cation-Selective Ionophores within Solvent Polymeric Membranes As Determined from Optode Ion-Exchange Constants<sup>84</sup>**

I <sup>z+</sup>	ionophore L	complex stoichiometry <i>n</i>	plasticizer	$\log \beta_{\text{IL},n}$
K <sup>+</sup>	valinomycin	1	DOS	9.3
Na <sup>+</sup>	valinomycin	1	DOS	6.4
K <sup>+</sup>	BME-44	1	DOS	7.9
Na <sup>+</sup>	BME-44	1	DOS	5.5
Na <sup>+</sup>	ETH 4120	2	BBPA	7.5
Ca <sup>2+</sup>	ETH 129	3	DOS	23.8
Ca <sup>2+</sup>	ETH 1001	2	DOS	19.7

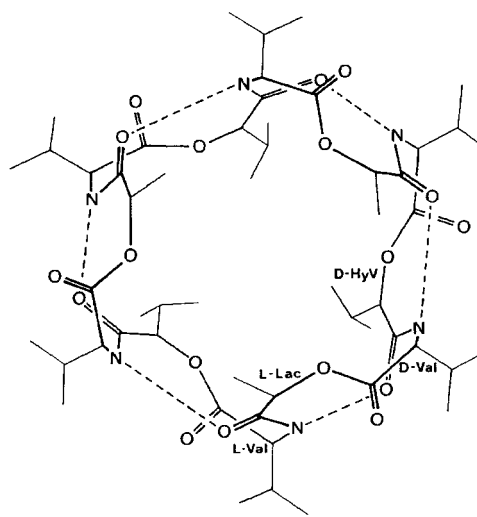
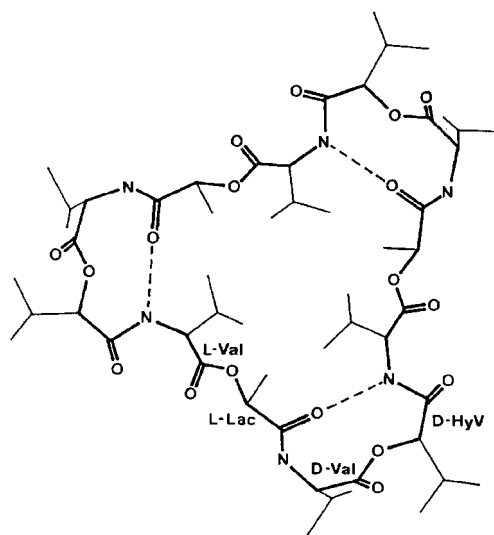
magnitude, from ca. 10<sup>4</sup> to 10<sup>9</sup> mol<sup>-1</sup> kg for a 1:1 stoichiometry.<sup>84</sup> The lower limit is set by the requirement that, in order to make full use of the ionophore's selectivity, ions must be present predominantly in complexed form, whereas the upper limit is determined by the fact that counterions from the sample must not enter the sensing film, otherwise the coextraction of the analyte ion and its counterion deteriorates the response of both potentiometric and optical sensors. For a given ligand, the limit of coextraction is influenced by the activity of the measuring ion and the lipophilicity of the counterion in the sample as well as by the membrane composition. While the interference in the response of cation-selective electrodes is most often caused by lipophilic sample anions such as perchlorate or thiocyanate, it can also occur with very hydrophilic ions for extremely stable complexes and/or if the site concentration in the membrane is low (see section II.1.A).<sup>50,181,182</sup>

Thermodynamic parameters for ion complexing reactions of numerous ionophores and related ligands have been mainly determined in polar solvents<sup>85,183–188</sup> in which complex formation constants were found to be lower by many orders of magnitude than those in ISE membranes (cf. Table 5). The differences are a consequence of the weak solvation properties of the rather apolar organic membrane phases. Voltammetry at the interface of two immiscible electrolyte solutions<sup>189,190</sup> has been applied to determine complex formation constants of lipophilic ligands in organic solvents, e.g., nitrobenzene (saturated with water), which in regard to its high polarity and lack of complexing functional groups resembles the polar *o*-nitrophenyl octyl ether (*o*-NPOE) often used as plasticizer in ISE membranes. Complex formation constants in the membrane phase have been determined recently for several cation-selective ionophores.<sup>84</sup> For 1:1 complexes of monovalent cations, they are up to 10<sup>9</sup> mol<sup>-1</sup> kg (cf. Table 6).

The selectivity behavior of ISEs and optodes is defined by the ion exchange constants which depend on the standard free energies of the respective ions in the aqueous and organic phases (cf. Table 7) as well as on the selectivity of complexation. The former

**Table 7. Standard Free Energies of Transfer (kJ mol<sup>-1</sup>) from Water to Nitrobenzene Obtained with the Extrathermodynamic Assumption That the Cation and the Anion of Tetraphenylarsonium Tetraphenylborate Have Equal Free Energies of Transfer<sup>189</sup>**

cations	$\Delta G_{\text{tr}}^0$	anions	$\Delta G_{\text{tr}}^0$
H <sup>+</sup>	32.5	F <sup>-</sup>	44.0
Li <sup>+</sup>	38.2	Cl <sup>-</sup>	31.4
Na <sup>+</sup>	34.2	Br <sup>-</sup>	28.4
K <sup>+</sup>	23.4	I <sup>-</sup>	18.8
Rb <sup>+</sup>	19.4	NO <sub>3</sub> <sup>-</sup>	24.4
Cs <sup>+</sup>	15.4	BF <sub>4</sub> <sup>-</sup>	11.0
Mg <sup>2+</sup>	69.6	ClO <sub>4</sub> <sup>-</sup>	8.0
Ca <sup>2+</sup>	67.3	SCN <sup>-</sup>	5.8
Sr <sup>2+</sup>	66.0	B(Ph) <sub>4</sub> <sup>-</sup>	-35.9
Ba <sup>2+</sup>	61.7	octanoate	-8.5
NH <sub>4</sub> <sup>+</sup>	26.8	picrate	-4.6
N(CH <sub>3</sub> ) <sub>4</sub> <sup>+</sup>	3.4	dodecyl sulfate	4.1
N(CH <sub>2</sub> CH <sub>3</sub> ) <sub>4</sub> <sup>+</sup>	-5.7		
As(Ph) <sub>4</sub> <sup>+</sup>	-35.9		

**Figure 37.** Conformation of valinomycin in nonpolar solvents (for the structural formula, see Figure 3). All six amide hydrogens form 1–4 intramolecular hydrogen bonds.<sup>18</sup>**Figure 38.** Conformation of valinomycin in solvents of medium polarity. Three intramolecular hydrogen bonds occur. In highly polar solvents, such as dimethyl sulfoxide or methanol, no intramolecular hydrogen bonds are present.<sup>18</sup>

can be influenced, to some extent, by choosing an appropriate plasticizer and polymer matrix for the

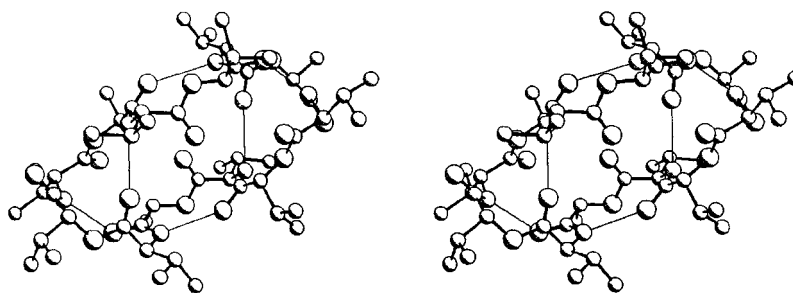


**Figure 39.** Stereoview of the X-ray structure of uncomplexed valinomycin.<sup>18</sup>

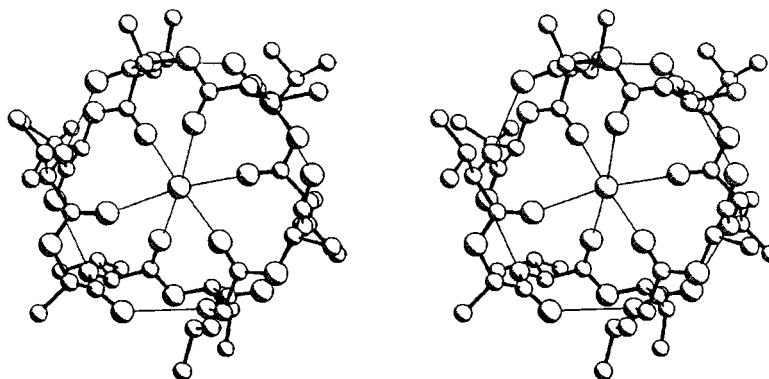


**Figure 40.** Stereoview of the X-ray structure of the valinomycin- $K^+$  complex.<sup>18</sup>

organic phase (see section III.2.A). Still, the most important means of realizing highly selective sensors is to use ligands that strongly complex the preferred ion and only weakly all the others. Notwithstanding, as mentioned above, there is an upper limit to the complex formation constant allowed (cf. eqs 44 and 47).

In general, both electrically neutral and charged ligands (referring to their uncomplexed state) can be used in ion sensors. The earlier notion that the complexation selectivity of charged ligands cannot be fully exploited in sensors<sup>29</sup> proved to be wrong.<sup>69</sup> However, adequate selection of ionic membrane additives is important (see section III.2.B). While in the past no clear distinction was made between charged monodentate ligands and lipophilic ions capable of forming ion pairs, they can be distinguished on the basis of the selectivity of interaction. Thus, tetraphenylborates and tetraalkylammonium salts, though forming ion pairs to some extent,<sup>191</sup> induce selectivities that are essentially determined by the free energies of solvation of their ions in the aqueous and membrane phases. In contrast, various charged porphyrin complexes are capable of binding anions and thus lead to selectivities that are very different from those obtained with ion exchangers (see section IV).<sup>71</sup>

In host-guest chemistry, it is widely believed that good complex stability requires a considerable degree of preorganization according to the principle that "the more highly hosts and guests are organized for binding and low solvation *prior* to their complexation, the more stable will be their complexes".<sup>192</sup> This principle is often understood in a geometric way, i.e., the free ligand is considered to be preorganized if its structure resembles that of the complex. In thermodynamic terms, however, it means that the free energy difference between the conformations of the two forms is small, even though their geometries may

be very different. Thus, valinomycin or 18-crown-6 can be considered as preorganized although their structures change substantially upon complexation.<sup>18,193,194</sup> Depending on the polarity of the solvent, different conformations have been observed in solution (cf. Figures 37 and 38).<sup>18</sup> None of them resembles the one observed by X-ray analysis of the free ionophore (cf. Figure 39),<sup>18</sup> which again differs from the structure of the  $K^+$ -complex (Figure 40).<sup>195</sup> For 18-crown-6, various model calculations showed the free energy differences between the geometrically very different conformations of the uncomplexed and complexed ligand to be small.<sup>196</sup> Moreover, a large number of highly selective nonmacrocyclic ionophores of practical relevance are available which do not exhibit an extensive geometric preorganization (see part 2<sup>6</sup>). The reason for the lower extent of required preorganization could be that, owing to the much larger interaction energies with ionic as compared to uncharged molecules, conformation energy differences between free and complexed hosts might be less relevant for ion carriers than for hosts complexing neutral guests. In general, ligands for use in sensors should possess high conformational flexibility, i.e., a limited geometric preorganization, in order to guarantee a rapid exchange (see section III.1.C).

Not only compounds that can form complexes are able to act as ionophores. Any reversible reaction involving covalent bond formation can be used if the equilibrium is established sufficiently fast. As examples, the response of carbonate ISEs based on trifluoroacetophenone derivatives (cf. Figure 41)<sup>197</sup> or of a bisulfite ion- and sulfur dioxide gas-selective optical sensor with a lipophilic benzaldehyde derivative as ionophore is due to covalent bond formation (cf. Figure 42).<sup>156,157</sup> In addition, lipophilic acids and bases can be used as  $H^+$ -selective charged and uncharged ionophores, respectively (see part 2<sup>6</sup>). Their  $pK_a$  in the membrane phase defines the limits

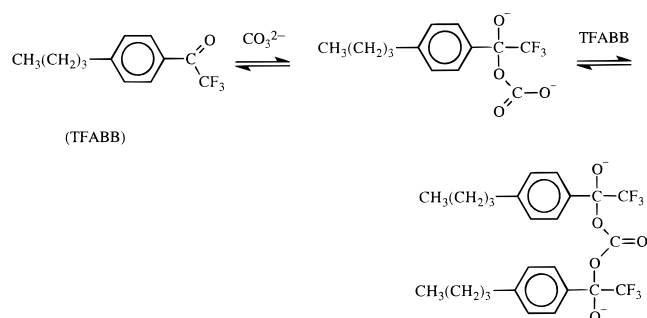


**Figure 41.** Reaction of trifluoroacetophenones with carbonate in sensor membranes.<sup>197</sup>

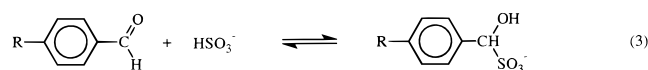
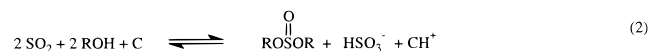


**Figure 42.** Reaction of  $\text{SO}_2$  with water (1) or an alcohol (2) in the membrane phase in the presence of a chromionophore C. The selective reaction of  $\text{HSO}_3^-$  with the lipophilic aldehyde is essential for the selectivity.<sup>157</sup>

R <sub>1</sub>	R <sub>2</sub>	Abbr.	pK <sub>a</sub>	
			MeOH	DOS-PVC
Ethyl	H	Nile Blue	12.2	14.0
Ethyl		ETH 5350	12.0	13.4
Ethyl		ETH 5294	10.6	12.0
Ethyl		ETH 2458	10.5	12.1
Methyl		ETH 5418	7.4	9.0
Methyl		ETH 2439	8.3	10.2

**Figure 43.** Structural formulae of chromionophores and pK<sub>a</sub> values in methanol and in the membrane phase.<sup>112</sup>

but not the extent of the measuring range of the corresponding ISEs (cf. eq 49).<sup>114</sup> If, upon protonation, such compounds change their UV/vis absorption or fluorescence, they can also be used as chromionophores or fluoroionophores in optical sensors (cf. II.2). A series of such compounds is available and their pK<sub>a</sub> values have been published (cf. Figure 43).<sup>112</sup> They are more basic in the membrane than in the aqueous phase. This can be explained by the fact that charges are stabilized to a lesser extent in the organic phase, an effect which is the largest for H<sup>+</sup>. Highly delo-

calized charges, such as in protonated chromionophores, are more stable than localized ones such as in tetraalkylammonium ions. Therefore, the relative basicities are not the same in the membrane as in the aqueous phase.<sup>157</sup> It is important, of course, to distinguish between the pK<sub>a</sub> in the organic membrane and the corresponding apparent one obtained from the protonation of the chromionophore as a function of the pH of the adjacent aqueous solution. The apparent pK<sub>a</sub> heavily depends on the membrane composition and the kind and concentration of other ions in the aqueous phase.

### B. Modeling of Ionophores

For the past 25 years, much work has been invested in theoretical studies on ion–ligand interactions since they are of considerable interest for analyzing the influence of different approximations in quantum chemistry. Thanks to unbiased reference values from mass spectrometric measurements,<sup>198–201</sup> these systems became ideal test cases. The calculations aimed at better understanding the interaction between known ionophores and ions, but very little work has been done to use them prospectively, i.e., with a view to designing new ligands.

It has been documented that semiempirical quantum chemical computations are inadequate for such calculations<sup>202</sup> since their results<sup>203</sup> contradict those obtained with more sophisticated techniques. In *ab initio* calculations, the influence of the basis sets is well-known. Small basis sets have to be specially designed, otherwise the interaction energies are heavily overestimated owing to the so-called basis set superposition error.<sup>204–206</sup> This error comes from the fact that in computing the energy of the complex, the wave functions of host and guest exert an enhancing influence on each other because the calculation is done with a virtually larger basis set than that for the individual components, and thus, the result is too negative. Although well-balanced small basis sets, insensitive to this kind of error, are available,<sup>207,208</sup> their success is partly due to error compensation,<sup>209,210</sup> so, whenever possible, large basis sets including polarization functions should be used. More sophisticated computations are usually not needed since, for example in the case of alkali metal and ammonium ions, the contribution of correlation effects to the calculated energy of hydration is less than 10% of the total interaction energy.<sup>209–212</sup>

Owing to the fact that computational demands increase with the fourth power of the number of basis functions, the size of molecules accessible to such calculations is the limiting factor. For the same reason, the enormous increase in available computational power in recent years is only slowly shifting this limit toward larger molecules. Direct self-consistent field methods<sup>213,214</sup> might be useful for large systems but the basic problem remains. Pseudopotentials,<sup>215–217</sup> to approximate the inner shell effects, or the density functional theory<sup>218,219</sup> might reduce computational demands. However, experience has to be gained first to show the reliability of interaction energies thus obtained. Another way to treat large systems is the application of approximate models based on *ab initio* calculations on small test

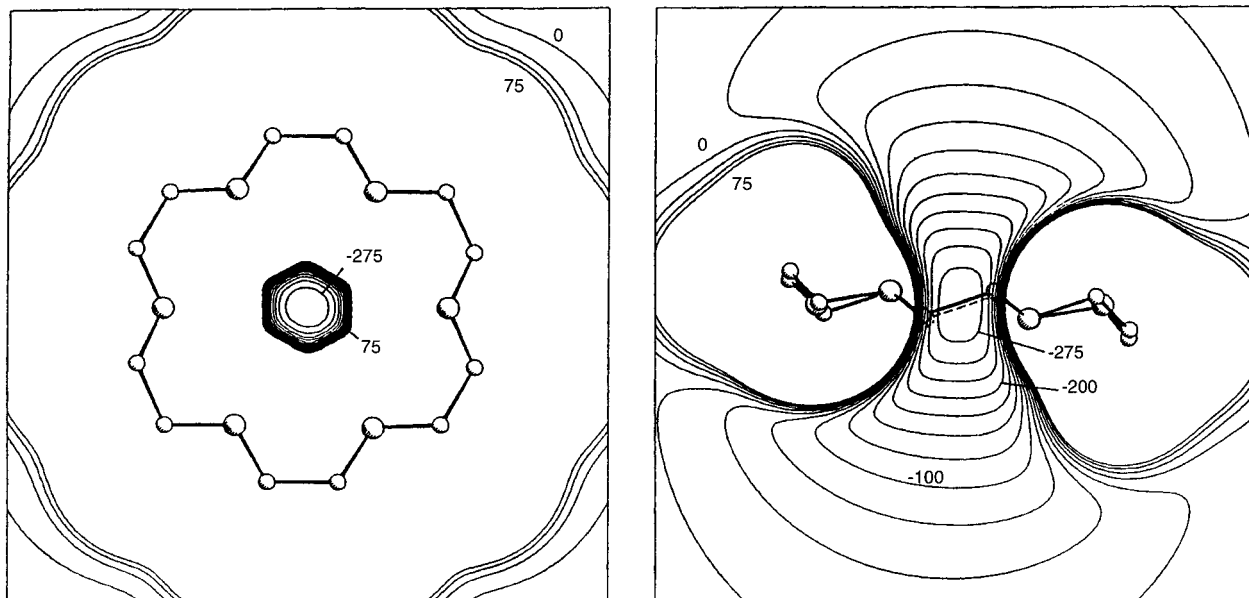


**Figure 44.** Isoenergy contour diagrams (energies in kJ/mol) for the interaction of  $K^+$  with 18-crown-6 as calculated with pair potentials derived from *ab initio* calculations.<sup>209</sup>

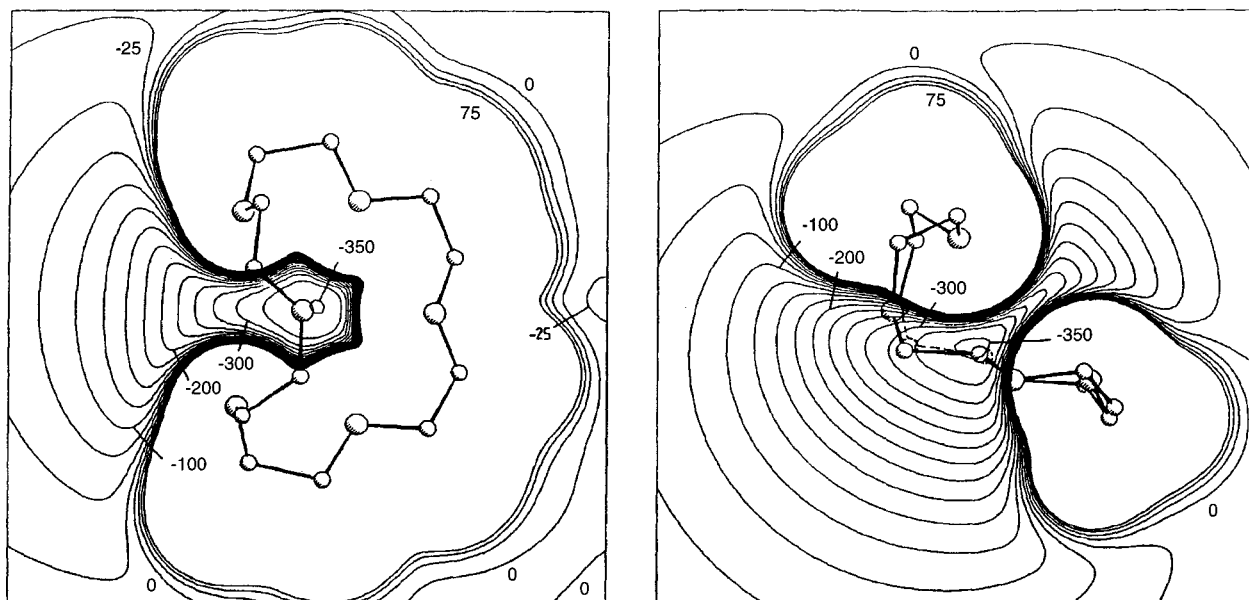


**Figure 45.** Isoenergy contour diagrams (energies in kJ/mol) for the interaction of  $Na^+$  with 18-crown-6 as calculated with pair potentials derived from *ab initio* calculations.<sup>209</sup>

molecules.<sup>220–222</sup> Interaction energies of various carriers have been computed by such methods.<sup>209,223,224</sup> Good correlations with ion selectivities measured in the condensed phase seem, however, fortuitous since the contribution of the neglected solvation and entropy effects is large. In addition, early calculations were sometimes based on the unrealistic assumption that the ligand conformation is frozen, as that obtained from X-ray studies on one of the complexes.<sup>223</sup> Moreover, all sophisticated computations published so far refer to the gas phase. Solvation effects can only be considered if approximate methods are used to describe the intramolecular (i.e., conformational) and intermolecular interaction energies involved.

For molecular mechanics and molecular dynamics calculations on complexes, ion–ligand interactions are generally represented by the sum of pairwise contributions of the individual atoms of the ligand

with the ion. Most frequently, Lennard–Jones type functions are used in combination with an electrostatic term. The parameters of these functions are either estimated by “learned guess”<sup>225,226</sup> or adjusted so that they reproduce interaction energies with small ligands, such as water and dimethyl ether,<sup>227</sup> or the X-ray structures of a set of complexes.<sup>228</sup> Another possibility is to use a large number of *ab initio* interaction energies of the ion under study with small model ligands whose atoms have the same environment as those of the target structure.<sup>209,229–231</sup> As an example for this approach, isoenergy contour diagrams are shown in Figures 44 and 45 for the interaction of  $K^+$  and  $Na^+$  with 18-crown-6.<sup>209</sup> The potentials derived by either of these techniques are combined with force fields in AMBER,<sup>232</sup> MM2,<sup>233</sup> MOLMEC,<sup>228</sup> and DISCOVER.<sup>234</sup> All these approximations have, however, severe limitations. Quite often, the energetically dominating ion–ligand in-

teraction energy is described with the lowest accuracy. But even if based on an extensive set of experimental or *ab initio* data, the model applied is only a crude approximation because fixed atomic charges (often adjusted empirically) are assumed and, hence, polarization effects of the guest ion are neglected. Another problem arises from the fact that, usually, the potentials describing intra- and intermolecular effects are developed independently. Since intermolecular interactions are very large when ions are involved and intramolecular force fields are only reliable close to the energy minima of the free ligands, the combination of the two effects might result in meaningless structures of the complex or require further adjustments during computation. In spite of these limitations, molecular mechanics calculations with such potentials have been used with remarkable success to reproduce experimental structures and selectivities of several ligands including the antibiotics valinomycin,<sup>235</sup> enniatin B,<sup>226</sup> and various crown ethers.<sup>209,227,236</sup>

One of the problems, especially in prospective calculations, i.e., of unknown structures (see below) is that of local energy minima. For example, the rather simple compound 18-crown-6 adopts 12 different conformations in 54 crystal structure analyses.<sup>196</sup> Even the building of a large number of starting geometries by the chemist would hardly guarantee that the relevant structures of minimum energy are found. Various automatic techniques have been used to solve this problem, including distance geometry<sup>237</sup> and simulated annealing (often referred to as the Monte Carlo method).<sup>238</sup> The application of genetic algorithms seems to be a promising alternative.<sup>239</sup>

All the techniques described so far provide only energy values. On the other hand, the free energy of solvation can be computed by applying the thermodynamic perturbation theory.<sup>240</sup> Molecular dynamics calculations<sup>241,242</sup> are used to sample the thermally accessible configurations of the system. An analogous technique allows free energy differences between two complexes (e.g., two different ions complexed by the same ligand in the same solvent, or the same ion and ligand forming complexes in two different solvents) to be calculated by "computational alchemy",<sup>243,244</sup> i.e., by stepwise interconverting two species (e.g.,  $K^+$  into  $Na^+$  or water into chloroform). As examples, the alkali ion-binding selectivities of 18-crown-6,<sup>245</sup> valinomycin,<sup>246,247</sup> and nonactin<sup>248</sup> have been studied by this technique. Mutations involving complete annihilation of the guest ion have been used to calculate absolute free energies of solvation<sup>249</sup> or complexation.<sup>250</sup> The reliability of such simulations depends both on adequate sampling and the accuracy of the potential energy functions, which exhibit the above-mentioned limitations. In spite of huge computational efforts, agreement between the results and experiments is only qualitative or semiquantitative, owing to the approximations involved.<sup>251,252</sup>

Given the enormous activities in this field, the question arises whether a more rational planning of new ionophores can be based on theoretical calculations. The answer is disappointing: "The prediction of the structure of a flexible receptor in solution, or

the binding and extraction properties of a given ionophore ... remains very difficult to answer by computations only."<sup>253</sup> So far, most of the calculations were performed to study known systems, i.e., retrospectively. Only very few prospective calculations aimed at the development of novel ionophores have been published.<sup>225,254</sup> They clearly show that, owing to the inaccuracies involved, prospective calculations only provide rough estimates. Nevertheless, if done with the appropriate care, they can be very useful as a filter for eliminating less promising candidates. This type of calculation is a step away from just assembling mechanical molecular models but is prone to remain far from providing true figures. Since ion selectivities, as mentioned above, are defined by small differences between large free energies of solvation and complexation, a much higher accuracy would be needed to reliably predict them.

### C. Exchange Kinetics, Reversibility

A prerequisite for the validity of the Nernst equation is a thermodynamic equilibrium between the adjacent aqueous and organic phases (see section II.1.A). This condition is fulfilled when the phase transfer kinetics and the involved complex formation are fast with respect to the diffusion processes involved. In electrochemical terms, the exchange current must be large compared to the current flowing through the membrane. In ideal cases, i.e., with only one ion species taking part in the charge transfer, its flux ( $J$ , in  $\text{mol cm}^{-2} \text{s}^{-1}$ ) into the membrane and back to the aqueous solution in the equilibrium state is the same by definition.

Kinetic limitations may influence the *slope* of the ISE response function.<sup>120</sup> In addition, the *response time* after a change in ion activity may be limited by the kinetics of interfacial reactions.<sup>29</sup> This is the case even when the membrane is conditioned in a solution containing the measuring ion, so the activity step only insignificantly alters the composition of the membrane bulk. When measuring selectivities, the surface composition of the membrane must change and, therefore, kinetic limitations may also bias selectivity coefficients.<sup>255</sup> With optodes, on the other hand, every measurement requires complete reconditioning of the sensing film and, therefore, kinetic limitations *on their response time* are more severe. However, diffusion, and not complexation or decomplexation, is usually the rate-limiting step (see section II.2.E).

To avoid kinetic limitations, the free energy of activation of the complexation process is a key factor to be considered when designing ionophores. The kinetics of complex formation of several naturally occurring ionophores in *aqueous solutions* was extensively investigated by the group of Eigen.<sup>256-258</sup> Because of very high free energies of hydration, the process of complexation would be extremely slow if the transition state of the complexation reaction involved nonsolvated ions. The very rapid complexation observed between alkali ions and carrier antibiotics, which is close to the limit set by diffusion control, can, therefore, only be explained by assuming that the water molecules are replaced stepwise by

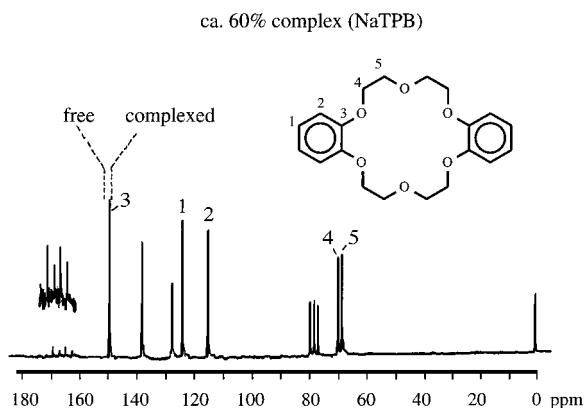


**Figure 46.**  $^{13}\text{C}$ -NMR spectrum of dibenzo(18-crown-6) in equilibrium with its  $\text{Na}^+$  complex (solvent,  $\text{CDCl}_3$ ).<sup>260</sup> As a consequence of a fast intermolecular exchange the signals of the free and complexed ionophore are averaged out.

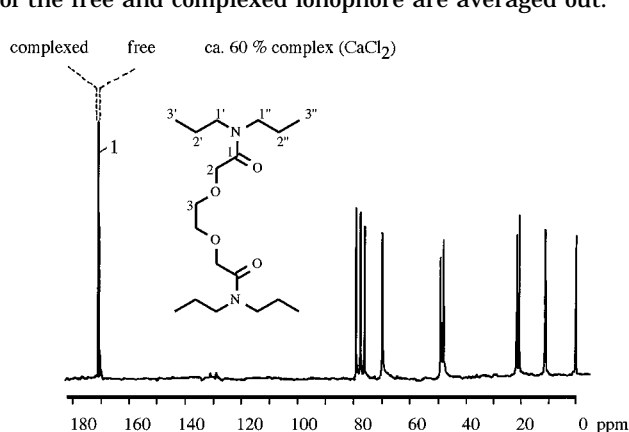


**Figure 47.**  $^{13}\text{C}$ -NMR spectrum of *N,N,N,N*-tetrapropyl-3,6-dioxaoctanediamide in equilibrium with its  $\text{Ca}^{2+}$  complex (solvent,  $\text{CDCl}_3$ ).<sup>260</sup> As a consequence of a fast intermolecular exchange the signals of the free and complexed ionophore are averaged out.

the coordination sites of the ionophore. In the case of valinomycin, it was shown that the rate-limiting step is a conformational change of the ligand, which occurs during the substitution of solvate molecules from the inner coordination sphere of the cation by the coordinating groups of the flexible ligand.<sup>259</sup> A consequence of this finding in view of designing new ionophores is that their structure should be flexible. Hence, ligands with a too rigid geometric preorganization seem to be inadequate components for ion sensors.

The exchange rate between free and complexed ligands in chloroform was investigated by  $^{13}\text{C}$ -NMR spectroscopy (cf. Figures 46–49).<sup>260</sup> It proved to be fast on the NMR time scale for the complexes of  $\text{Na}^+$  with dibenzo-18-crown-6 (Figure 46) and of  $\text{Ca}^{2+}$  with *N,N,N,N*-tetrapropyl-3,6-dioxaoctanedioic acid amide (an ionophore related to ETH 1001, Figure 47) but slow for that of  $\text{Ba}^{2+}$  with cryptand[2,2,2], for which separate sharp signals were observed for the free ligand and for the complex (Figure 48). In contrast to the cryptands, the antibiotic nonactin yields perfectly working ammonium-selective ISEs. Interestingly, the exchange rate between its free form and the  $\text{NH}_4^+$  complex is rather slow as well (Figure 49). The free energy of activation for the exchange reaction of various cations with the  $\text{Cd}^{2+}$ -selective iono-

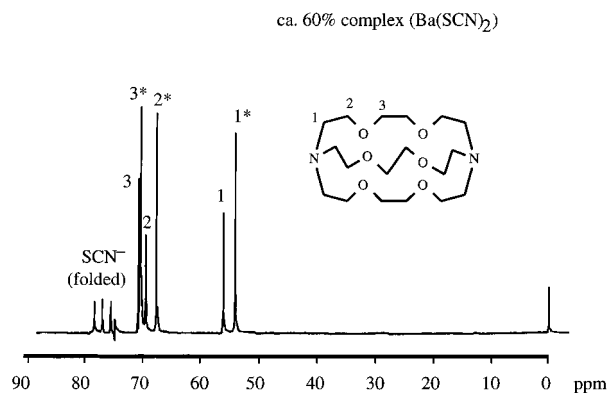


**Figure 48.**  $^{13}\text{C}$ -NMR spectrum of the cryptand[2,2,2] in equilibrium with its  $\text{Ba}^{2+}$  complex (solvent,  $\text{CDCl}_3$ ).<sup>260</sup> The signals of the complex are marked with an asterisk (\*).

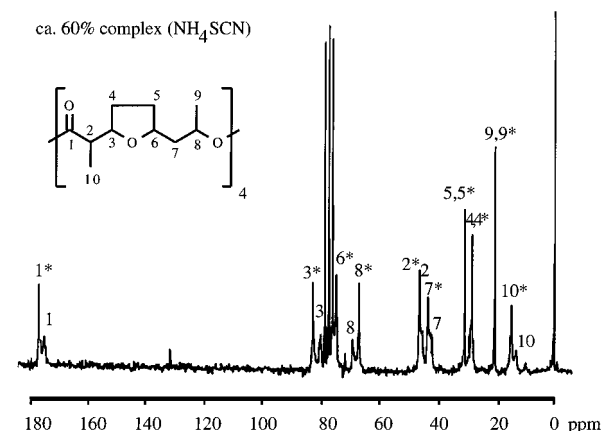


**Figure 49.**  $^{13}\text{C}$ -NMR spectrum of the antibiotic nonactin in equilibrium with its  $\text{NH}_4^+$  complex (solvent,  $\text{CDCl}_3$ ).<sup>260</sup> The signals of the complex are marked with an asterisk (\*).

phore *N,N,N,N*-tetrapropyl-3,6-dioxaoctanedithioamide,<sup>261</sup> determined in acetonitrile in the presence of a cation excess,<sup>262</sup> was up to  $45 \text{ kJ mol}^{-1}$  for  $\text{Cd}^{2+}$  and  $\text{Zn}^{2+}$ , for both of which cationic functions of the corresponding ISE are observed, but over  $65 \text{ kJ mol}^{-1}$  for  $\text{Pt}^{2+}$  and  $\text{Pd}^{2+}$ , which induce an anionic response. It was, however, not established unambiguously whether the latter is due to kinetic limitations or to coextraction caused by a too high complex stability.

Time-dependent impedance studies to investigate ISEs, first carried out by Buck and co-workers,<sup>263,264</sup> can be used under certain assumptions to determine apparent ion exchange current densities. For a valinomycin–PVC membrane with dibutyl phthalate as plasticizer and ca. 50 mol % of a tetraphenylborate, the following results were reported for 1 M sample solutions:<sup>265</sup>  $2.6 \times 10^{-2}$  (KCl),  $5.7 \times 10^{-6}$  (NaCl), and  $3.2 \times 10^{-6} \text{ A cm}^{-2}$  (LiCl). The charge transfer resistances for 1 and  $10^{-2}$  M solutions were, respectively, 0.001 and  $0.150 \text{ k}\Omega \text{ cm}^2$  (KCl), 4.5 and  $15 \text{ k}\Omega \text{ cm}^2$  (NaCl), and 7.9 and  $20 \text{ k}\Omega \text{ cm}^2$  (LiCl). However, the values obtained may be influenced by changes at the membrane surface<sup>47,266</sup> and cannot be interpreted unequivocally. A further possible bias may arise for the discriminated ions  $\text{Na}^+$  and  $\text{Li}^+$  because they are not capable of fully replacing  $\text{K}^+$  (cf. Figure 18).<sup>92</sup>

The kinetics of phase transfer equilibria are more complex than that of single-phase reactions because various mechanisms are conceivable.<sup>267</sup> In the case of a homogeneous phase reaction taking place in the aqueous or in the organic phase, either the lipophilic ionophore must be extracted into the sample solution or the hydrophilic sample ion into the membrane. As a third possibility, complexation can take place at the boundary phase. In all three cases, ion-pair formation with counterions might catalyze the reaction. It seems very difficult to unambiguously prove which process prevails. Even for the well-studied complexation of valinomycin with  $K^+$ , different mechanisms have been proposed from electrochemical measurements on related systems. For example, Armstrong and co-workers<sup>268,269</sup> investigated the influence of the composition of a DOS–PVC membrane on the complex impedance plots. They found a simple one-step reaction in the presence of excess free valinomycin and a two-step mechanism including the diffusion of the uncomplexed  $K^+$  into the membrane when no excess of the free ligand was available. On the basis of voltammetric experiments at the water/nitrobenzene interface, Koryta *et al.* also proposed two parallel mechanisms, a one-step reaction at the surface and a two-step process including the extraction of the uncomplexed  $K^+$  into the membrane phase.<sup>270</sup> Contrary to this, Yoshida and Freiser, from studies on the same system presented evidence that the complex formation between valinomycin and  $K^+$  occurs in the aqueous phase,<sup>271</sup> but this mechanism was later disproved by further experiments.<sup>272</sup> A series of other ionophores have been investigated including non-macrocyclic  $Ca^{2+}$ - and  $Na^+$ -selective carriers,<sup>273,274</sup> dibenzo-18-crown-6,<sup>267,275</sup> and nonactin.<sup>275,276</sup> The authors deduced that complexation occurred either at the membrane surface or in the organic phase, again different mechanisms being proposed in some cases for the same system. Even if the experimental findings can be interpreted unequivocally, they should not be generalized. The contribution of the various above-mentioned mechanisms to the overall reaction depends on the relative lipophilicities of the ion and the ionophore. Notwithstanding, the main result from these studies is that the complexation and decomplexation reactions were fast for all ionophores investigated, so no kinetic limitation of the phase transfer was observed with adequate sensor components. As long as this condition is fulfilled, the exact mechanism is of no relevance with respect to ISE and optode applications. Moreover, it is important to keep in mind that changes occur only at the boundary surface (space-charge region) after changing the sample, if the electrode responds according to the Nernst equation. This process is faster by many orders of magnitudes than the ISE response.

#### D. Lipophilicity

Since the three membrane components, ionophore, ionic additive, and plasticizer, are generally dissolved in the organic polymer phase, their leaching rate into the sample must be kept as low as possible. This is usually achieved by attaching lipophilic groups, such as long alkyl chains, to their molecular frames. Oesch and Simon<sup>277,278</sup> and later Dinten *et al.*<sup>279</sup> developed a model that allows one to relate the

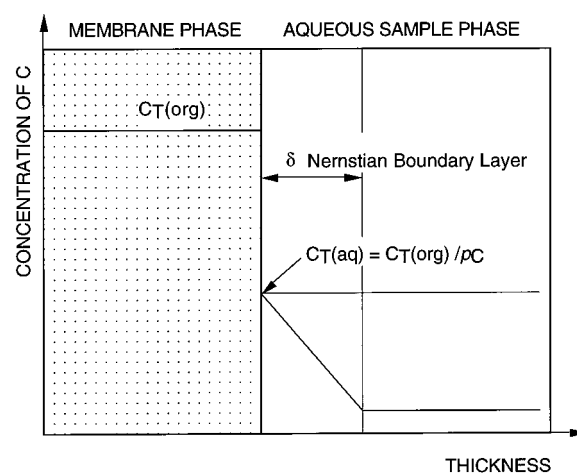


**Figure 50.** Schematic representation of the leaching behavior of a compound C from an ion-selective membrane into a liquid sample.<sup>174,279</sup> Since this leaching process is slow, it can be assumed that no concentration gradients within the organic membrane phase occur and that equilibrium holds at the membrane–sample interface. A linear concentration gradient within the Nernst diffusion layer into the sample is assumed that leads to gradual depletion of compound C. A large partition coefficient  $p_C$  of C will lead to a small local concentration of C at the aqueous phase boundary and to a slow loss from the membrane. Upper horizontal line on side of the aqueous sample: Sample concentration of C at equilibrium.

leaching rate of a given compound, C, to its partition coefficient (or lipophilicity)

$$\ln \frac{c_{\text{tot}}(\text{org}, 0)}{c_{\text{tot}}(\text{org}, t)} = \frac{D_{\text{aq}}}{p_C d \delta} t \quad (76)$$

where  $c_{\text{tot}}(\text{org}, 0)$  and  $c_{\text{tot}}(\text{org}, t)$  are the total concentrations of C in the membrane phase at the time  $t = 0$  and  $t > 0$ , respectively,  $D_{\text{aq}}$  is the diffusion coefficient of C in the aqueous phase,  $d$  the thickness of the sensing film, and  $\delta$  that of the Nernstian boundary layer contacting the organic phase, whereas the lipophilicity,  $p_C$ , is the total equilibrium partition coefficient of C between the aqueous and the organic phases:

$$p_C = \frac{c_{\text{tot}}(\text{org})}{c_{\text{tot}}(\text{aq})} \quad (77)$$

This model is based on the assumption that the leaching process of membrane components out of an organic membrane into the aqueous sample phase is relatively slow compared to diffusional processes inside the membrane and at the liquid–liquid interface. Thus, no appreciable concentration gradients across the organic phase are encountered and the membrane/sample interface is in chemical equilibrium at all times. This assumption has been found to be valid for membrane compounds with a minimum lipophilicity of  $p_C \sim 1000$ .<sup>174</sup> The leaching process is schematically represented in Figure 50. If the two phases were in chemical equilibrium, the concentration of C in the aqueous phase,  $c_{\text{tot}}(\text{aq})$ , would reach the value of  $c_{\text{tot}}(\text{org})/p_C$ , as indicated by the upper horizontal line. However, in a flow-through system or in a stirred solution of large volume, a linear concentration profile of C within the unstirred Nernstian



boundary layer of the aqueous phase is assumed, while directly at the membrane interface, the concentration still corresponds to the equilibrium value defined by  $p_C$ . Equation 76 allows one to quantify the required lipophilicity of any compound leaching from the organic phase. The required lipophilicity,  $\log p_C$ , for an allowed decrease of 1% in the concentration within  $t = 30$  d obtained with typical values of the parameters ( $D_{\text{aq}} = 5 \times 10^{-6} \text{ cm}^2 \text{ s}^{-1}$ ,<sup>279</sup>  $\delta = 30 \text{ }\mu\text{m}$ ,<sup>279</sup> and  $d = 2$  or  $200 \text{ }\mu\text{m}$  for optode or ISE membranes, respectively) is 9.3 for optodes and 7.3 for ISEs.

For uncharged species that are present in both phases prevailing in their free form,  $p_C$  can be approximated by the equilibrium constant,  $P_C$ , corresponding to the concentration ratio of C between the two phases:

$$p_C \approx P_C = \frac{[\text{C}]_{\text{org}}}{[\text{C}]_{\text{aq}}} \quad (78)$$

This assumption is valid for plasticizers and predominantly uncomplexed, uncharged ionophores which exhibit only very weak ion binding properties in aqueous solutions.<sup>183,258</sup> The lipophilicity of these compounds was shown to follow a linear relationship with  $\log P_C$  obtained in the extraction system octanol/water:<sup>279</sup>

$$\log P_C(\text{membrane/aqueous sample}) = a + b \log P_C(\text{octanol/water}) \quad (79)$$

The  $P_C$  values for octanol/water can be determined by thin layer chromatography<sup>279</sup> or computed from structural lipophilicity increments as proposed by Hansch and Leo.<sup>280,281</sup> The parameters  $a$  and  $b$ , respectively, were found to be 0.4 and 0.8 for the system membrane phase/aqueous solution<sup>172</sup> and 0.48 and 0.33 for membrane phase/undiluted serum.<sup>278</sup> These values show that especially optodes and miniaturized ISEs exhibit greatly reduced lifetimes in prolonged contact with lipophilic samples.

If an uncharged ionophore, L, in the membrane phase forms a significant amount of the complex  $\text{ML}_n^{z+}$  with the cation  $\text{M}^{z+}$ , its overall lipophilicity is somewhat higher than that given by the thermodynamic equilibrium constant of the free ligand:

$$p_L = \frac{[\text{L}]_{\text{org}} + n[\text{ML}_n^{z+}]_{\text{org}}}{[\text{L}]_{\text{aq}}} = P_L + \frac{n[\text{ML}_n^{z+}]_{\text{org}}}{[\text{L}]_{\text{aq}}} \quad (80)$$

Again, complexation of L in the aqueous phase is neglected here. However, with certain membrane components, complexation and/or protonation in the aqueous phase must be taken into account. This is the case, e.g., with electrically neutral  $\text{H}^+$ -selective ionophores and chromoionophores that are readily protonated in aqueous solutions, so their lipophilicity corresponds to<sup>112</sup>

$$p_C = \frac{[\text{C}]_{\text{org}} + [\text{CH}^+]_{\text{org}}}{[\text{C}]_{\text{aq}} + [\text{CH}^+]_{\text{aq}}} \quad (81)$$

While for protonation in the aqueous phase, the  $pK_a$  of the (chromo)ionophore and the sample pH must be considered, the concentration of the protonated form in the organic phase depends on the membrane composition. In liquid membrane pH electrodes<sup>114</sup> and optical sensors with membranes of optimized composition, the concentrations of the protonated and deprotonated forms are usually about equal ( $[\text{C}]_{\text{org}} \approx [\text{CH}^+]_{\text{org}}$ ). Hence, eq 81 yields

$$p_C = \frac{[\text{C}]_{\text{org}}}{[\text{C}]_{\text{aq}}} \frac{2K_a}{K_a + [\text{H}^+]_{\text{aq}}} = P_C \frac{2K_a}{K_a + [\text{H}^+]_{\text{aq}}} \quad (82)$$

While values of  $P_C$  still may be calculated according to the method of Hansch and Leo<sup>280</sup> (after correcting with eq 79), the lipophilicity is also influenced by the sample pH. Basic ionophores having a  $pK_a$  of 9–11 show a lipophilicity that is greatly reduced even in only mildly acidic solutions.<sup>112</sup> Such effects have to be taken into account in real-world applications of the corresponding sensors.

Covalent attachment of the ionophore to the polymer matrix has been shown to yield functional electrodes having improved lifetimes.<sup>175,176,282–284</sup> A significant influence on the response time of the ISE was only reported in the case of a  $\text{H}^+$ -selective electrode.<sup>284</sup> However, small amounts of unbound ionophore might have a decisive influence on the response. Immobilization of chromoionophores by covalently binding them to the polymer matrix has been shown to prolong the lifetime of  $\text{Ca}^{2+}$ -selective bulk optodes as well.<sup>158</sup> In this case, however, an approximately 5-fold increase in response time had to be reckoned with, probably because the diffusion rate within the sensing film was limited.

## 2. Other Membrane Components

### A. Membrane Solvent (Plasticizer)

Solvent polymeric membranes used in ion sensors are usually based on a matrix containing about 33% (w/w) of PVC and 66% of a membrane solvent.<sup>23,285</sup> Films with such a high amount of plasticizer have optimum physical properties<sup>286</sup> and ensure relatively high mobilities of their constituents. As <sup>13</sup>C-NMR relaxation times show, the membrane solvent is in a highly viscous liquid state,<sup>57,287</sup> this finding being in agreement with the self-diffusion coefficient of  $(8.7 \pm 1) \times 10^{-8} \text{ cm}^2 \text{ s}^{-1}$  determined for the plasticizer in a dicresyl butyl phosphate–PVC (78:22%, w/w) membrane.<sup>288</sup> When the amount of plasticizer in PVC membranes with valinomycin–DOS or ETH1001–*o*-NPOE decreases from 67 to 20% (w/w), the specific membrane resistance rapidly increases from ca.  $10^8$  to ca.  $10^{13} \text{ }\Omega \text{ cm}$  owing to reduced mobilities.<sup>172</sup> However, lower solubilities upon changes in membrane composition may also account for such effects.<sup>289</sup>

In order to give a homogeneous organic phase, the membrane solvent must be physically compatible with the polymer, i.e., have plasticizer properties. Otherwise, it exudes, yielding membranes of unstable composition. For various reasons, it also has an influence on the selectivity behavior. For a ligand-free ISE membrane based on an ion exchanger that

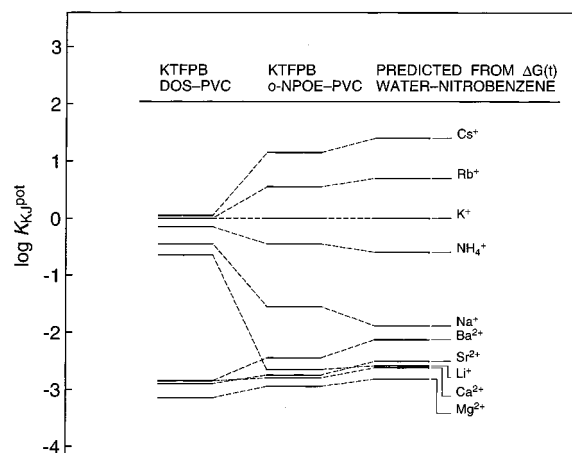


**Figure 51.** Potentiometric selectivities of cation-exchanger-based membrane electrodes compared to the values obtained from standard Gibbs energies of transfer from water to nitrobenzene (for calculating selectivity coefficients from free energies of transfer, see refs 29 and 36).

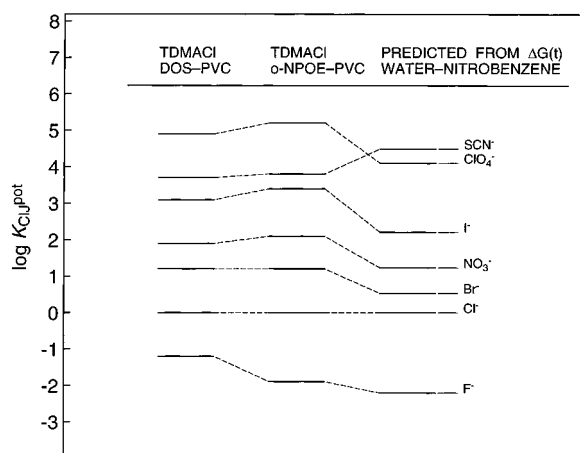


**Figure 52.** Potentiometric selectivities of anion-exchanger-based membrane electrodes compared to the values obtained from standard Gibbs energies of transfer from water to nitrobenzene (for calculating selectivity coefficients from free energies of transfer, see refs 29 and 36).

is incapable of specific interactions, the selectivities are determined by the difference between the standard free energies of the ions in the aqueous and organic phases, which is only influenced by the plasticizer. The selectivity sequence obtained with such membranes is always the same as shown by Figures 51 and 52. The potentiometrically obtained values (columns 1 and 2)<sup>70,290</sup> nicely correlate with those measured by voltammetry on liquid-liquid interfaces.<sup>189</sup> It is usually named after Hofmeister, who, in 1888 at the Pharmacological Institute in Prague, studied the effect of various salts on the coagulation of egg proteins and aimed at finding correlations with their diuretic and laxative properties.<sup>291</sup> The sequences he obtained for some cations and anions were later shown to agree with those of the free energies of hydration of the ions.<sup>292</sup>

On the other hand, selectivities of carrier-based ISEs are highly influenced by the membrane solvent. For example, the change in plasticizer from the polar *o*-NPOE to the apolar dibutyl sebacate (DBS) or dioctyl sebacate (DOS) reduces the  $\text{Ca}^{2+}$ -selectivity of the ISE with the ionophore ETH 1001 by orders of magnitude.<sup>293,294</sup> It has been assumed that this

influence is due to the polarity of the plasticizer, which can be estimated from the interaction of charged species with a continuum of given dielectric constant (Born model).<sup>295</sup> With more polar solvents, divalent ions are preferred over monovalent ones, the effect being especially pronounced with thin ligand layers.<sup>296,297</sup> This correlation is, however, only qualitative, as shown by a recent study of a large number of lipophilic compounds with respect to their applicability as plasticizers in  $\text{Mg}^{2+}$ -selective ISE membranes.<sup>298</sup>

The membrane solvent strongly influences also the measuring range (i.e., the upper and lower detection limits) of ion-selective sensors. Here again, no simple correlation with its polarity alone is to be expected. The lower detection limit, e.g., of a  $\text{H}^+$ -selective liquid membrane electrode, brought about by the exchange of  $\text{Na}^+$  against  $\text{H}^+$ , is for example lower with the polar *o*-NPOE ( $\epsilon_{\text{mem}} = 14$ )<sup>299</sup> than with the nonpolar DOS ( $\epsilon_{\text{mem}} = 4.8$ ),<sup>300</sup> which is obviously due to the better coordinating abilities of the latter (cf. II.1.C).<sup>114</sup>

Another factor highly influenced by the membrane solvent is the formation of ion-pairs. Those between complexed ions and lipophilic counterions<sup>117,191,301</sup> seem to be negligible in polar membranes, but are relevant in nonpolar ones.<sup>301</sup> Formation of ion-pairs or coordination compounds may influence the *slope* of the response function. If, for example, divalent cations  $\text{M}^{2+}$  form associates with a monovalent anion  $\text{X}^-$  so that predominantly monovalent species  $\text{MX}^+$  take part in the phase transfer equilibrium<sup>302</sup> and/or occur in the membrane,<sup>303</sup> a slope characteristic for monovalent ions can be obtained.<sup>29,302</sup> Furthermore, ion association may influence the selectivity factors as well. The formation of ion-pairs in the membrane decreases the concentration of the uncomplexed ions and has thus a similar effect as an increase of the complex formation constant. However, this influence is likely to be nonspecific, i.e., similar for primary and interfering ions, and, therefore, deteriorates the selectivity. Such a loss in selectivity is expected to be especially significant for sterically unhindered ionic sites (such as sulfonates) and for ionophores forming weaker complexes. A detailed model describing these effects was published together with measurements confirming these predictions.<sup>82</sup>

The choice of plasticizer also depends on what the ISE is used for. During measurements in blood or serum, deposits of charged species (mainly proteins) on the membrane surface give rise to potential drifts. These effects are more severe with polar solvents. Therefore, in some cases, the preparation of  $\text{Ca}^{2+}$ -selective membranes with low polarity solvents, and, hence, reduced selectivities toward monovalent ions, has been proposed.<sup>294</sup> Another concern is that, at least to some extent, even highly lipophilic solvents leach from the membrane phase and thereby cause inflammation if applied in living organisms.<sup>304</sup> This can be avoided by using a plasticizer of high molecular weight<sup>305</sup> or by photopolymerizing it after membrane preparation.<sup>306</sup>

Bulk optodes have usually been prepared with the same plasticizers as used for ISEs. Since the highly polar *o*-NPOE has a weak absorption in the visible

range, it was sometimes replaced with *o*-trifluoromethyl octyl ether, the exact polarity of which is however not known.<sup>307</sup>

### B. Ionic Additives

The prerequisite for obtaining a theoretical response with ISE membranes is their permselectivity, which means that no significant amount of counterions may enter the membrane phase (cf. section II.1.A.). To achieve this so-called Donnan exclusion with *electrically neutral carriers*, counterions (ionic sites) confined to the membrane must be present. Although neutral-carrier-based ISE membranes may work properly even when they contain only a very small amount of ionic sites (e.g., as impurities, see below), the addition of a salt of a lipophilic ion is advisable and beneficial for various other reasons as well. The original motive for adding a tetraphenylborate salt to the membrane of a cation-selective electrode was to reduce the anionic interference observed in the presence of lipophilic anions like thiocyanate or perchlorate.<sup>96,116</sup> At the same time, the electrical resistance of the membrane is lowered, which is especially important with microelectrodes.<sup>123</sup> Ionic additives are ion exchangers which themselves induce a selective response if no or only an insufficient amount of ionophore is present. Therefore, their concentration must be adjusted carefully. The electrical resistance may also be lowered by adding a salt of two lipophilic ions.<sup>308,309</sup> Such a salt has no ion-exchanger properties and can be applied in excess relative to the ionophore.

Ionic sites, moreover, have a selectivity-modifying influence in that their amount in the membrane determines that of the exchangeable ions of opposite charge. Hence, by adjusting the molar ratio of ionic sites to ionophore so that the latter is present in excess with respect to the primary ion but in deficiency regarding the interfering ions, the selectivity behavior of ISEs can be improved. This is always possible in case the primary ion has a higher charge and/or forms a complex of lower stoichiometry than the interfering ions (cf. section II.1.B). In the case of neutral carrier-based H<sup>+</sup>-selective electrodes, the measuring range can be maximized by adding an optimal amount of anionic sites, which was shown to be 50 mol % relative to the ionophore (see section II.1.D).<sup>114</sup>

In *charged-carrier-based* ISE membranes, on the other side, ionic sites are not required to obtain a Nernstian response because the carrier itself induces the Donnan exclusion. However, their presence is beneficial, as was shown recently,<sup>69,71</sup> but in contrast to neutral-carrier-based membranes, they must bear the *same* charge as the analyte ion (cf. section II.1.B). In general, the selectivity of ion complexation can only be fully exploited when these membranes contain ionic additives. From the different effects the charge of added ionic sites has on neutral- and charged-carrier-based ISEs, the carrier mechanism may be evaluated by investigating membranes that contain ionic sites of opposing charges (cf. section II.1.B).<sup>71,72</sup> For example, the antibiotic monensin, which had been assumed to be a charged ionophore,<sup>310</sup> was shown to act as neutral carrier (in the form of the undissociated carboxylic acid) when in contact with unbuffered solutions (see Figure 53).<sup>72</sup>

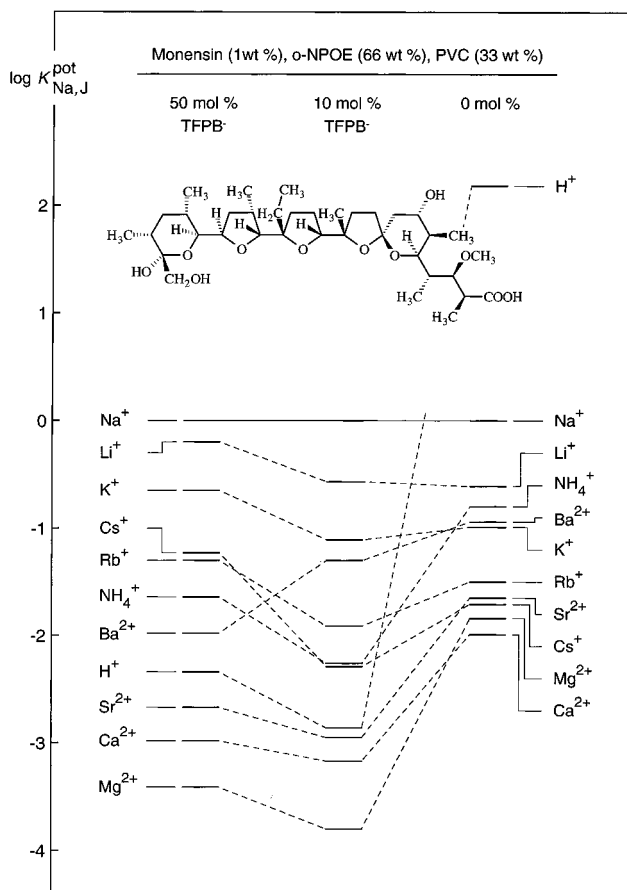


**Figure 53.** Potentiometric selectivity coefficients of Na<sup>+</sup>-selective electrodes based on the antibiotic monensin.<sup>69</sup> The addition of negative sites (TFPB<sup>-</sup>) improves the selectivities. Membranes containing cationic sites show an anionic response ruling out a charged carrier mechanism.

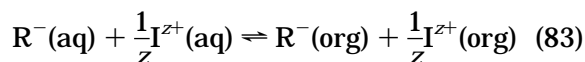
If both the electrically neutral and the charged form of an ionophore are able to give complexes, either of the two mechanisms can be made to prevail by choosing ionic sites of the appropriate charge<sup>72</sup> or by changing the pH of the sample. Organophosphoric esters, for example, have been used as charged carriers in Ca<sup>2+</sup>-selective membranes.<sup>21</sup> As shown recently, they exhibit similar selectivity in the presence of cationic or anionic sites.<sup>72</sup> In the latter case, the organophosphoric acid is protonated in the membrane and acts as a neutral carrier.<sup>72</sup>

*Optode films* may contain three kinds of charged species, namely, the complexed analyte ion, the lipophilic ionic site incorporated into the membrane, and, additionally, a charged form of the chromoionophore. The latter can have either a positive or negative charge, i.e., it is either a protonated base (uncharged chromoionophore) or a deprotonated acid (charged chromoionophore). Because of the presence of the charged form of the chromoionophore, the concentration ratios of ion/ligand is not fixed by weighing parameters. It rather changes with the optode response. Since the selectivity may vary with this relative concentration, weighing parameters do not influence ion selectivities of optodes in the same way as those of ISEs. This is the reason why no Mg<sup>2+</sup>-selective optodes are obtained with the ionophores used for assaying Mg<sup>2+</sup> with ISEs.<sup>84</sup> Nonetheless, the absolute and relative concentrations of the different components of the sensing film do have

an important effect on the selectivities.<sup>113,167</sup> Once the ion exchange constants,  $K_{\text{exch}}$ , are determined, the optimum membrane composition can be calculated from eq 63.

Another important feature of optodes is that their signal intensity is directly influenced by the concentration of ionic sites, which is in contrast to ISE membranes, where small changes (e.g., through leaching or decomposition) have no bearing on the response behavior. Hence, with optical sensors, measurements at several wavelengths may be necessary in order to control this effect.

The *lipophilicity*, i.e., the equilibrium partition coefficient,  $p_{R^-}$ , of the ionic additive  $R^-$  required to guarantee a certain sensor lifetime is the same as that of electrically neutral compounds (cf. section III.1.D) but its actual value in a given membrane system depends on the kind and concentration of counterions (i.e.,  $I^{z+}$ ).<sup>174</sup> For a membrane without an ionophore,  $p_{R^-}$  can be expressed in good approximation as a function of the coextraction constant,  $K_{\text{IR}}$ , of the equilibrium 83 of the salt  $\text{IR}_Z$  (analogous expressions hold for cationic sites,  $R^+$ ):<sup>174</sup>



$$p_{R^-} \approx \frac{[R^-]}{c_{R^-}} = K_{\text{IR}} \left( \frac{c_{I^{z+}}}{[I^{z+}]} \right)^{1/z} \quad (84)$$

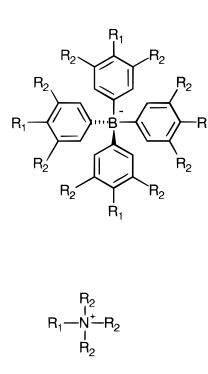
Equation 84 is based on the assumption that the effect of ion-pair formation is negligible in the aqueous and organic phases, which is sufficiently fulfilled in the case of the sterically hindered ionic sites usually incorporated into sensor membranes (cf. Figure 54).<sup>174,299</sup> It shows that the lipophilicity of the added ions depends both on the concentration and lipophilicity of the counterions. For the distribution of the potassium salts of  $\text{TPB}^-$ ,  $\text{TpCIPB}^-$ , and  $\text{TFPB}^-$  between a DOS–PVC (2:1, w/w) membrane and water,  $\log K_{\text{KR}}$  values of 4.6, 5.8, and 8.4, respectively, were obtained.<sup>174</sup>

If, in addition, the sensor membrane contains a lipophilic ionophore capable of forming strong complexes, the concentration,  $[I^{z+}]$ , of the free analyte cation in the organic phase greatly decreases so that the lipophilicity of  $R^-$  is enhanced:<sup>174</sup>

$$p_{R^-} \approx \frac{[R^-]}{c_{R^-}} = K_{\text{IR}} (\beta_{\text{IL}_n})^{1/z} \left( \frac{c_{I^{z+}} [L]^n}{[I^{z+}]_n} \right)^{1/z} \quad (85)$$

For example, if valinomycin is added to a DOS–PVC (2:1, w/w) membrane contacted with a 0.01 M KCl solution,  $\log p_{\text{TpCIPB}^-}$  increases from 5.8 to 13.1.<sup>174</sup> This explains the observation made earlier<sup>311</sup> that the  $\text{TPB}^-$  concentration is self-adjusting in a membrane in which it was initially present in a molar excess relative to valinomycin. After short conditioning in an aqueous solution, this excess is lost and the expected ion selectivity for  $\text{K}^+$  is obtained.

The structural formulas of the most important salts used as lipophilic additives are shown in Figure 54. Various tetraphenylborate derivatives are currently used as anionic additives. Unfortunately their chemical stability is limited, especially in the presence of



$R_1$	$R_2$	Acronym	$\log K_{\text{KR}} (\text{K}^+ \text{ SALT})$
H	H	$\text{TPB}^-$	4.6
Cl	H	$\text{TpCIPB}^-$	5.8
H	$\text{CF}_3$	$\text{TFPB}^-$	8.4
H	$\text{C}(\text{CF}_3)_2\text{OCH}_3$	$\text{HFPPB}^-$	N/A

$R_1$	$R_2$	Acronym	$\log K_{\text{RCI}} (\text{Cl}^- \text{ SALT})$
$\text{CH}_3$	$(\text{CH}_2)_{11}\text{CH}_3$	$\text{TDDMA}^+$	$7.1 \pm 2.2$
$(\text{CH}_2)_{11}\text{CH}_3$	$(\text{CH}_2)_{11}\text{CH}_3$	$\text{TDDA}^+$	N/A

**Figure 54.** Anionic and cationic sites currently used in ion-selective electrodes and optodes and their membrane-water distribution coefficients.<sup>174,313</sup>

acids, oxidants, and light. The decomposition is due to an attack of  $\text{H}^+$  on the phenyl substituents.<sup>177</sup> The stability could be increased by introducing electron-withdrawing substituents.<sup>177,178</sup> Because of their chemical stability and lipophilicity, sodium tetrakis[3,5-bis(1,1,1,3,3,3-hexafluoro-2-methoxy-2-propyl)phenyl]borate trihydrate ( $\text{NaHFPPB}$ )<sup>312</sup> and potassium tetrakis[3,5-bis(trifluoromethyl)phenyl]borate ( $\text{KTFPB}$ )<sup>178</sup> (cf. Figure 54) are the best anionic additives available.<sup>174</sup> The stability issue may be more critical when using optode membranes with chromoionophores of low basicity since the rate of decomposition is expected to linearly correlate with their acidity constant.<sup>82</sup> Lipophilic tetraalkylammonium salts such as tridodecyl methylammonium chloride ( $\text{TDMACl}$ , membrane–water distribution coefficient ca.  $10^7$ <sup>313</sup>) are suitable cationic additives. The hydrophilic counterions of these lipophilic additives are exchanged for the primary ion as soon as the ISE is conditioned in the respective solutions.

Leaching of ionic sites may be avoided by bonding them covalently to the polymer matrix as, for example, in sulfonated PVC.<sup>82</sup> This polymer, however, has been shown to modify the selectivity behavior because of direct interaction of the sulfonate group with cations.<sup>82</sup> Although, when using nonpolar plasticizers, ion-pairs are formed to some degree also with tetraphenylborates,<sup>299</sup> these interactions are weaker and unspecific and do not have a significant selectivity modifying effect. Recently, tetraphenylborate covalently bonded to a polymer matrix has been reported.<sup>175,303,314</sup> Since ionic sites in the presence of ionophores show an increase in lipophilicity, their covalent attachment to the polymer phase seems necessary in special cases only, such as for miniaturized sensors or when leaching even of minor amounts must be avoided because of possible toxicity. If these compounds are used in ion-exchanger-based ISE membranes, i.e., without a lipophilic ionophore, they will leach out more readily. This is especially the case if they are in prolonged contact with a flowing system, e.g., when applied as chromatographic detectors.<sup>315–318</sup>

### C. The Polymer Matrix

Originally, liquid ISE membranes were obtained by soaking porous materials (e.g., filter paper) with a solution of the ionophore in a water-immiscible, nonvolatile, viscous organic liquid.<sup>319,320</sup> Polymers as

homogeneous membrane matrices came first in use with charged carriers.<sup>20,285</sup> According to common practice typically  $\approx 33\%$  (w/w) of PVC,  $\approx 66\%$  of plasticizer, and  $\approx 1\%$  of ionophore are used.<sup>23,285</sup> The first neutral-carrier-based polymer ISE membranes were prepared with valinomycin in silicone rubber<sup>321</sup> or PVC<sup>321,322</sup> but without adding lipophilic ionic sites. At that time, the polymer was considered to be just an inert matrix providing the necessary physical properties, such as mechanical stability and elasticity. Nowadays, it is well-established that these ISEs only exhibited a Nernstian response owing to the fortuitous presence of ionic impurities in PVC<sup>47,48,311</sup> and in other membrane components.<sup>49</sup> It was demonstrated that membranes having no ionic sites at all do not give any electrode response.<sup>49,50</sup> By radiotracer studies<sup>182</sup> as well as by ion exchange and atomic absorption,<sup>311</sup> the total concentration of anionic impurities in cation-selective PVC membranes was found to be 0.5 and 0.05–0.6 mmol kg<sup>-1</sup>. Recently, their electrochemically relevant concentration was determined more precisely by measuring potentiometric selectivity coefficients of a series of membranes that only differed in the amount of tetraphenylborate salt added.<sup>83</sup> When prepared with commercially available PVC and *o*-NPOE, membranes were shown to contain  $0.063 \pm 0.016$  mmol kg<sup>-1</sup> of anionic impurities. This is much less than the usually applied concentrations of ionophore and ionic additive ( $\approx 1$ –15 mmol kg<sup>-1</sup>). Although the nature of the impurities in commercial PVC is not fully elucidated, it is established that some of them are compounds having sulfate or sulfonate groups.<sup>48</sup> Impedance measurements seem to indicate that these anionic sites, which may come from emulsifier residues, are not covalently bonded to the polymer matrix.<sup>48</sup> Of course, the kind and concentration of impurities may greatly vary with the source of PVC and be very different with other polymers. For example, membranes made with a commercially available polyurethane, Tecoflex, have  $0.044 \pm 0.006$  mmol kg<sup>-1</sup> of cationic impurities, i.e., salts with lipophilic cations.<sup>83</sup>

Sensor membranes based on PVC are known to take up water from the aqueous phase. It has been observed for many years that certain transparent membranes become opaque upon contact with water or moist air, the process being reversed upon drying. This opacity was attributed to the formation of water droplets. In recent years, the process has been thoroughly investigated by Harrison and co-workers. Using a spatial imaging technique<sup>323</sup> and water indicators such as CoCl<sub>2</sub>, these authors were able to follow the diffusion of dissolved, i.e., homogeneous, water, whereas light scattering allowed them to monitor the droplet formation, i.e., the presence of heterogeneous water. It could be shown that this water uptake is a two-stage process: The diffusion of homogeneous water is fast ( $D \approx 10^{-6}$  cm<sup>2</sup> s<sup>-1</sup>), whereas the apparent diffusion of heterogeneous water is slow ( $D \approx 10^{-8}$ – $10^{-7}$  cm<sup>2</sup> s<sup>-1</sup>, varying with time and membrane composition). As expected, the diffusion of water through a water-saturated membrane is fast again.<sup>165,324</sup> The presence of these two states of water was also confirmed by IR and NMR

spectroscopy.<sup>66</sup> Further studies revealed that there exists a water-rich surface region, showing that water is not evenly distributed in the membrane.<sup>266,325</sup> The water taken up by a typical PVC membrane (33% PVC and 67% bis(2-ethylhexyl) adipate, DOA) corresponds to  $\approx 0.6\%$  (w/w) or  $\approx 0.35$  M (density of the membrane, 1.08 g cm<sup>-3</sup>).<sup>325</sup> However, this amount strongly depends on the composition (more hydrophilic components induce a higher water uptake) as well as on the ionic concentration (ionic strength) in the aqueous phase. Thus, when the concentration of KCl in the sample is lowered from 1 to 10<sup>-3</sup> M, the water content in a carrier-free *o*-NPOE–PVC membrane increases from 0.10 to 0.40% (w/w) and in the analogous one with valinomycin from 0.10 to 0.24% (w/w).<sup>326</sup>

Of course, PVC is not the only polymer suitable for sensor membranes. As pointed out very early by Fiedler and Ruzicka,<sup>322</sup> apart from having the necessary solubility, for a polymer to serve as sensor matrix, the most important factor is that its glass transition temperature ( $T_g$ ) must be below room temperature. With polymers of high  $T_g$  (e.g., high molecular weight PVC:  $T_g \approx 80^\circ$ ), plasticizers must be used, while those of low  $T_g$  (e.g., soft polyurethanes with a low content of crystalline units,<sup>304</sup> silicone rubber,<sup>321</sup> poly(vinylidene chloride),<sup>327</sup> and polysiloxanes<sup>175</sup>) can be used without, thus avoiding the handicap of plasticizer leaching but, at the same time also losing the possibility to modify ion selectivities by varying the plasticizer. A number of other polymers have also been investigated.<sup>328</sup> Although the polymer has only a slight effect on the performance of ISEs, detailed investigations show that it is not just an inert matrix but that it may influence various membrane properties. For example, the polarity of a membrane differs significantly from that of the plasticizer alone (cf. section III.2.A). Thus the widely used plasticizers DOS and *o*-NPOE exhibit dielectric constants of 4.2 and 21, respectively, whereas the values for the corresponding membrane phases with 33% PVC are 4.8 and 14.<sup>299</sup> As to the extent of ion-pair formation, it is much lower in a DOS–PVC membrane than in DOS alone.<sup>300</sup>

Several chemically modified forms of PVC containing hydroxy, amino, or carboxylate groups have been synthesized in order to improve the adhesion properties of the membranes on electrode surfaces.<sup>311,329,330</sup> Most investigations focused on derivatives of PVC containing about 1.8% of carboxylate groups. The corresponding sensors based on various neutral carriers were shown to exhibit similar characteristics as those of PVC matrices, which is explained by the fact that the COOH groups are predominantly undissociated.<sup>311,330,331</sup> Aminated PVC<sup>330,332</sup> or related polymers<sup>333</sup> are at least partly protonated upon contact with aqueous samples and have been used to prepare so-called ionophore-free H<sup>+</sup>-selective liquid membrane electrodes.<sup>334,335</sup> Neutral-carrier-based Na<sup>+</sup>-selective ISEs with a vinyl chloride–vinyl alcohol copolymer (OH-PVC) matrix exhibited reduced protein-induced asymmetry effects.<sup>336</sup>

For clinical applications, the biocompatibility of ISE membranes is essential. During *in vitro* measurements, protein deposits on membrane surfaces

give rise to membrane asymmetries and instabilities, so frequent recalibration and skilled personnel are needed. For *in vivo* applications, on the other hand, leaching components having inflammatory, toxic,<sup>304</sup> and/or thrombogenic properties are of concern. Polyurethanes were shown to reduce the inflammatory response<sup>304</sup> and are attractive also because of their excellent adhesive properties.<sup>337</sup> Moreover, by covalently bonding hydrophilic poly(ethylene oxide) to the surface of polyurethane membranes, their biocompatibility is improved.<sup>338</sup> Blood compatibility can be also improved by covalently attaching heparin to the membrane surface.<sup>339</sup> Owing to their good adhesive properties, polyurethanes are a highly promising alternative to PVC in optical sensors as well.<sup>340</sup>

For preparing miniaturized electrodes by standard photolithography, as applied in microelectronics technology, photocurable polymer matrices are of interest. Among them, acrylates and methacrylates,<sup>341</sup> methacrylated siloxane resins,<sup>175,342</sup> epoxyacrylates,<sup>343</sup> polystyrene,<sup>344</sup> and acrylates of urethane oligomers<sup>345,346</sup> have been studied in ISE membranes. For miniaturized electrodes, covalent attachment of all membrane components including the ionophore is advisable. Both charged<sup>282</sup> and uncharged<sup>175,176,283</sup> ionophores have been covalently bonded to the polymer matrix, seemingly without any significant loss of electrode performance. The use of templates during polymer preparation was proposed as an alternative way of preparing selective electrodes. Early attempts of copolymerizing a Ca<sup>2+</sup>-selective ligand in divinylbenzene-based polymers was of limited success.<sup>347</sup> More recently, electrochemically mediated molecular imprinting was successfully applied for preparing NO<sub>3</sub><sup>-</sup>-selective polypyrrole membranes.<sup>348</sup>

#### IV. Conclusions

Carrier-based ion-selective electrodes have been known for about 30 years and have found many applications in research and routine analysis. Nonetheless, research and development activities have not declined over time but are still increasing, especially in the field of anion sensors. In the past, the theoretical description of the ISE response has been quite demanding and often not understood by experimental scientists. As a consequence, experimentation under nonoptimal conditions is still not uncommon. Typical examples are the use of membranes containing inadequate or no intentionally added ionic sites or inappropriate conditioning of membranes. It has been shown only recently that significant parts of the established theory are not really relevant in most cases, so a simplified and chemically more intuitive treatment is fully adequate. One of the goals of this paper has been to review this theoretical basis in a comprehensive form.

In spite of the different transduction principles, the response of bulk optodes and ISEs rely on very similar chemical equilibria. This allowed the development of numerous new sensors within only a few years. In this paper we stressed the relation of the two fields because the mutual benefits of the interactions between them are manifold. It is shown that fundamental parameters obtained by one of the techniques are valid and can be advantageously used

for the other. We hope that the simultaneous treatment of the theoretical basis and a comparison of the analytically relevant parameters will catalyze useful interactions of these sensor fields.

The parallel treatment will also be the focus of part 2 of this pair of reviews, in which a large number of sensors will be presented and critically discussed. Since a comprehensive list of sensors would fill volumes, we will focus on the most relevant ones both from historical and practical points of view. While we will try to mention as many analytes as possible for which carrier-based ISEs or bulk optodes are known, it is clear that any attempt to give a complete list is futile. The summary of the best available sensors will show some of the still-remaining needs, and the knowledge of historical developments may help to optimize strategies for the design of future sensors. Currently, enormous efforts are invested into the field of chemical sensor technologies, but as shown by the actual performance and fundamental limitations of instruments using arrays of *non-specific* sensing elements, selective chemical recognition is at the heart of truly useful sensors. Part 2 will show the huge amount of work analytical chemists have done in applied molecular recognition. Given the state-of-the-art in the theory of ISEs and optodes, the development of ever more selective ionophores and their application in sensors has, however, become more and more of a challenge also for organic chemists.

#### V. Acknowledgments

The authors acknowledge support from the Petroleum Research Fund, the Swiss National Science Foundation, Hitachi Ltd., Orion Research Inc., and the Ministry of Education, Science and Culture, Japan. We thank Dr. D. Wegmann, Dr. T. Sokalski, and D. Ertékes for careful reading of parts of the manuscript.

#### Note Added in Proof

II.1.B: Very recently a detailed analysis of acidic ionophores showed that apparently "twice-Nernstian" responses can be generated for divalent cations by using negative sites (Amemiya, S.; Bühlmann, P.; Umezawa, Y. *Anal. Chem.*, in press).

III.3.C: Very recently a detailed analysis of the underlying membrane processes (Mathison, S.; Bakker, E. *Anal. Chem.*, in press) led to a large improvement of the detection limit of ISEs (Sokalski, T.; Ceresa, A.; Zwickl, T.; Pretsch, E. *J. Am. Chem. Soc.*, in press).

#### VI. References

- (1) MacDonald, N. F.; Williams, P. Z.; Burton, J. I.; Batsakis, J. G. *Am. J. Clin. Pathol.* **1981**, *76* (Suppl.), 575.
- (2) Gunaratna, P. C.; Koch, W. F.; Paule, R. C.; Cormier, A. D.; D'Orazio, P.; Greenberg, N.; O'Connell, K. M.; Malenfant, A.; Okorodudu, A. O.; Miller, R.; Kus, D. M.; Bowers, G. N., Jr. *Clin. Chem.* **1992**, *38*, 1459.
- (3) D'Orazio, P., Pittsburgh Conference, Chicago, IL, 1994; Abstract 152.
- (4) Stefanac, Z.; Simon, W. *Chimia* **1966**, *20*, 436.
- (5) Pioda, L. A. R.; Stankova, V.; Simon, W. *Anal. Lett.* **1969**, *2*, 665.
- (6) Bühlmann, P.; Bakker, E.; Pretsch, E. Manuscript in preparation.
- (7) Izatt, R. M.; Lindh, G. C.; Bruening, L. R.; Bradshaw, J. S.; Lamb, J. D.; Christensen, J. J. *Pure Appl. Chem.* **1986**, *58*, 1453.

- (8) Visser, H. C.; Reinhoudt, D. N.; de Jong, F. *Chem. Soc. Rev.* **1994**, 23, 75.
- (9) Morf, W. E.; Wuhmann, P.; Simon, W. *Anal. Chem.* **1976**, 48, 1031.
- (10) Behr, J. P.; Kirch, M.; Lehn, J.-M. *J. Am. Chem. Soc.* **1985**, 107, 241.
- (11) Buck, R. P.; Nahir, T. M.; Cosofret, V. V.; Lindner, E.; Erdösy, M. *Anal. Proc. Incl. Anal. Comm.* **1994**, 31, 301.
- (12) Moore, C.; Pressman, B. C. *Biochem. Biophys. Res. Commun.* **1964**, 15, 562.
- (13) Stefanac, Z.; Simon, W. *Microchem. J.* **1967**, 12, 125.
- (14) Pioda, L. A. R.; Wipf, H.-K.; Simon, W. *Chimia* **1968**, 22, 189.
- (15) Pedersen, C. J., *J. Am. Chem. Soc.* **1967**, 89, 2495–2496; **1967**, 89, 7017–7036; **1970**, 92, 386–391; **1970**, 92, 391–394.
- (16) Dietrich, B.; Lehn, J. M.; Sauvage, J. P. *Tetrahedron Lett.* **1969**, 34, 2885.
- (17) Lehn, J. M.; Sauvage, J. P. *J. Chem. Soc., Chem. Commun.* **1971**, 440.
- (18) Dobler, M. *Ionophores and their Structures*; Wiley-Interscience: New York, 1981.
- (19) Shatkay, A. *J. Phys. Chem.* **1967**, 71, 3858.
- (20) Shatkay, A. *Anal. Chem.* **1967**, 39, 1056.
- (21) Ross, J. W. *Science* **1967**, 156, 1378.
- (22) Moody, G. J.; Thomas, J. D. R. *Selective Ion Sensitive Electrodes*; Merrow: Watford, England, 1971.
- (23) Craggs, A.; Moody, G. J.; Thomas, J. D. R. *J. Chem. Edu.* **1974**, 51, 541.
- (24) Ammann, D.; Pretsch, E.; Simon, W. *Tetrahedron Lett.* **1972**, 2473.
- (25) Ammann, D.; Pretsch, E.; Simon, W. *Anal. Lett.* **1972**, 5, 843.
- (26) Ammann, D.; Anker, P.; Meier, P. C.; Morf, W. E.; Pretsch, E.; Simon, W. *Ion-Sel. Electr. Rev.* **1983**, 5, 3.
- (27) Lehn, J. M. *Supramolecular Chemistry*; VCH: Weinheim, 1995.
- (28) Ciani, S. M.; Eisenman, G.; Szabo, G. *J. Membrane Biol.* **1969**, 1, 1.
- (29) Morf, W. E. *The Principles of Ion-Selective Electrodes and of Membrane Transport*; Elsevier: New York, 1981.
- (30) Boles, J. H.; Buck, R. P. *Anal. Chem.* **1973**, 45, 2057.
- (31) Theorell, T. *Proc. Soc. Exp. Biol. Med.* **1935**, 33, 282.
- (32) Meyer, K. H.; Sievers, J.-F. *Helv. Chim. Acta* **1936**, 19, 649.
- (33) Pungor, E. *Pure Appl. Chem.* **1992**, 64, 503.
- (34) Umezawa, K.; Lin, X. M.; Nishizawa, S.; Sugawara, M.; Umezawa, Y. *Anal. Chim. Acta* **1993**, 282, 247.
- (35) Bakker, E.; Nägele, M.; Schaller, U.; Pretsch, E. *Electroanalysis* **1995**, 7, 817.
- (36) Bakker, E.; Meruva, R. K.; Pretsch, E.; Meyerhoff, M. E. *Anal. Chem.* **1994**, 66, 3021.
- (37) Dix, J. P.; Vögltle, F. *Chem. Ber.* **1981**, 114, 638.
- (38) Morf, W. E.; Seiler, K.; Lehmann, B.; Behringer, C.; Hartman, K.; Simon, W. *Pure Appl. Chem.* **1989**, 61, 1613.
- (39) Morf, W. E.; Seiler, K.; Rusterholz, B.; Simon, W. *Anal. Chem.* **1990**, 62, 738.
- (40) Bakker, E.; Simon, W. *Anal. Chem.* **1992**, 64, 1805.
- (41) Janata, J. *Anal. Chem.* **1987**, 59, 1351.
- (42) Janata, J. *Anal. Chem.* **1992**, 64, 921 A.
- (43) Umezawa, Y. *Handbook of Ion-Selective Electrodes: Selectivity Coefficients*; CRC Press: Boca Raton, FL, 1990.
- (44) Perry, M.; Löbel, E.; Bloch, R. *J. Membr. Sci.* **1976**, 1, 223.
- (45) Karpfen, F. M.; Randles, J. E. B. *Trans. Faraday Soc.* **1953**, 49, 823.
- (46) Morf, W. E.; Simon, W. *Helv. Chim. Acta* **1986**, 69, 1120.
- (47) Horvai, G.; Graf, E.; Tóth, K.; Pungor, E.; Buck, R. P. *Anal. Chem.* **1986**, 58, 2735.
- (48) van den Berg, A.; van der Wal, P. D.; Skowronska-Ptasinska, M.; Sudhölter, E. J. R.; Reinhoudt, D. N.; P., B. *Anal. Chem.* **1987**, 59, 2827.
- (49) Bühlmann, P.; Yajima, S.; Tohda, K.; Umezawa, K.; Nishizawa, S.; Umezawa, Y. *Electroanalysis* **1995**, 7, 811.
- (50) Bühlmann, P.; Yajima, S.; Tohda, K.; Umezawa, Y. *Electrochim. Acta* **1995**, 40, 3021.
- (51) Henderson, L. J. *J. Biol. Chem.* **1921**, 46, 411.
- (52) Sigel, H.; Zuberbühler, A. D.; Yamauchi, O. *Anal. Chim. Acta* **1991**, 255, 63.
- (53) Theorell, T. *Trans. Faraday Soc.* **1937**, 1053.
- (54) Rakhman'ko, E. M.; Yegorov, V. V.; Gulevich, A. L.; Lushchik, Y. F. *Sel. Electrode Rev.* **1991**, 13, 5.
- (55) Meier, P. C.; Morf, W. E.; Läubli, M.; Simon, W. *Anal. Chim. Acta* **1984**, 156, 1.
- (56) Eugster, R.; Gehrig, P. M.; Morf, W. E.; Spichiger, U. E.; Simon, W. *Anal. Chem.* **1991**, 63, 2285.
- (57) Büchi, R.; Pretsch, E.; Simon, W. *Helv. Chim. Acta* **1976**, 59, 2327.
- (58) Büchi, R.; Pretsch, E.; Morf, W. E.; Simon, W. *Helv. Chim. Acta* **1976**, 59, 2407.
- (59) Buck, R. P.; Tóth, K.; Gräf, E.; Horvai, G.; Pungor, E. *J. Electroanal. Chem.* **1987**, 223, 51.
- (60) Guggenheim, E. A. *J. Phys. Chem.* **1930**, 34, 1540.
- (61) Tohda, K.; Umezawa, Y.; Yoshiyagawa, S.; Hashimoto, S.; Kawasaki, M. *Anal. Chem.* **1995**, 67, 570.
- (62) Davies, M. L.; Tighe, B. J. *Sel. Electrode Rev.* **1991**, 13, 159.
- (63) Jones, D. L.; Moody, G. J.; Thomas, J. D. R. *Analyst* **1981**, 106, 974.
- (64) Espadas-Torre, C.; Bakker, E.; Barker, S.; Meyerhoff, M. E. *Anal. Chem.* **1996**, 68, 1623.
- (65) Anzai, J.; Liu, C. C. *Anal. Chim. Acta* **1991**, 248, 323.
- (66) Chan, A. D. C.; Harrison, D. J. *Anal. Chem.* **1993**, 65, 32.
- (67) Hodinar, A.; Jyo, A. *Anal. Chem.* **1989**, 61, 1169.
- (68) Huser, M.; Morf, W. E.; Fluri, K.; Seiler, K.; Schulthess, P.; Simon, W. *Helv. Chim. Acta* **1990**, 73, 1481.
- (69) Schaller, U.; Bakker, E.; Spichiger, U. E.; Pretsch, E. *Anal. Chem.* **1994**, 66, 391.
- (70) Schaller, U.; Bakker, E.; Spichiger, U. E.; Pretsch, E. *Talanta* **1994**, 41, 1001.
- (71) Bakker, E.; Malinowska, E.; Schiller, R. D.; Meyerhoff, M. E. *Talanta* **1994**, 41, 881.
- (72) Schaller, U.; Bakker, E.; Pretsch, E. *Anal. Chem.* **1995**, 67, 3123.
- (73) Badr, I. H. A.; Meyerhoff, M. E.; Hassan, S. S. M. *Anal. Chem.* **1995**, 67, 2613.
- (74) Oesch, U.; Ammann, D.; Simon, W. *Clin. Chem.* **1986**, 32, 1448.
- (75) Gadzekpo, V. P. Y.; Christian, G. D. *Anal. Chim. Acta* **1984**, 164, 279.
- (76) Morf, W. E.; Simon, W. In *Ion-Selective Electrodes in Analytical Chemistry*; Freiser, H., Ed.; Plenum Press: New York, 1978.
- (77) Morf, W. E.; Ammann, D.; Pretsch, E.; Simon, W. *Pure Appl. Chem.* **1973**, 36, 421.
- (78) Eisenman, G.; Rudin, D. O.; Casby, J. U. *Science* **1957**, 126, 831.
- (79) Eugster, R.; Spichiger, U. E.; Simon, W. *Anal. Chem.* **1993**, 65, 689.
- (80) Horvai, G. *Trends Anal. Chem.* **1997**, 16, 260.
- (81) Oesch, U.; Anker, P.; Ammann, D.; Simon, W. In *Ion-Selective Electrodes*; Pungor, E., Buzás, I., Eds.; Akadémiai Kiadó: Budapest, 1984; Vol. 4.
- (82) Rosatzin, T.; Bakker, E.; Suzuki, K.; Simon, W. *Anal. Chim. Acta* **1993**, 280, 197.
- (83) Nägele, M.; Pretsch, E. *Mikrochim. Acta* **1995**, 121, 269.
- (84) Bakker, E.; Willer, M.; Lerchi, M.; Seiler, K.; Pretsch, E. *Anal. Chem.* **1994**, 66, 516.
- (85) Eyal, E.; Rechnitz, G. A. *Anal. Chem.* **1971**, 43, 1090.
- (86) Wuhmann, H.-R.; Morf, W. E.; Simon, W. *Helv. Chim. Acta* **1973**, 56, 1011.
- (87) Bliggendorfer, R.; Suter, G.; Simon, W. *Helv. Chim. Acta* **1989**, 72, 1164.
- (88) Kirsch, N. N. L.; Simon, W. *Helv. Chim. Acta* **1976**, 59, 357.
- (89) Guilbault, G. G.; Durst, R. A.; Frant, M. S.; Freiser, H.; Hansen, E. H.; Light, T. S.; E. Pungor; Rechnitz, G.; Rice, N. M.; Rohm, T. J.; Simon, W.; Thomas, J. D. R. *Pure Appl. Chem.* **1976**, 48, 127.
- (90) Diamond, D.; Forster, R. J. *Anal. Chim. Acta* **1993**, 276, 75.
- (91) Hartnett, M.; Diamond, D. *Anal. Chem.* **1997**, 69, 1909.
- (92) Bakker, E. *J. Electrochem. Soc.* **1996**, 143, L83.
- (93) Umezawa, Y.; Umezawa, K.; Sato, H. *Pure Appl. Chem.* **1995**, 67, 507.
- (94) Buck, R. P.; Lindner, E. *Pure Appl. Chem.* **1994**, 66, 2527.
- (95) Buck, R. P.; Cosofret, V. V.; Lindner, E. *Anal. Chim. Acta* **1993**, 282, 273.
- (96) Morf, W. E.; Ammann, D.; Simon, W. *Chimia* **1974**, 28, 65.
- (97) Fu, B.; Bakker, E.; Yun, J. H.; Yang, V. C.; Meyerhoff, M. E. *Anal. Chem.* **1994**, 66, 2250.
- (98) Wang, E. J.; Meyerhoff, M. E.; Yang, V. C. *Anal. Chem.* **1995**, 67, 522.
- (99) Fu, B.; Bakker, E.; Yang, V. C.; Meyerhoff, M. E. *Macromolecules* **1995**, 28, 5834.
- (100) Sokalski, T.; Maj-Zurawska, M.; Hulanicki, A. *Mikrochim. Acta* **1991**, 1, 285.
- (101) Christian, G. D. *Analyst* **1994**, 119, 2309.
- (102) Bakker, E. *Electroanalysis* **1997**, 9, 7.
- (103) Macca, C. *Anal. Chim. Acta* **1996**, 321, 1.
- (104) Ammann, D.; Bühner, T.; Schefer, U.; Müller, M.; Simon, W. *Pflügers Arch.* **1987**, 409, 223.
- (105) Ruzicka, J.; Hansen, E. H.; Tjell, J. C. *Anal. Chim. Acta* **1973**, 67, 155.
- (106) Bakker, E. *Anal. Chem.* **1997**, 69, 1061.
- (107) Midgley, D. *Analyst* **1979**, 104, 248.
- (108) Bricker, J.; Daunert, S.; Bachas, L. G.; Valiente, M. *Anal. Chem.* **1991**, 63, 1585.
- (109) Cosofret, V. V.; Nahir, T. M.; Lindner, E.; Buck, R. P. *J. Electroanal. Chem.* **1992**, 327, 137.
- (110) Schefer, U.; Ammann, D.; Pretsch, E.; Oesch, U.; Simon, W. *Anal. Chem.* **1986**, 58, 2282.
- (111) Bakker, E.; Willer, M.; Pretsch, E. *Anal. Chim. Acta* **1993**, 282, 265.
- (112) Bakker, E.; Lerchi, M.; Rosatzin, T.; Rusterholz, B.; Simon, W. *Anal. Chim. Acta* **1993**, 278, 211.
- (113) Lerchi, M.; Orsini, F.; Cimerman, Z.; Pretsch, E.; Chowdhury, D. A.; Kamata, S. *Anal. Chem.* **1996**, 68, 3210.
- (114) Bakker, E.; Xu, A.; Pretsch, E. *Anal. Chim. Acta* **1994**, 295, 253.
- (115) Oesch, U.; Ammann, D.; Brzozka, Z.; Pham, H. V.; Pretsch, E.; Rusterholz, B.; Simon, W.; Suter, G.; Welti, D. H.; Xu, A. P. *Anal. Chem.* **1986**, 58, 2285.
- (116) Morf, W. E.; Kahr, G.; Simon, W. *Anal. Lett.* **1974**, 7, 9.

- (117) Verpoorte, E. M. J.; Chan, A. D. C.; Harrison, D. J. *Electroanalysis* **1993**, *5*, 845.
- (118) Sears, J. K.; Darby, J. R. *The Technology of Plasticizers*; Wiley & Sons: New York, 1982.
- (119) Dinten, O., Diss. ETH Zürich, No. 8591, 1988.
- (120) Lindner, E.; Tóth, K.; Pungor, E. *Dynamic Characteristics of Ion-Selective Electrodes*; CRC Press: Boca Raton, FL, 1988.
- (121) Guilbault, G. G. *IUPAC Inf. Bull.* **1978**, *1*, 69.
- (122) Uemasu, I.; Umezawa, Y. *Anal. Chem.* **1982**, *54*, 1198.
- (123) Ammann, D. *Ion-Selective Microelectrodes*; Springer-Verlag: Berlin, 1986.
- (124) Schneider, B.; Zwickl, T.; Federer, B.; E. Pretsch; Lindner, E. *Anal. Chem.* **1996**, *68*, 4342.
- (125) Lindner, E.; Niegreisz, Z.; Tóth, K.; Pungor, E.; Berube, T. R.; Buck, R. P. *J. Electroanal. Chem.* **1989**, *259*, 67.
- (126) Morf, W. E.; Lindner, E.; Simon, W. *Anal. Chem.* **1975**, *47*, 1596.
- (127) Lindner, E.; Tóth, K.; Pungor, E.; Morf, W. E.; Simon, W. *Anal. Chem.* **1978**, *50*, 1627.
- (128) Huser, M.; Gehrig, P. M.; Morf, W. E.; Simon, W.; Lindner, E.; Jeney, J.; Tóth, K.; Pungor, E. *Anal. Chem.* **1991**, *63*, 1380.
- (129) Berube, T. R.; Buck, R. P. *Anal. Lett.* **1989**, *22*, 1221.
- (130) Seiler, K.; Simon, W. *Sens. Actuators, B* **1992**, *6*, 295.
- (131) Seiler, K.; Simon, W. *Anal. Chim. Acta* **1992**, *266*, 73.
- (132) Arnold, M. A. *Anal. Chem.* **1992**, *64*, 1015.
- (133) Yoshiyagawa, S.; Tohda, K.; Umezawa, Y.; Hashimoto, S.; Kawasaki, M. *Anal. Sci.* **1993**, *9*, 715.
- (134) Mohr, G. J.; Wolfbeis, O. S. *Anal. Chim. Acta* **1995**, *316*, 239.
- (135) Gantzer, M. L.; Hemmes, P. R.; Wong, D., Eur. Pat. Appl. EP 153.641.
- (136) Morf, W. E.; Seiler, K.; Sørensen, P. R.; Simon, W. In *Ion-Selective Electrodes*; Pungor, E., Ed.; Akadémiai Kiadó: Budapest, 1989; Vol. 5.
- (137) Morf, W. E.; Seiler, K.; Lehmann, B.; Behringer, C.; Tan, S. S. S.; Hartman, K.; Sørensen, P. R.; Simon, W. In *Ion-Selective Electrodes*; Pungor, E., Ed.; Akadémiai Kiadó: Budapest, 1989; Vol. 5.
- (138) Roe, J. N.; Szoka, F. C.; Verkman, A. S. *Analyst* **1990**, *115*, 353.
- (139) Suzuki, K.; Tohda, K.; Tanda, Y.; Ohzora, H.; Nishihama, S.; Inoue, H.; Shirai, T. *Anal. Chem.* **1989**, *61*, 382.
- (140) Suzuki, K.; Ohzora, H.; Tohda, K.; Miyazaki, K.; Watanabe, K.; Inoue, H.; Shirai, T. *Anal. Chim. Acta* **1990**, *237*, 155.
- (141) He, H. R.; Uray, G.; Wolfbeis, O. S. *Anal. Chim. Acta* **1991**, *246*, 251.
- (142) He, H.; Li, H.; Mohr, G.; Kovacs, B.; Werner, T.; Wolfbeis, O. S. *Anal. Chem.* **1993**, *65*, 123.
- (143) McCarrick, M.; Harris, S. J.; Diamond, D. *Analyst* **1993**, *118*, 1127.
- (144) Tóth, K.; Lan, B. T. T.; Jeney, J.; Horvath, M.; Bitter, I.; Grün, A.; Agai, B.; Toke, L. *Talanta* **1994**, *41*, 1041.
- (145) Shortreed, M.; Bakker, E.; Kopelman, R. *Anal. Chem.* **1996**, *68*, 2656.
- (146) Lerchi, M.; Reitter, E.; Simon, W.; Pretsch, E. *Anal. Chem.* **1994**, *66*, 1713.
- (147) Wang, E.; Meyerhoff, M. E. *Anal. Chim. Acta* **1993**, *283*, 673.
- (148) Hauser, P. C.; Litten, J. C. *Anal. Chim. Acta* **1994**, *294*, 49.
- (149) West, S. J.; Ozawa, S.; Seiler, K.; Tan, S. S. S.; Simon, W. *Anal. Chem.* **1992**, *64*, 533.
- (150) Wang, K.; Seiler, K.; Rusterholz, B.; Simon, W. *Analyst* **1992**, *117*, 57.
- (151) Tan, S. S. S.; Hauser, P. C.; Chaniotakis, N. A.; Suter, G.; Simon, W. *Chimia* **1989**, *43*, 257.
- (152) Wang, K.; Seiler, K.; Haug, J. P.; Lehmann, B.; West, S.; Hartman, K.; Simon, W. *Anal. Chem.* **1991**, *63*, 970.
- (153) Seiler, K.; Wang, K. M.; Kuratli, M.; Simon, W. *Anal. Chim. Acta* **1991**, *244*, 151.
- (154) Ozawa, S.; Hauser, P. C.; Seiler, K.; Tan, S. S. S.; Morf, W. E.; Simon, W. *Anal. Chem.* **1991**, *63*, 640.
- (155) Ozawa, S.; Simon, W., in K. T. V. Grattan, A. T. Augousti (eds), *Sensors & their Applications VI*, Institute of Physics Publishing, Manchester, 1993.
- (156) Kuratli, M.; Badertscher, M.; Rusterholz, B.; Simon, W. *Anal. Chem.* **1993**, *65*, 3473.
- (157) Kuratli, M.; Pretsch, E. *Anal. Chem.* **1994**, *66*, 85.
- (158) Rosatzin, T.; Holy, P.; Seiler, K.; Rusterholz, B.; Simon, W. *Anal. Chem.* **1992**, *64*, 2029.
- (159) Lerchi, M.; Bakker, E.; Rusterholz, B.; Simon, W. *Anal. Chem.* **1992**, *64*, 1534.
- (160) Seiler, K., Diss. ETH Zurich No. 9221, 1990.
- (161) Bakker, E. *Anal. Chim. Acta* **1997**, *350*, 329.
- (162) Crank, J. *The Mathematics of Diffusion*; Oxford University Press: New York, 1993.
- (163) Seiler, K.; Morf, W. E.; Rusterholz, B.; Simon, W. *Anal. Sci.* **1989**, *5*, 557.
- (164) Shortreed, M.; Kopelman, R.; Kuhn, M.; Hoyland, B. *Anal. Chem.* **1996**, *68*, 1414.
- (165) Li, Z.; Li, X.; Petrovic, S.; Harrison, D. J. *Anal. Chem.* **1996**, *68*, 1717.
- (166) Dohner, R. E.; Spichiger, U. E.; Simon, W. *Chimia* **1992**, *46*, 215.
- (167) Seiler, K.; Wang, K.; Bakker, E.; Morf, W. E.; Rusterholz, B.; Spichiger, U. E.; Simon, W. *Clin. Chem.* **1991**, *37*, 1350.
- (168) Gehrig, P.; Rusterholz, B.; Simon, W. *Anal. Chim. Acta* **1990**, *233*, 295.
- (169) Rouilly, M. V.; Badertscher, M.; Pretsch, E.; Suter, G.; Simon, W. *Anal. Chem.* **1988**, *60*, 2013.
- (170) Maj-Zurawska, M.; Sokalski, T.; Hulanicki, A. *Talanta* **1988**, *35*, 281.
- (171) Wang, K.; Seiler, K.; Morf, W. E.; Spichiger, U. E.; Simon, W.; Lindner, E.; Pungor, E. *Anal. Sci.* **1990**, *6*, 715.
- (172) Oesch, U.; Simon, W. *Anal. Chem.* **1980**, *52*, 692.
- (173) Griffin, J. J.; Christian, G. D. *Talanta* **1983**, *30*, 201.
- (174) Bakker, E.; Pretsch, E. *Anal. Chim. Acta* **1995**, *309*, 7.
- (175) Reinhoudt, D. N.; Engbersen, J. F. J.; Brózka, Z.; van den Vlekkert, H. H.; Honig, G. W. N.; Holterman, H. A. J.; Verkerk, U. H. *Anal. Chem.* **1994**, *66*, 3618.
- (176) Daunert, S.; Bachas, L. G. *Anal. Chem.* **1990**, *62*, 1428.
- (177) Meisters, M.; Vandenberg, J. T.; Cassaretto, F. P.; Posvic, H.; Moore, C. E. *Anal. Chim. Acta* **1970**, *49*, 481.
- (178) Nishida, H.; Takada, N.; Yoshimura, M.; Sonoda, T.; Kobayashi, H. *Bull. Chem. Soc. Jpn.* **1984**, *57*, 2600.
- (179) Caroni, P.; Gazzotti, P.; Vuilleumier, P.; Simon, W.; E. Carafoli, E. *Biochim. Biophys. Acta* **1977**, *470*, 437.
- (180) Prestipino, G.; Falugi, C.; Falchetto, R.; Gazzotti, P. *Anal. Biochem.* **1993**, *210*, 119.
- (181) Tóth, K.; Lindner, E.; Pungor, E.; Zippel, E.; Kellner, R. *Fresenius Z. Anal. Chem.* **1988**, *331*, 448.
- (182) Thoma, A. P.; Viviani-Nauer, A.; Arvanitis, S.; Morf, W. E.; Simon, W. *Anal. Chem.* **1977**, *49*, 1567.
- (183) Inoue, Y.; Hakushi, T. In *Cation binding by macrocycles*; Inoue, Y., Gokel, G. W., Eds.; Marcel Dekker Inc.: New York, 1990.
- (184) Feinstein, M. B.; Felsenfeld, H. *Proc. Natl. Acad. Sci. USA* **1971**, *68*, 2037.
- (185) Funck, T.; Eggert, F.; Grell, E. *Chimia* **1972**, *26*, 637.
- (186) Shemyakin, M. M.; Ovchinnikov, Y. A.; Ivanov, V. T.; Antonov, V. K.; Vinogradova, E. I.; Shkrob, A. M.; Malenkov, G. G.; Evstratov, A. V.; Laine, I. T.; Melnik, E. I.; Ryabova, I. D. *J. Membr. Biol.* **1969**, *1*, 402.
- (187) Möschler, H. J.; Weder, H.-G.; Schwyzer, R. *Helv. Chim. Acta* **1971**, *54*, 1437.
- (188) Grell, E.; Funck, T.; Eggert, F. In *Mechanisms of antibiotic Action on Protein Biosynthesis and Membranes*; Muñoz, E., García-Ferrándiz, F., Vazquez, D., Eds.; Elsevier Scientific Publishing Co.: Amsterdam, 1972.
- (189) Vanýsek, P. *Electrochemistry on Liquid/Liquid Interfaces*; Springer: Berlin, 1985.
- (190) Koryta, J. *Electrochim. Acta* **1979**, *24*, 293.
- (191) Armstrong, R. D.; Todd, M. *J. Electroanal. Chem.* **1987**, *237*, 181.
- (192) Cram, D. J.; Lein, G. M. *J. Am. Chem. Soc.* **1985**, *107*, 3657.
- (193) Pinkerton, M.; Steinrauf, L. K.; Dawkins, P. *Biochem. Biophys. Res. Commun.* **1969**, *35*, 512.
- (194) Steinrauf, L. K.; Hamilton, J. A.; Sabesan, M. N. *J. Am. Chem. Soc.* **1982**, *104*, 4085.
- (195) Neupert-Laves, K.; Dobler, M. *Helv. Chim. Acta* **1977**, *60*, 1861.
- (196) Dobler, M. *Chimia* **1984**, *12*, 415.
- (197) Meyerhoff, M. E.; Pretsch, E.; Welty, D. H.; Simon, W. *Anal. Chem.* **1987**, *59*, 144.
- (198) Dzidic, I.; Kebarle, P. *J. Phys. Chem.* **1970**, *74*, 1466.
- (199) Yamdagni, R.; Kebarle, P. *J. Am. Chem. Soc.* **1972**, *94*, 2940.
- (200) Davidson, W. R.; Kebarle, P. *Can. J. Chem.* **1976**, *54*, 2594.
- (201) Woodin, L. R.; Beauchamp, J. L. *J. Am. Chem. Soc.* **1978**, *100*, 501.
- (202) Schuster, P.; Jakubetz, W.; Marius, W. *Top. Curr. Chem.* **1975**, *60*, 1.
- (203) Renugopalakrishnan, V.; Urry, D. W. *Biophys. J.* **1978**, *24*, 729.
- (204) Pullman, B.; Pullman, A.; Berthod, H.; Gresh, N. *Theor. Chim. Acta* **1975**, *40*, 93.
- (205) Kolos, W. *Theor. Chim. Acta* **1979**, *51*, 219.
- (206) Kolos, W. *Theor. Chim. Acta* **1980**, *54*, 187.
- (207) Gianolio, L.; Pavani, R.; Clementi, E. *Gazz. Chim. Ital.* **1978**, *108*, 181.
- (208) Gianolio, L.; Clementi, E. *Gazz. Chim. Ital.* **1980**, *179*.
- (209) Portmann, P.; Maruizumi, T.; Welty, M.; Badertscher, M.; Neszmélyi, A.; Simon, W.; Pretsch, E. *J. Chem. Phys.* **1987**, *87*, 493.
- (210) Portmann, P.; Maruizumi, T.; Welty, M.; Badertscher, M.; Neszmélyi, A.; Simon, W.; Pretsch, E. *J. Chem. Phys.* **1988**, *88*, 1477.
- (211) Del Bene, J. E.; Mettee, H. D.; Frisch, M. J.; Luke, B. T.; Pople, J. A. *J. Phys. Chem.* **1983**, *87*, 3279.
- (212) Kistenmacher, H.; Popkie, H.; Clementi, E. *J. Chem. Phys.* **1973**, *58*, 5842.
- (213) Almlöf, J.; Faegri, K.; Korsell, K. *J. Comput. Chem.* **1982**, *3*, 385.
- (214) Haesser, M.; Ahlrichs, R. *J. Comput. Chem.* **1989**, *10*, 104.
- (215) Pullman, A.; Gresh, N.; Daudey, J. P.; Moskowitz, J. W. *Int. J. Quantum Chem., Quantum Chem. Symp.* **1977**, *11*, 501.
- (216) Ortega-Blake, I.; Les, A.; Rybak, S. *J. Theor. Biol.* **1983**, *104*, 571.



- (217) Krauss, M.; Stevens, W. J. *Annu. Rev. Phys. Chem.* **1984**, *35*, 357.
- (218) Parr, R. G.; Yang, W. *Density-Functional Theory of Atoms and Molecules*; Oxford University Press: New York, 1983.
- (219) Ha, Y. L.; Chakraborty, A. K. *J. Phys. Chem.* **1992**, *96*, 6410.
- (220) Clementi, E. *Lecture Notes in Chemistry*; Springer-Verlag: Berlin, 1976.
- (221) Gresh, N.; Claverie, P.; Pullman, A. *Int. J. Quantum Chem. Symp.* **1979**, *13*, 243.
- (222) Badertscher, M.; Welti, M.; Portmann, P.; Pretsch, E. *Top. Curr. Chem.* **1986**, *136*, 17.
- (223) Gresh, N.; Etchebest, C.; De la Luz Rojas, O.; Pullman, A. *Int. J. Quantum Chem. Quantum Biol. Symp.* **1981**, *8*, 109.
- (224) Gresh, N.; Pullman, A. *Int. J. Quantum Chem.* **1982**, *23*, 709.
- (225) Lifson, S.; Felder, C. E.; Shanzer, A. *J. Am. Chem. Soc.* **1983**, *105*, 3866.
- (226) Lifson, S.; Felder, C. E.; Shanzer, A. *Biochemistry* **1984**, *23*, 2577.
- (227) Wipff, G.; Weiner, P.; Kollman, P. *J. Am. Chem. Soc.* **1982**, *104*, 3249.
- (228) Adam, K. R.; Antolowich, M.; Brigden, L. G.; Lindoy, L. F. *J. Am. Chem. Soc.* **1991**, *113*, 3346.
- (229) Corongiu, G.; Clementi, E.; Pretsch, E.; Simon, W. *J. Chem. Phys.* **1979**, *70*, 1266.
- (230) Corongiu, G.; Clementi, E.; Pretsch, E.; Simon, W. *J. Chem. Phys.* **1980**, *72*, 3096.
- (231) Welti, M.; Pretsch, E.; Clementi, E.; Simon, W. *Helv. Chim. Acta* **1982**, *65*, 1996.
- (232) Weiner, S. J.; Kollman, P. A.; Nguyen, D. T.; Case, D. A. *J. Comput. Chem.* **1986**, *7*, 230.
- (233) Burkert, U.; Allinger, N. L. *Molecular Mechanics*; American Chemical Society: Washington, DC, 1982.
- (234) Discover ; Biosym Technologies: San Diego, CA, 1994.
- (235) Lifson, S.; Felder, C. E.; Shanzer, A. *J. Biomol. Struct. Dyn.* **1984**, *2*, 641.
- (236) Badertscher, M.; Maruizumi, T.; Musso, S.; Welti, M.; Ha, T. K.; Pretsch, E. *J. Comput. Chem.* **1990**, *11*, 819.
- (237) Crippen, G. M.; Havel, T. F. *Distance Geometry and Molecular Conformation*; Research Studies Press: Taunton, Somerset, 1988.
- (238) Laarhoven, P. J. M.; Aarts, E. H. L. *Simulated Annealing: Theory and Applications*; D. Reidel: Dordrecht, 1987.
- (239) Brodmeier, T.; E. Pretsch, E. *J. Comput. Chem.* **1994**, *15*, 588.
- (240) Jorgensen, W. L. *Acc. Chem. Res.* **1989**, *22*, 184.
- (241) Jorgensen, W. L. *J. Phys. Chem.* **1983**, *87*, 5304.
- (242) van Gunsteren, W. F.; Berendsen, H. J. C. *Angew. Chem. Int. Ed. Engl.* **1990**, *29*, 992.
- (243) Tembe, B. L.; McCammon, J. A. *Comput. Chem.* **1984**, *8*, 281.
- (244) Straatsma, T. P.; McCammon, J. A. *Ann. Rev. Phys. Chem.* **1992**, *407*.
- (245) van Eerden, J.; Harkema, S.; Feil, D. *J. Phys. Chem.* **1988**, *92*, 5076.
- (246) Eisenman, G.; Alvarez, O.; Aqvist, J. *J. Inclusion Phenom. Mol. Recognit. Chem.* **1992**, *12*, 23.
- (247) Aqvist, J.; Alvarez, O.; Eisenman, G. *J. Phys. Chem.* **1992**, *96*, 10019.
- (248) Marrone, T. J.; Merz, K. M., Jr. *J. Am. Chem. Soc.* **1992**, *114*, 7542.
- (249) Jorgensen, W. L.; Buckner, J. K.; Boudon, S.; Tirado-Rives, J. *J. Chem. Phys.* **1988**, *89*, 3742.
- (250) Miyamoto, S.; Kollman, P. A. *J. Am. Chem. Soc.* **1992**, *114*, 3668.
- (251) Kollman, P. A. In *Computational Approaches in Supramolecular Chemistry*; Wipff, G., Ed.; Kluwer Academic Publishers: Dordrecht, 1994.
- (252) Wipff, G.; Troxler, L. In *Computational Approaches in Supramolecular Chemistry*; Wipff, G., Ed.; Kluwer Academic Publishers: Dordrecht, 1994.
- (253) Wipff, G. In *Computational Approaches in Supramolecular Chemistry*; Wipff, G., Ed.; Kluwer Academic Publishers: Dordrecht, 1994.
- (254) Adam, K. R.; Lindoy, L. F. In *Crown Compounds, Toward Future Applications*; Cooper, S. R., Ed.; VCH: Weinheim, 1992.
- (255) Lewenstam, A.; Hulanicki, A. *Selective Electrode Rev.* **1990**, *12*, 161.
- (256) Diebler, H.; Eigen, M.; Ilgenfritz, M.; Maass, G.; Winkler, R. *Pure Appl. Chem.* **1969**, *20*, 93.
- (257) Winkler, R. In *Structure and Bonding*; Springer-Verlag: Heidelberg, 1972; Vol. 10.
- (258) Burgermeister, W.; Winkler-Oswatitsch, R. In *Topics in Current Chemistry*; Springer-Verlag: Heidelberg, 1977; Vol. 60.
- (259) Grell, E.; Oberbäumer, I. In *Molecular Biology, Biochemistry and Biophysics*; Pecht, I., Rigler, R., Eds.; Springer-Verlag: Berlin, 1977; Vol. 24.
- (260) Pretsch, E.; Büchi, R.; Ammann, D.; Simon, W. In *Analytical Chemistry, Essays in Memory of Anders Ringbom*; Wänninen, E., Ed.; Pergamon Press: Oxford, 1977.
- (261) Schneider, J. K.; Hofstetter, P.; Pretsch, E.; Ammann, D.; Simon, W. *Helv. Chim. Acta* **1980**, *63*, 217.
- (262) Hofstetter, P.; Pretsch, E.; Simon, W. *Helv. Chim. Acta* **1983**, *66*, 2103.
- (263) Mathis, D. E.; Buck, R. P. *J. Membr. Sci.* **1979**, *4*, 379.
- (264) Mathis, D. E.; Stover, F. S.; Buck, R. P. *J. Membr. Sci.* **1979**, *4*, 395.
- (265) Xie, S. H.; Cammann, K. *J. Electroanal. Chem.* **1987**, *229*, 249.
- (266) Tóth, K.; Graf, E.; Horvai, G.; Pungor, E.; Buck, R. P. *Anal. Chem.* **1986**, *58*, 2741.
- (267) Kakutani, T.; Nishiwaki, Y.; Osakai, T.; Senda, M. *Bull. Chem. Soc. Jpn.* **1986**, *59*, 781.
- (268) Armstrong, R. D.; Lockhart, J. C.; Todd, M. *Electrochim. Acta* **1986**, *31*, 591.
- (269) Armstrong, R. D. *Electrochim. Acta* **1987**, *32*, 1549.
- (270) Vanysek, P.; Ruth, W.; Koryta, J. *J. Electroanal. Chem.* **1983**, *148*, 117.
- (271) Yoshida, Z.; Freiser, H. *J. Electroanal. Chem.* **1984**, *179*, 31.
- (272) Koryta, J.; Kozkov, Y. N.; Skalicky, M. *J. Electroanal. Chem.* **1987**, *234*, 335.
- (273) Samec, Z.; Homolka, D.; Marecek, V. *J. Electroanal. Chem.* **1982**, *135*, 265.
- (274) Wang, E.; Yu, Z.; Qi, D.; Xu, C. *Electroanalysis* **1993**, *5*, 149.
- (275) Hofmanova, A.; Hung, L. Q.; Khalil, W. *J. Electroanal. Chem.* **1982**, *135*, 257.
- (276) Homolka, D.; Hung, L. Q.; Hofmanova, A.; Khalil, M. W.; Koryta, J.; Marecek, V.; Samec, Z.; Sen, S. K.; Vanysek, P.; Weber, J.; Brezina, M.; Janda, M.; Stibor, I. *Anal. Chem.* **1980**, *52*, 1606.
- (277) Oesch, U.; Simon, W. *Helv. Chim. Acta* **1979**, *62*, 754.
- (278) Oesch, U.; Dinten, O.; Ammann, D.; Simon, W. In *Ion Measurements in Physiology and Medicine. Proceedings of the International Symposium on the Theory and Application of Ion-Selective Electrodes in Physiology and Medicine, Burg Rabenstein, BRD, September 12-14*; Kessler, M., D. K., H., Höper, J., Eds.; Springer-Verlag: Berlin, 1985.
- (279) Dinten, O.; Spichiger, U. E.; Chaniotakis, N.; Gehrig, P.; Rusterholz, B.; Morf, W. E.; Simon, W. *Anal. Chem.* **1991**, *63*, 596.
- (280) Hansch, C.; Leo, A. *Substituent Constants for Correlation Analysis in Chemistry and Biology*; Wiley: New York, 1979.
- (281) Kubinyi, H. *QSAR: Hansch Analysis and Related Approaches*; VCH: Weinheim, 1993.
- (282) Ebdon, L.; Ellis, A. T.; Corfield, G. C. *Analyst* **1982**, *107*, 288.
- (283) Brunink, J. A. J.; Lugtenberg, R. J. W.; Brzozka, Z.; Engbersen, J. F. J.; Reinhoudt, D. N. *J. Electroanal. Chem.* **1994**, *378*, 185.
- (284) Lindner, E.; Cosofret, V. V.; Kusy, R. P.; Buck, R. P.; Rosatzin, T.; Schaller, U.; Simon, W.; Jeney, J.; Tóth, K.; Pungor, E. *Talanta* **1993**, *40*, 957.
- (285) Moody, G. J.; Oke, R. B.; Thomas, J. D. R. *Analyst* **1970**, *95*, 910.
- (286) Simon, M. A.; Kusy, R. P. *Polymer* **1993**, *34*, 5106.
- (287) Chan, A. D. C.; Harrison, D. J. *Talanta* **1994**, *41*, 849.
- (288) Jagur-Grodzinski, J.; Marian, S.; Vofsi, D. *Sep. Sci.* **1973**, *8*, 33.
- (289) Malinowska, E.; Oklejas, V.; Hower, R. W.; Brown, R. B.; Meyerhoff, M. E. *Proceedings of International Conference on Transducers '95*; 1995; p 851.
- (290) Schaller, U., Diss ETH Zürich, No 10948, 1994.
- (291) Hofmeister, F. *Arch. Exp. Pathol. Pharmacol.* **1888**, *24*, 247.
- (292) Marcus, Y. *Biophysical Chemistry* **1994**, *51*, 111.
- (293) Ammann, D.; Bissig, R.; Güggi, M.; Pretsch, E.; Simon, W.; Borowitz, I. J.; Weiss, L. *Helv. Chim. Acta* **1975**, *58*, 1535.
- (294) Anker, P.; Wieland, E.; Ammann, D.; Dohner, R. E.; Asper, R.; Simon, W. *Anal. Chem.* **1981**, *53*, 1970.
- (295) Born, M. *Z. Physik* **1920**, *1*, 45.
- (296) Morf, W. E.; Simon, W. *Helv. Chim. Acta* **1971**, *54*, 2683.
- (297) Simon, W.; Morf, W. E.; Meier, P. C. In *Structure and Bonding*; Springer-Verlag: Heidelberg, 1973; Vol. 16.
- (298) Eugster, R.; Rosatzin, T.; Rusterholz, B.; Aebersold, B.; Pedrazza, U.; Rüegg, D.; Schmid, A.; Spichiger, U. E.; Simon, W. *Anal. Chim. Acta* **1994**, *289*, 1.
- (299) Armstrong, R. D.; Horvai, G. *Electrochim. Acta* **1990**, *35*, 1.
- (300) Armstrong, R. D.; Covington, A. K.; Proud, W. G. *J. Electroanal. Chem.* **1988**, *257*, 155.
- (301) Armstrong, R. D.; Todd, M. *J. Electroanal. Chem.* **1988**, *257*, 161.
- (302) Lindner, E.; Tóth, K.; Pungor, E.; Behm, F.; Oggenfuss, P.; Welti, D. H.; Ammann, D.; Morf, W. E.; Pretsch, E.; Simon, W. *Anal. Chem.* **1984**, *56*, 1127.
- (303) Cobben, P. L. H. M.; Egberink, R. J. M.; Bomer, J. G.; Bergveld, P.; Reinhoudt, D. N. *J. Electroanal. Chem.* **1994**, *368*, 193.
- (304) Lindner, E.; Cosofret, V. V.; Ufer, S.; Buck, R. P.; Kao, W. J.; Neuman, M. R.; Anderson, J. M. *J. Biomed. Mater. Res.* **1994**, *28*, 591.
- (305) Igarashi, I.; Ito, T.; Taguchi, T.; Tabata, O.; Inagaki, H. *Sens. Actuators, B* **1990**, *1*, 8.
- (306) Harrison, D. J.; Teclerariam, A.; Cunningham, L. L. *Anal. Chem.* **1989**, *61*, 246.
- (307) Watanabe, K.; Nakagawa, E.; Yamada, H.; Hisamoto, H.; Suzuki, K. *Anal. Chem.* **1993**, *65*, 2704.
- (308) Nieman, T. A.; Horvai, G. *Anal. Chim. Acta* **1985**, *170*, 359.
- (309) Ammann, D.; Pretsch, E.; Simon, W.; Lindner, E.; Bezegh, A.; Pungor, E. *Anal. Chim. Acta* **1985**, *171*, 119.
- (310) Kraig, R. P.; Nicholson, C. *Science* **1976**, *194*, 725.
- (311) Lindner, E.; Graf, E.; Nigreis, Z.; Tóth, K.; Pungor, E.; Buck, R. P. *Anal. Chem.* **1988**, *60*, 295.

- (312) Zhang, G. H.; Imato, T.; Asano, Y.; Sonoda, T.; Kobayashi, H.; Ishibashi, N. *Anal. Chem.* **1990**, *62*, 1644.
- (313) Maj-Zurawska, M.; Hulanicki, A. *Microchim. Acta* **1990**, *1*, 209.
- (314) Tsujimura, Y.; Sunagawa, T.; Yokoyama, M.; Kimura, K. *Analyst* **1996**, *121*, 1705.
- (315) Manz, A.; Simon, W. *J. Chromatogr. Sci.* **1983**, *21*, 326.
- (316) Manz, A.; Simon, W. *Anal. Chem.* **1987**, *59*, 74.
- (317) Haber, C.; Silvestri, I.; Rösli, S.; Simon, W. *Chimia* **1991**, *45*, 117.
- (318) Nann, A.; Pretsch, E. *J. Chromatogr. A* **1994**, *676*, 437.
- (319) Pioda, L. A. R.; Simon, W. *Chimia* **1969**, *72*.
- (320) Frant, M. S.; Ross, J. W. *Science* **1970**, *167*, 987.
- (321) Pick, J.; Tóth, K.; Vasák, M.; Pungor, E.; Simon, W. In *Ion Selective Electrodes*; Pungor, E., Buzás, I., Eds.; Akadémiai Kiadó: Budapest, 1973.
- (322) Fiedler, U.; Ruzicka, J. *Anal. Chim. Acta* **1973**, *67*, 179.
- (323) Li, Z.; Li, X.; Petrovic, S.; Harrison, D. J. *Anal. Methods Instrum.* **1993**, *1*, 30.
- (324) Li, Z.; Li, X.; Rothmeier, M.; Harrison, D. J. *Anal. Chem.* **1996**, *68*, 1726.
- (325) Chan, A. D. C.; Li, X.; Harrison, D. J. *Anal. Chem.* **1992**, *64*, 2512.
- (326) Zwickl, T.; Schneider, B.; Cimerman, Z.; Lindner, E.; Sokalski, T.; Schaller, U.; Pretsch, E. *Manuscript in preparation*.
- (327) Wotring, V. J.; Prince, P. K.; Bachas, L. G. *Analyst* **1991**, *116*, 581.
- (328) Moody, G. J.; Saad, B. B.; Thomas, J. D. R. *Sel. Electrode Rev.* **1988**, *10*, 71.
- (329) Satchwill, T.; Harrison, D. J. *J. Electroanal. Chem.* **1986**, *202*, 75.
- (330) Ma, S. C.; Chaniotakis, N. A.; Meyerhoff, M. E. *Anal. Chem.* **1988**, *60*, 2293.
- (331) Cosofret, V. V.; Buck, R. P.; Erdosy, M. *Anal. Chem.* **1994**, *66*, 3592.
- (332) Ma, S.-C.; Meyerhoff, M. E. *Mikrochim. Acta* **1990**, *1*, 197.
- (333) Kusy, R. P.; Whitley, J. Q.; Buck, R. P.; Cosofret, V. V.; Lindner, E. *Polymer* **1994**, *35*, 2141.
- (334) Cosofret, V. V.; Lindner, E.; Buck, R. P.; Kusy, R. P.; Whitley, J. Q. *J. Electroanal. Chem.* **1993**, *345*, 169.
- (335) Cosofret, V. V.; Lindner, E.; Buck, R. P.; Kusy, R. P.; Whitley, J. Q. *Electroanalysis* **1993**, *5*, 725.
- (336) Dürselen, L. F. J.; Wegmann, D.; May, K.; Oesch, U.; Simon, W. *Anal. Chem.* **1988**, *60*, 1455.
- (337) Cha, G. S.; Liu, D.; Meyerhoff, M. E.; Cantor, H. C.; Midgley, A. R.; Goldberg, H. D.; Brown, R. B. *Anal. Chem.* **1991**, *63*, 1666.
- (338) Espadas-Torre, C.; Meyerhoff, M. E. *Anal. Chem.* **1995**, *67*, 3108.
- (339) Brooks, K. A.; Allen, J. R.; Feldhoff, P. W.; Bachas, L. G. *Anal. Chem.* **1996**, *68*, 1439.
- (340) Wang, E.; Meyerhoff, M. E. *Anal. Lett.* **1993**, *26*, 1519.
- (341) Moody, G. J.; Slater, M. J. M.; Thomas, J. D. R. *Analyst* **1988**, *113*, 103.
- (342) van der Wal, P. D.; van den Berg, A.; de Rooij, N. F. *Sens. Actuators, B* **1994**, *18-19*, 200.
- (343) Cardwell, T. J.; Cattrall, R. W.; Iles, P. J.; Hamilton, I. C. *Anal. Chim. Acta* **1989**, *219*, 135.
- (344) Tietje-Girault, J.; McInnes, I.; Schroder, M.; Tennat, G.; Girault, H. H. *Electrochim. Acta* **1990**, *35*, 777.
- (345) Bratov, A. V.; Abramova, N.; Munoz, J.; Dominguez, C.; Alegret, S.; Bartoli, J. *J. Electrochem. Soc.* **1994**, *141*, L111.
- (346) Bratov, A.; Abramova, N.; Munoz, J.; Dominguez, C.; Alegret, S.; Bartoli, J. *Anal. Chem.* **1995**, *67*, 3589.
- (347) Rosatzin, T.; Andersson, L. I.; Simon, W.; Mosbach, K. *J. Chem. Soc., Perkin Trans. 2* **1991**, 1261.
- (348) Hutchins, R. S.; Bachas, L. G. *Anal. Chem.* **1995**, *67*, 1654.

CR940394A